ABSTRACT

The research about biodegradable polymers has grown so quickly during last decades. One of the main reasons is their application in the field of biomedicine. These polymers are nontoxic for the organism and could be metabolized by the human body after a controlled degradation. Gene therapy success depends on safety and effective of the gene carriers. For that reason the creation of new synthetic vectors is necessary. The temporary scaffolds are one of the most important applications of biodegradable polymers. Temporary scaffolds are used to replace a tissue of the human body that has been broken or weakened by an illness, injury or surgery.

In this project new synthetized biodegradable polymers based on arginine are employed and characterized through FTIR, RMN, DSC, X-rays and GPC. Electrospun PLA scaffolds containing either this new family of polymers or pure arginine are prepared. To obtain the optimal quality of the scaffold it is necessary to tune the electrospinning operational parameters (e.g. flow rate, voltage, needle-collector distance, collector type). Furthermore, both the conditions of the solution (e.g. polymer type and concentration, viscosity, conductivity) as well as the ambient parameters play an important role to get the optimal electrospinning conditions.

The scaffolds are characterized with different techniques, SEM for the morphologic study and fiber diameter measurement, contact angle to evaluate the hydrophobicity of the surface, infrared analysis to assess the addition of the different arginine compounds, and thermal analysis to determine variations on thermal stability and characteristic transition temperatures.

The use of bacteriophages is an interesting alternative for drug-resistant infections that has shown many good results in recent studies. The bacteriophages are a type of virus that only infects bacteria.

Once characterized, the new prepared electrospun mats are loaded by adsorption with bacteriophages, which are specific for the *Staphylococcus Aureus* bacteria. The antibacterial ability of the loaded scaffolds is tested. PHMB is a well-known antibacterial compound that is used as positive control. Biocompatibility of new samples is also tested through cell adhesion and proliferation studies. Finally, the potential use in biomedicine for tissue engineering and infection control is evaluated.

RESUMEN

Durante las últimas décadas la investigación sobre polímeros biodegradables ha crecido notablemente. Su aplicación en el campo de la biomedicina es una de las principales razones. Este tipo de polímeros se caracterizan por no ser tóxicos para el organismo, y poder ser metabolizados tras su degradación. El éxito de la terapia con genes depende en la seguridad y la efectividad de estos. Por este motivo es necesaria la creación de nuevos vectores sintéticos. Los andamios o "scaffolds" temporales son una de las principales aplicaciones de los polímeros biodegradables. Normalmente son utilizados para reemplazar algún tejido del cuerpo humano que ha sido debilitado o se ha roto por algún tipo de lesión u operación quirúrgica.

En el presente proyecto se trabaja con nuevos polímeros biodegradables basados en la arginina caracterizándolos mediante FTIR, RMN, DSC, rayos X y GPC. Diferentes scaffolds de PLA conteniendo tanto estos nuevos polímeros como diferentes cantidades de arginina serán preparados mediante la técnica de *electrospinning*. Para obtener la calidad óptima del scaffold es necesario ajustar los parámetros operacionales del proceso (velocidad de flujo, distancia entre la aguja y el colector, tipo de colector, etc.). Tanto los parámetros de la disolución (concentración y tipo de polímero, viscosidad, conductividad) así como los parámetros ambientales juegan también un papel importante en la obtención de las condiciones óptimas de *electrospinning*.

Los scaffolds se caracterizan mediante diferentes técnicas, SEM para el estudio morfológico y la medida del diámetro de fibra, ángulo de contacto para evaluar la hidrofobicidad de la superficie, análisis infrarrojo para valorar los diferentes compuestos de arginina y un análisis térmico para determinar variaciones en la estabilidad térmica o en las temperaturas de transición características.

El uso de bacteriófagos es una alternativa muy interesante para el tratamiento de infecciones resistentes a los antibióticos que ha mostrado muy buenos resultados en estudios recientes. Los bacteriófagos son un tipo de virus que solo infecta a bacterias.

Una vez caracterizados, los scaffolds son cargados por adsorción con bacteriófagos, los cuales son específicos para la bacteria *Staphylococcus aureus*. La capacidad antibacteriana de los scaffolds cargados con bacteriófagos es ensayada mediante la inhibición del crecimiento de *S.aureus*, y una matriz cargada con

PHMB, que es un conocido bactericida, fue usada como control positivo. La biocompatibilidad de las nuevas matrices de fibras cargadas también fue estudiada mediante los ensayos de adhesión y proliferación celular.

ACKNOWLEDGMENTS

First and foremost, I would like to start thanking my supervisors, Prof. Dr, Jordi Puiggalí, for taking a chance and believe in me when he give me the opportunity to do my master thesis project in this laboratory, his wisdom and ideas help me to understand new concepts that I had never seen before; and Dr. Luis Javier del Valle, for his guidance, inspiration and constant encouragement and patience throughout the project. His many trick and tips make me easier to finish the project on time. Both of them have taken considerable amount of time and energy to teach me, and their ideas and suggestions always lead to a better understanding of my thesis topic.

I would like to thank Dr. Lourdes Franco for her time invested in explaining and helping me with the calorimetric analysis. I am exceedingly grateful to Angelica Diaz for helping me with the GPC as well as the RMN analysis. I also would like to thank Cristian Olmo for the Synchrotron analysis and the data treatment.

I must also extend thanks to research fellow labmates: Jose, Ina and especially to Noel who show me how to do the TEM observation and sample preparation.

Lastly, I want to express my biggest appreciation to my parents and brothers, for their unconditional love and selfless support through all my academic formation. Also to some friends who helped me either correcting the English grammar or letting me to distress having a break with them. Thank you María, Daniel, and Chen.

TABLE OF CONTENTS

ABSTRACT iii

RESUMEN v

ACKNOWLEDGMENTS vii

TABLE OF CONTENTS ix

LIST OF TABLES xii

LIST OF FIGURES xiii

GLOSSARY xvii

CHAPTER I: PREFACE 1

1.1. - Project origin 1
1.2. - Motivation 1
1.3. - Previous requirements 1

CHAPTER II: BACKGROUND AND LITERATURE REVIEW 3

2.1. - Biodegradable polymers 3
2.1.1. - General aspects 3
2.1.2. - Degradation process 3
2.1.3. - Classification 4
2.1.4. - Polylactide 5
2.1.5. - Poly (ester amide)s 8
2.1.6. - Polyurethanes 9
2.1.7. - Arginine-based biodegradable ether-ester polymers 9

2.2. - Polyhexamethylenebiguanide 10
2.3. - Bacteriophages 11
2.3.1. - Fundamentals 11
2.3.2. - Bacteriophages versus antibiotics 13
2.3.3. - Bibliographic antecedents 14
2.4. - Biomedical applications of biodegradable polymers 15
2.4.1. - Fundamentals 15
2.4.2. - Temporary scaffolds 16
2.4.3. - Tissue engineering 16
2.5. - Electrospinning 18
2.5.1. - Introduction 18
2.5.2. - Technique principles 18
2.5.3. - Electrospinning set-up 19
2.5.4. - Processing parameters 21
2.5.5. - General applications 23
2.5.6. - Biomedical applications 24

CHAPTER III: OBJECTIVES 27

3.1. - General objectives 27
3.2. - Specific objectives 27

CHAPTER IV: MATERIALS AND METHODS 29

4.1. - Chemical products 29
4.2. - Electrospinning 32
4.3. - Morphology and fiber diameter 34
4.4. - Infrared analysis 37
4.5. -Thermal analysis 39
4.6. - Nuclear magnetic resonance 41
4.7. - Synchrotron radiation 43
4.8. - Gel permeation chromatography 44
4.9. - Contact angle 46
4.10. - Bacterial culture growth inhibition 47
4.10.1. - Media preparation and bacterial strain 47
4.10.2. - Bacteriophage 48

4.10.3. - Plaque assay of soft-agar overlay 48
4.10.4. - Bacteriophage adsorption onto the fiber mats 48
4.11. - In-Vitro biocompatibility assays: cell adhesion and proliferation 49

CHAPTER V: RESULTS AND DISCUSSION 53

5.1. - Characterization of the Arg-based polymers 53
5.1.1. - Thermal analysis 53
5.1.2. - Infrared analysis 55
5.1.3. - Nuclear magnetic resonance 57
5.1.4. - Synchrotron radiation 58
5.1.5. - Gel permeation chromatography 60
5.2. - Optimal preparation of electrospinnable polymer solutions 61
5.3. - Optimization of the electrospinning conditions 63
5.4. - Fiber characterization 65
5.4.1. - Optical microscope analysis 65
5.4.2. - SEM morphology 66
5.4.3. - Fiber diameter 67
5.4.4. - Infrared analysis 72
5.4.5. - Thermal analysis 76
5.4.6. - Contact angle 80
5.4.7. - Synchrotron radiation 83
5.5. - Observation of phages by TEM 83
5.6. - Bacterial growth inhibition 84
5.7. - In-Vitro biocompatibility assay: cell adhesion and proliferation 86

CHAPTER VI: CONCLUSIONS AND RECOMMENDATIONS 91

CHAPTER VII: SUSTAINABILITY OF THE PROJECT 93

7.1. - Environmental, health and social impact evaluation 94
7.2. - Economic evaluation of the project 96
REFERENCES 99

LIST OF TABLES

Table **Page**

Table 2. 1: Effects of the processing parameters in the electrospinning technique. 22

Table 4. 1: Arginine based polymers designation. 29
Table 4. 2: Basic characteristics of the monomer M1..... 31

Table 5. 1: Glass transition temperatures of the different Arg-based polymers... 53
Table 5. 2: Degradation temperature for Arg-based polymers. 54
Table 5. 3: Molecular weight and dispersity index. 60
Table 5. 4: Solubility tests for solvent selection. 61
Table 5. 5: Complete description of the required materials for the manufacture of the produced mats. 63
Table 5. 6: Optimal electrospinning parameters for each sample produced..... 65
Table 5. 7: Obtained fiber diameter (Data: $\bar{x}$ ± SEM). Tukey's test: a, $p < 0.05$ VS PLA; b, $p < 0.05$ VS PLA-0.25%PHMB; c, $p < 0.05$ VS PLA-5%Arg; d, $p < 0.05$ VS PLA-10%Arg; e, $p < 0.05$ VS PLA*; f, $p < 0.05$ VS PLA-PE; g, $p < 0.05$ VS PLA-20%Arg. 72
Table 5. 8: Thermal properties of the samples loaded with arginine. 80
Table 5. 9: Thermal properties of electrospun samples loaded with the different Arg-based polymers. 80

LIST OF FIGURES

Figure **Page**

Figure 2. 1: PLA synthesis by polycondensation and by ring opening processes.. 6
Figure 2. 2: Repetitive unit of polylactic acid. 7
Figure 2. 3: L-Lactide, D-lactide and *meso*-lactide monomers and their derived polymers. 7
Figure 2. 4: PLA life cycle. 8
Figure 2. 5: Parts and structure of a bacteriophage [25]. 11
Figure 2. 6: Lytic an lysogenic replication cycles of bacteriophages [28]. 12
Figure 2. 7: Scaffold development for tissue engineering [46], [47]. 18
Figure 2. 8: Electrospinning scheme. 20
Figure 2. 9: Forces acting one against the other in the drop. 20

Figure 4. 1: "Scheme 1": The first step of synthesis of the Arg-based polymers: Synthesis of the monomers M1. 30
Figure 4. 2: "Scheme 2": Second step for the Arg-based polymer syntheses. 31
Figure 4. 3: Scheme of the electrospinning setup. 32
Figure 4. 4: Camera equipped optical microscope. 34
Figure 4. 5: Focus Ion Beam microscope used during the research. 37
Figure 4. 6: Vibrational modes of molecules. 38
Figure 4. 7: Double beam spectrometer. 39
Figure 4. 8: Fourier transform infrared spectrometer. 39
Figure 4. 9: *Jasco FTIR 4100.* 39
Figure 4. 10: DSC *Q100 (TA Instruments).* 41
Figure 4. 11: Scheme of the experimental setup for simultaneous SAXS/WAXS experiments performed at the NCD beam line of synchrotron ALBA. The main parts of the goniometer are rotation unit (1), arm (2), counterweight (3), and hot stage (4). The vacuum chamber is made of cylindrical parts of different lengths and a square based truncated pyramid at the front [64]. 43
Figure 4. 12: Representative scheme of the different parameters that interfere in the Bragg's law. 44
Figure 4. 13: Scheme of the GPC equipment and separation of molecular sizes.. 45
Figure 4. 14: Contact angle equipment used for measurements. 46
Figure 4. 15: Water drop dispensation in a sample. 47
Figure 4. 16: Automatic microplate reader *EZ-READ 400 ELISA.* 51

Figure 5. 1: Example for glass transition temperature determination of the PEA and PEUR. 54
Figure 5. 2: Weight and derivative weight loss of a representative group of samples of Arg-based polymers. 55
Figure 5. 3: Comparison between the FTIR spectra of PEA, PEUR and PEEUR-3 samples. 56
Figure 5. 4: FTIR spectra of different PEEUR's show no significant differences. . 57
Figure 5. 5: Part of the NMR spectra of the PEEUR-2 sample. 58
Figure 5. 6: Crystalline peaks of arginine. 59
Figure 5. 7: X-rays analysis of the Arg-based polymers. 59
Figure 5. 8: Amorphous and crystalline halos for different polymers and pure arginine. 60
Figure 5. 9: GPC distribution curve the studied PEA. 61
Figure 5. 10: Example of the electrospinning optimization process. 64
Figure 5. 11: Different captions (20X) of the optimal electrospinning conditions: a) PLA; b) PLA-0.25%PHMB; c) PLA-10%Arg; d) PLA-20%Arg., e)PLA-PEA, f) PLA-PEEUR-1 66
Figure 5. 12: SEM micrographs (10.000 X) of: a) PLA; b) PLA-0.25%PHMB; c) PLA-20%Arg; d) PLA-PEEUR-4 67
Figure 5. 13: Diameter distribution and SEM micrographs of (5.000 X): a), PLA, b) PLA-0.25%PHMB, c) PLA-5%Arg, d) PLA-10%Arg, e) PLA-20%Arg, f) PLA*, g) PLA-PEA, h) PLA-PEUR, i) PLA-PEEUR-1, j) PLA- PEEUR-2, k) PLA- PEEUR-3, l) PLA- PEEUR-4. 71
Figure 5. 14: Typical peaks observed in the PLA mat. 73
Figure 5. 15: FTIR spectra of the pure PHMB powder. 73
Figure 5. 16: Effect of the addition a 0.25% of PHMB to the PLA compared with the pure PLA sample. 74
Figure 5. 17: Typical peaks observed in an arginine FTIR spectrum. 75
Figure 5. 18: Comparison of different percentages of arginine samples. 75
Figure 5. 19: Comparison of the FTIR spectra between PLA* and PLA-PEA. 76
Figure 5. 20: Effects produced in the characteristic temperatures of the electrospun samples containing arginine. 77
Figure 5. 21: DSC analysis of an arginine rich zone of the PLA-20%Arg sample. 79
Figure 5. 22: Comparison of the contact angle measured in the PLA and PLA + 0.25%PHMB. Tukey's test: *, $p < 0.05$ VS PLA. 81
Figure 5. 23: Influence of the quantity of arginine on the contact angle. 82
Figure 5. 24: Structural formula of the PLA, PHMB and arginine. 82

Figure 5. 26: TEM images of bacteriophages. a) *Siphoviridae* phage with non-contractile tail. b) *Myoviridae* phage with its characteristics contractile tail. 84
Figure 5. 27: Adhesion assay. 87

GLOSSARY

% v/v – Volume concentration
% w/v – Weight-volume concentration
^{1}H-NMR – Proton nuclear magnetic resonance spectroscopy
A.U. – Arbitrary units
Arg. – Arginine
C_3H_6O – Acetone
C_3H_7NO – Dimethylformamide
CA – Contact angle
$CDCL_3$ – Deuterated chloroform
CH_2CL_2 – Dichloromethane
CH_2O_2 – Formic acid
$CHCL_3$ – Chloroform
CLP – Classification labeling and packaging
C_p – Heat capacity
DCM – Dichloromethane
DDS – Drug delivery systems
DMEM – Dulbecco Modified Eagle medium
DMF – Dimethylformamide
DMSO – Dimethyl sulfoxide
DSC – Differential scanning calorimeter
FTIR – Fourier Transform Infrared spectroscopy
GPC – Gel permeation chromatography
H_c – Crystallization enthalpy
HDPE – High density polyethylene
H_m – Melting enthalpy
IR – Infrared
MTT – Tetrazolium salt, 3-4,5 dimethylthiazol-2,5 diphenyl tetrazolium bromide
NMR – Nuclear magnetic resonance
OM – Optical microscope
PBS – Phosphate buffered saline
PCL – Polycaprolactone
PEA –Poly(ester amide)
PEEUR – Poly (ether ester urethane)
PEG – Polyethylene glycol
PEUR – Poly (ester urethane)
PEVOH - Poly (ethylene vinyl alcohol)
PHA – Polyhydroxyalkanoate

PHB – Polyhydroxybutyrate
PHMB – Poly(hexamethylene) biguanide hydrochloride
PLA – Polylactid acid
PMMA - Poly(methyl methacrylate)
PU – Polyurethane
PVOH – Polyvinyl alcohol
SAXS – Small angle X-ray scattering
T% - Transmittance
T_c – Crystallization temperature
TEA – Triethanolamine
T_g – Glass transition temperature
TGA – Thermal gravimetric analysis
T_m – Melting temperature
UV – Ultra-violet
WAXD – Wide angle X-ray diffraction

CHAPTER I: PREFACE

1.1. - Project origin

During last decades, the investigation about biodegradable polymers has grown so quickly. One of the main reasons is its application in the field of biomedicine. These polymers are nontoxic for the organism and could be metabolized by the human body after a controlled degradation. This project come up with the use of electrospun–scaffolds of biodegradable polymers loaded with bacteriophages. The scaffolds are three dimensional and porous structures that are used as cellular support for the preparation and regeneration of human tissues. The use of bacteriophages is an interesting alternative for drug-resistant infections that has shown many good results in recent studies.

1.2. - Motivation

The main motivation for choosing this project is my curiosity to acquire new professional and academic competencies. More precisely, in the field of polymers and their biomedical applications, such as for instance those referring to tissue engineering.

This project makes me possible to obtain new experiences in the field of investigation such as learning different techniques, methodologies or get familiarized with a lot of laboratory equipment. It also allows me to enhance my group working skills.

1.3. - Previous requirements

This master thesis has been accomplished in an investigation laboratory on its majority. For that reason, it is important to have a previous knowledge about material science and be familiarized with laboratory work. It is also important to know about the equipment used as well as the materials employed. Accordingly, a literature review has been carried out during the whole progress of the work in order to fix and achieve the proposed objectives.

CHAPTER II: BACKGROUND AND LITERATURE REVIEW

2.1. - Biodegradable polymers

2.1.1. - General aspects

Polymers are macromolecules created by the covalent bond of small monomers. They could be made up from one single type of monomer or from different ones, being named thus homopolymers or copolymers, respectively. Depending on how these monomeric units are arranged along the polymeric chain they can result in random copolymers, alternating copolymers, block copolymers or grafted copolymers. The number of repeating units forming the polymeric chain is known as the degree of polymerization. The degree of polymerization is a way to express the length of the chain, which will influence the polymer physical properties.

It is possible to distinguish between natural and synthetic polymers depending on the polymers origin source. Equally, if comparing their life cycle there are biodegradable and non-biodegradable polymers.

Over time, the field of material science has being continuously improved everyday seeking for new materials and new applications. More precisely, biodegradable polymers are studied and created for two main reasons. The first one is the idea of avoiding the earth contamination with other materials that remain on the planet perpetually. The other reason is because the biggest source for synthetic polymers (petroleum) is being depleted. However, not all polymers come from renewable sources. Nowadays their prices are still high but the perspectives are promising and therefore this topic is receiving much attention.

2.1.2. - Degradation process

On biomedicine many different types of polymers are nowadays used. The major applications, since decades, are the regeneration and the substitution of organs or human tissues. The materials used in medicine have either temporal or permanent use. Biodegradable polymers (also known as bioabsorbable polymers in medicine) are of great importance within these temporal materials.

When a polymer can be decomposed in different chemical elements which conform itself is called biodegradable polymer. The process of degradation may be the consequence of the attack of biological agents such as bacteria, fungi, yeast and their enzymes, which lead under aerobic conditions to the formation of carbon dioxide, water, biomass and residues [1]. Furthermore, it is possible for the polymer to suffer the degradation due to environmental conditions that may cause the breaking of labile groups. This rupture is made by an external that agent could be chemical (e.g. hydrolysis caused by water) or physical.

The chemical changes that could occur in the polymer are the chain rupture, crosslinking reactions, and change in the lateral substituents, among others. The physical changes that the polymer could suffer in the degradation process go from the discoloration to the brightness loss, as well as the superficial erosion, the greasy surface, the appearing of flaws and the loss of mechanical properties.

The polymer degradation process implies the decrease of the molecular mass and consequently the polymerization degree. A polymer with many groups sensitive to the environment will degrade much faster than others depending on the pH, the humidity, the temperature and the sunlight exposure [2].

In conclusion, the degradation process is different depending on the external agent involved. The main degradation processes are listed below [3]:

1. Photodegradation: Sunlight.
2. Thermodegradation: Temperature.
3. Chemical degradation:
    a. Hydrolytic: Humidity.
    b. Oxidative: Chemical or atmospheric agents.
4. Mechanical: Stresses.
5. Biodegradation: Microorganisms such as algae, fungi or bacteria.

2.1.3. - Classification

Biodegradable polymers are classified in two main groups depending on their origin:

- Natural or renewables: those that come from natural resources.
- Synthetic: Polymers created from fossil or petroleum resources.

Natural polymers are divided in four groups from the chemical point of view:

I. Polysaccharides.
    a. Homopolysacharides: starch, quitin or cellulose.
    b. Heteropolysacharides: natural rubbers.
II. Proteins.
III. Lipids.
IV. Aliphatic polyesters.
    a. Polyesters produced from organisms or plants: PHA, PHB.
    b. Polyesters synthetized from renewable sources: PLA.

Synthetic polymers are divided in six main groups:

I. Aliphatic polyesters: PCL.
II. Aromatic-aliphatic polyesters.
III. Polyamides: nylon 4 and nylon 6.
IV. Polyethers: PEG.
V. Polyvinylalcohols: PVOH, PEVOH.
VI. Modified polyolefins: PE-starch blends.

Polymers from natural resources are mainly associated to the biodegradability concept. In fact, nowadays the development of biodegradable polymers from synthetic resources is growing up. The main aim for this development is the ease in optimizing the properties of these polymers to be at the same time both biodegradable and biocompatible. Some of the required properties are [4]:

- Organism compatibility.
- Ability to develop the desired task.
- Controlled degradation rate.

2.1.4. - Polylactide

Polyesters are characterized by the presence of labile ester bonds (-COO-) on the main chain. The properties are determined by the number of bonds that are present in the structure as well as by the geometry, the polarity and the mobility of their repetitive units. The importance of the polyester biomaterials lies on their ester bond type and their hydrolytic degradation capacity. As there are not very strong molecular interactions, the properties of polyesters are more sensitive to variations in the structure in comparison to other polymers.

Linear polyesters are classified in aliphatic polyesters and polyesters that contain aromatic units. Depending on the number of monomers required for its synthesis, aliphatic polyesters are divided in two groups [2]:

I. Polyhydroxy acids: synthetized by polycondensation of a hydroxyacid or by ring opening polymerization of a lactone or a lactide ring.
II. Poly(alkylene dicarboxylate)s obtained by the polycondensation of a diol and a dicarboxylic acid.

The polylactic acid is a natural biopolymer because its monomer is mainly obtained by fermentation. It could also be obtained by fossil or petrol resources and, therefore, is classified as a synthetic biopolymer [5].

PLA could be obtained, as above indicated, by lactic acid polycondensation as well as by lactide ring opening polymerization. With the first process the obtained polymer has a low molecular weight. On the other hand by the ring opening process the resulting PLA has a high molecular weigth that could lead to a slightly higher melting point.

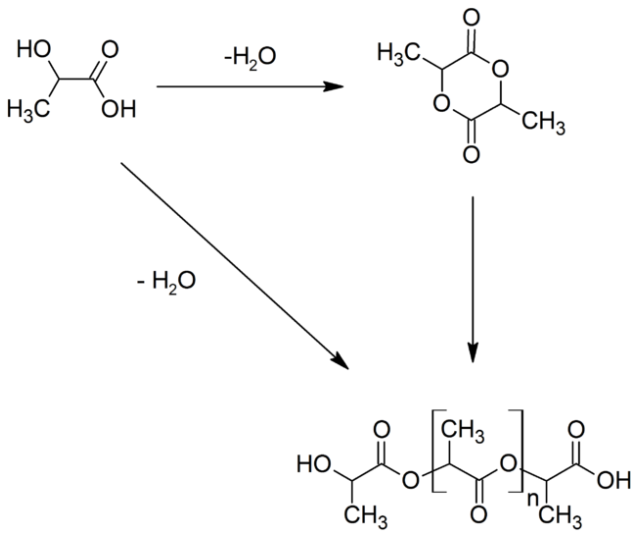

Figure 2. 1: PLA synthesis by polycondensation and by ring opening processes

Direct condensation is an equilibrium reaction where the presence of water traces in the final stages of the reaction limits the molecular weigth. Due to this difficulty the most used process to obtain PLA is the ring opening reaction. This process combine both the economic and the environmental benefits of synthetizing the lactide dimer as well as the PLA on its melted phase [6].

The repetitive unit of the PLA consists of an ester group and a –CH(CH_3) group. From the chemical structure point of view, the alpha carbon from the repetitive unit is a chiral carbon (asymmetric) and consequently it could present two different configurations

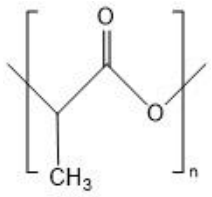

PLA

Figure 2. 2: Repetitive unit of polylactic acid.

Lactide is a cyclic dimer that can be formed by any combination of the two different optical isomers. D and L-Lactide are presented in Figure 2. 3. The two cyclic monomers have two isochiral carbons that lead to the formation of isotactic polymers. The resulting polymer from the natural monomer, L-Lactide (L-PLA), is a semicrystalline polymer (i.e. the degree of crystallinity is close to 37%) due to its stereoregularity. It present high strength and low deformation, and consequently has a high Young modulus, which makes the polymer suitable for applications where the supporting ability is crucial (i.e. sutures or orthopedic devices) [4], [7]. Its melting point is around 175 °C and its glass transition temperature is between 60 °C and 65 °C.

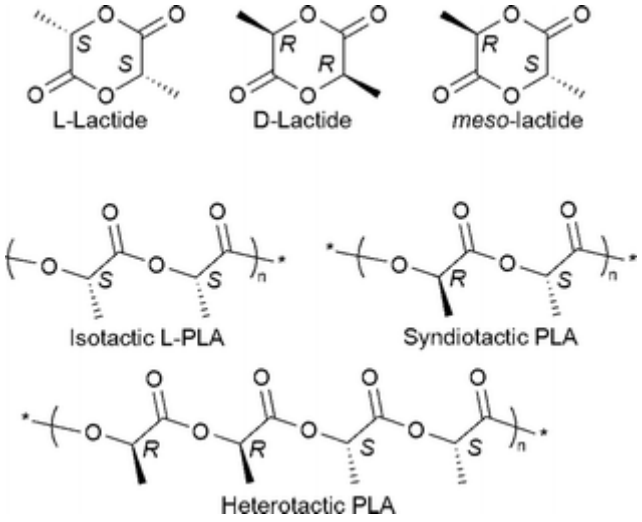

Figure 2. 3: L-Lactide, D-lactide and *meso*-lactide monomers and their derived polymers.

D,L-lactide (*meso*-lactide, Figure 2.3.) consist of the two lactic acid stereoisomers and lead to an atactic and amorphous sample after polymerization. Hence, the strength of the polymer is lower and the deformation capacity is much higher than found for the two isotactic polymers. The *meso* derivative is characterized by its high degradation rate making itself an interesting polymer for drug delivery. Also copolymers of both chiral and achiral monomers are sometimes prepared in order to tune the crystallinity and control the degradation process [4], [7].

Nowadays DLPLA is also used for sutures, screws, drug delivery, coronary stents, nails for ligament fixation and many more biomedical applications. Indeed, one of the most recent applications is within the tissue engineering field. The main aim of this field is to regenerate human tissues from its own cells guiding the cell in-situ by reabsorbable scaffolds [8].

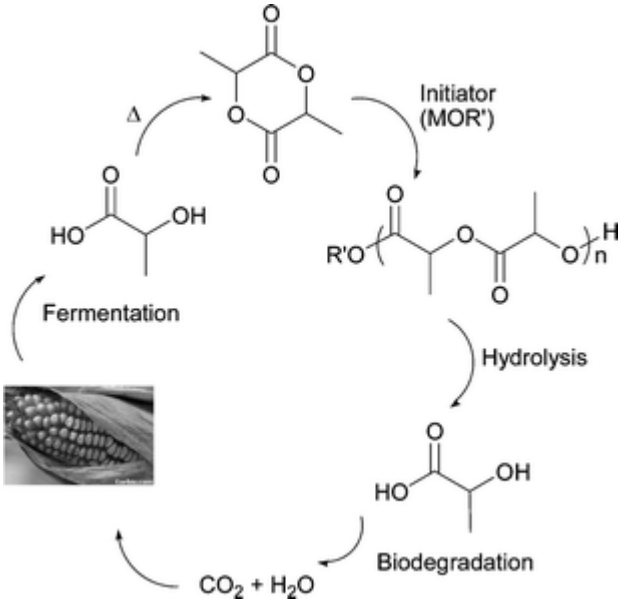

Figure 2. 4: PLA life cycle.

2.1.5. - Poly (ester amide)s

Nowadays the poly(ester amide)s are a group of biodegradable polymers that are becoming more interesting for the society as they can be considered commodity as well as specialty polymers. They have amide and ester groups on their chemical structure, being thus degradable (due to the presence of the ester groups), besides they also have a good thermal and mechanical properties (due to the presence of amide groups that lead to strong intermolecular hydrogen bonding interactions). PEAs could be prepared from different monomers and

following many diverse synthetic methodologies. Therefore, there are a huge variety of microstructures (e.g. blocky, sequential or random) that allows to prepare PEAs with properties appropriate to the expected application. It is also possible to obtain PEAs by ring opening polymerization (the monomer is constituted in this case by an α-amino acid and an α-hydroxyacid and lead to the so named polydepsipeptides) or by polycondensation. In summary properties of PEAs can be easily tuned (e.g. hydrophilic or hydrophobic behavior) due to the change of easily modify their microstructure and composition. such as the [9]

The applications of these materials are increasing during the last years (e.g. adhesives or smart materials). Specially, in biomedicine PEAs are used in controlled drug delivery systems (DDS), hydrogels and tissue engineering [10].

2.1.6. - Polyurethanes

The biomedical application of polyurethanes start around the 1950s with the work of Pangam [11]. Typical PUs morphology is composed of two different structural phases that constitute the so named hard and soft segments. The hard segments promote the mechanical performance of the polymer, and the soft ones provide elasticity and some other properties. The soft segments correspond to the polyols (e.g. polyethers or polyesters) [12]. Nowadays the main use of polyurethanes for biomedical applications is constituted by the manufacturing of catheters, scaffolds, membranes for wound dressing or DDS [13]. PUs are show also good results in surface functionalization studies being hereby a suitable alternative for cell adhesion applications [14].

2.1.7. - Arginine-based biodegradable ether-ester polymers

In gene therapy different polymers are being explored to treat serious diseases. For gene therapy one of the most important factors is the effectiveness of the vector. A successful gene transfer must accomplish the following characteristics: cell penetration, nucleic acid protection and sometimes integration of the delivered gene [15].

Nowadays there are some gene carriers that have shown good but not really satisfactory results, for instance poly(ethyleneimine) (PEI), poly(L-lysine) (PLL) or poly(L-arginine) (poly-arg). The improvement of these polymers and the creation of some new synthetic vectors are a topic of great interest. These new vectors present much lower cytotoxicity. Specifically, new cationic arginine-

based ether-ester polymers have been developed. They consist of different main groups: ester, ether, amide and urethane. The ester bonds obviously enhance biodegradability the ether bond could enhance solubility (like PEG [16], [17]) and finally amide and urethane groups improve intermolecular interactions.

2.2. - Polyhexamethylenebiguanide

The polyhexamethylenebiguanide is a cationic biocide commercialized over the world as a result of its high antimicrobial activity, its chemical stability, low toxicity and reasonable cost.

Its effectivity against microorganisms results from the biguanide group linked to the hexamethylene. The PHMB is one of the most extended antiseptics when a long exposure or contact is required [18].

The presence of PHMB during daily activities is really broad [19]:

- Swimming pool antiseptics.
- Cosmetics.
- Leather preservatives.
- Contact lenses liquid.
- Food handling.
- Textile and fibers.

The effectivity of PHMB is related to its capacity to be linked to the head groups of the phospholipids present in the cellular walls of the bacteria, increasing thus the rigidity. This increase leads to the non-polar segments to the hydrophobic domain and creates a disturbance in the cell membrane ending with the cell death [19], [20].

PHMB could be synthetized by different routes. Usually it is obtained by polycondensation of sodium dicyanamide and hexamethylenediamine in two steps [21]. The five amines present in the PHMB are able to be bonded to the neighboring molecules by hydrogen bonds [22].

2.3. - Bacteriophages

The use of bacteriophages in the treatment of infectious diseases caused by bacteria is a technique which began to be developed in the sixties [23]. There are regulations about biological products and viral vaccines that mark the guidelines for the safety of the bacteriophages in the treatment of diseases, although there are not yet a specific regulation for them [24]–[26].

2.3.1. - Fundamentals

The bacteriophages are a type of virus that only infects the bacteria. They consist on a protein cover named capsid that surround the genetic material The other main part of the phage is the tail which could be different depending on the phage type [27]. Their total size goes from 20 to 200 nm. Depending on their structure they could be classified in filament, helical or icosahedral. In Figure 2. 5 it is presented an icosahedral phage and its constitutive parts. As it could be observed the genetic material is hosted in the capsid. Through the tail fibers the virus is attained to the bacteria and therefore it could inject the genetic material.

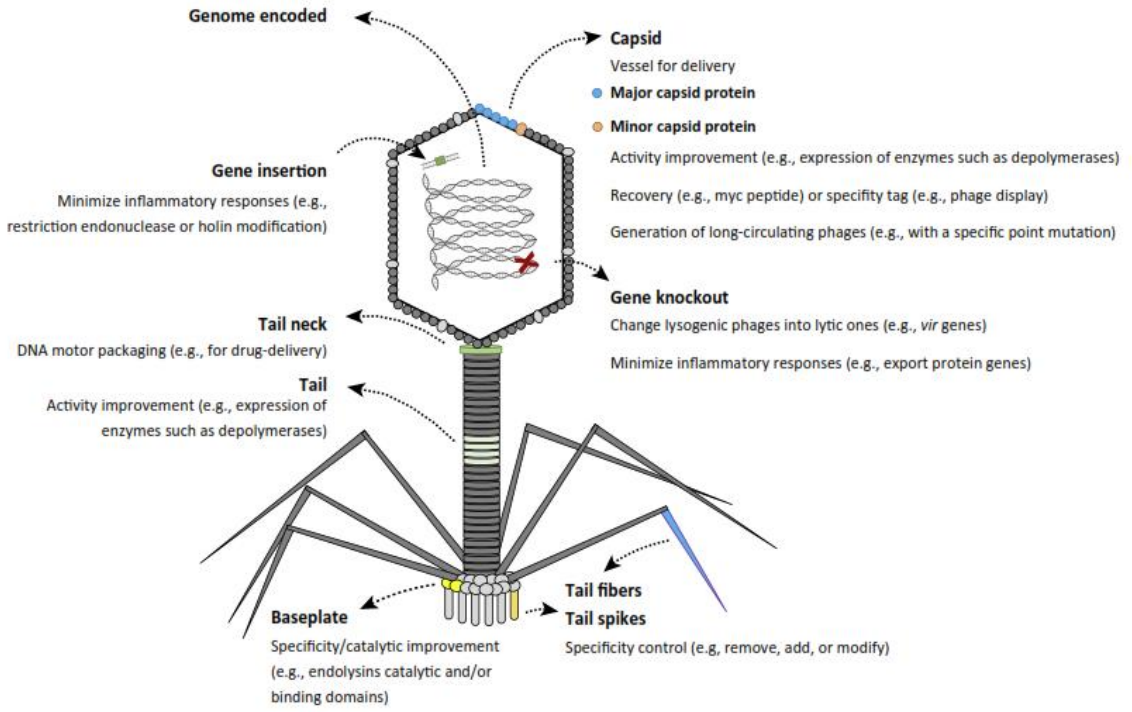

Figure 2. 5: Parts and structure of a bacteriophage [25].

The bacteriophages are attached to different bacterial surfaces through receptors. Any attachment begins with a recognition process between the bacteria and the

phage through its receptors. It drifts in a lytic or lysogenic replication cycle after the genetic materials have been inserted in the bacteria by the phage. On one hand, the lytic cycle results on the lysis destruction of the bacteria that host the bacteriophage after the replication and the encapsulation of the viral particles, which releases the new virus to infect other bacterial cells. On the other hand the lysogenic cycle does not imply an instantaneous lysis. The bacteriophage inserts its genome in the bacteria, which integrates in the DNA of the bacteria and replicates as a bacterial genome. Hence it is transmitted to all progeny of the infected bacteria every time that it is divided by fission. Compared to lytic cycles, in lysogenic cycles the bacteriophage remains in a latency state inside of the bacteria until the proper environmental conditions are achieved. Then, the phages are activated and produce the bacteria death by cellular lysis.

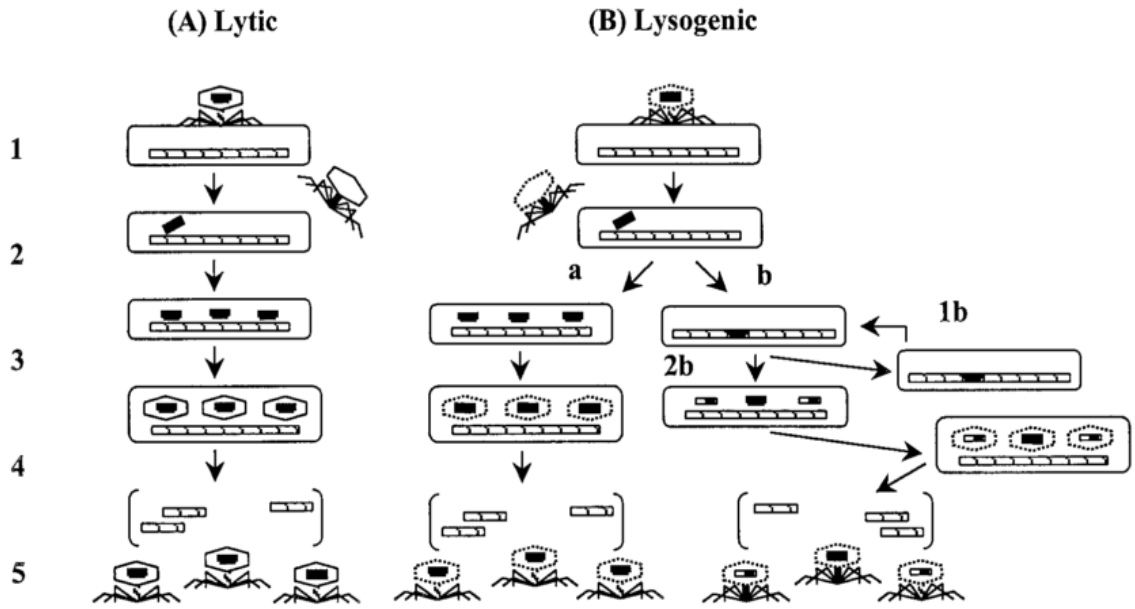

Figure 2. 6: Lytic an lysogenic replication cycles of bacteriophages [28].

The different steps for replication followed by bacteriophages are described below [28]:

A. "Lytic phages: step 1, attachment; step 2, injection of phage DNA into the bacterial host; step 3, shutoff of synthesis of host components, replication of phage DNA, and production of new capsids; step 4, assembly of phages; step 5, release of mature phages (lysis)."

B. "Lysogenic phages: steps 1 and 2 are similar to those of lytic phages (i.e., attachment and injection, respectively); starting with step 3, lysogenic phages can, among other possibilities, initiate a reproductive cycle similar to that of lytic phages (a) or integrate their DNA into the host bacterium's chromosome (lysogenization) (b). Lysogenized cells can replicate normally for many generations (1b) or at some point undergo lysogenic induction (2b) spontaneously or because of inducing agents such as radiation or carcinogens, during which time the integrated phage DNA is excised from the bacterial chromosome and may pick up fragments of bacterial DNA."

Generally a bacteriophage needs around 30 minutes to replicate. The amount of virus that could be released for each infection goes between 50 and 100, apart from the genetic material fragments and protein coating.

2.3.2. - Bacteriophages versus antibiotics

The use of bacteriophages as well as antibiotics in the disease treatment has a common objective but the different mechanism could produce really different consequences in the human body. First of all, antibiotic affects both the pathogen bacteria and the natural body microflora. This has positive effects over itself and consequently secondary infections could be developed, or even allergies or digestive disorders. On the other side, the bacteriophages are only able to attack those kinds of bacteria that contain the appropriate receptors. Hence the natural microflora does not suffer any disturbance, limiting thus the development of secondary infections [29].

Antibiotics and bacteriophages are also different when looking to their operation range. The antibiotics are not only focused where the infection is located but they are distributed in a more broad way, indeed they are metabolized and finally removed from the body. The bacteriophages need the bacteria to replicate, being this the reason why they are concentrated where the infection is allocated. The antibiotics are not always effective in the infection treatment because sometimes the infection becomes resistant to the antibiotic. However bacteriophage could completely suppress the infection from the organism. Furthermore, if the bacteria becomes resistant to antibiotics the bacteriophage could act against them too [30].

The reason why the use of bacteriophages is not spread is the difficulty to develop solid pharmaceutical formulas. Nevertheless, the selection of new bacteriophages affective against antibiotic resistant bacteria is a relatively fast process. However, to obtain the pharmaceutical formula to combat these resistant bacteria is a process that could take years [31].

2.3.3. - Bibliographic antecedents

At an international level there are many articles published that refer to the use of phage therapy in human beings. Most of them come from the east of Europe and from the Soviet Union. In this section some different articles about phage therapy are presented in order to show the potential of this healing treatment. In these articles the use of biodegradable polymers is presented by focusing in their application to adsorb/encapsulate bacteriophages:

- R. Caparelli *et al.* [32] showed a potential perspective for phage use in human cases. In this study they treated mice infected with methicillin-resistant staphylococcal strains with a bacteriophage active against *staphylococcus aureus*. Results were positive from either *in vitro* or *in vivo* observation. According to their conclusions, the phage used can also prevent abscess formation and reduce the load and weigth of abscesses.

- E. Morello *et al.* [33] showed a particular case of lung infection disease which is resistant to antibiotics. A significant number of mice were infected with the *Pseudomonas aeruginosa.* After one single dose treatment the onset of the infection allowed over 95% survival. Moreover, after a four-day preventive treatment resulted in a 100% survival. This study provides an incentive to further studies in on pulmonary phage therapy.

- K. Markoishvili *et al.* [34] developed a degradable matrix of poly(ester amide) that was impregnated with bacteriophages and with an antibiotic to combat the infection presented in ulcers due to vascular problems. In this case, the antibiotic treatment was not effective because of the lack of blood supply and the possibility of the bacteria to become resistant. A 70% of the bacteriophage treated patients healed their ulcers completely.

- H. Pearson *et al*. [23] investigated how to establish covalent links between bacteriophages and inert polymers while biological activity was

preserved. The results were positive because the linked bacteriophages maintain their activity against *Escherichia Coli* and *Staphylococcus aureus.*

- D. Jikia *et al.* [29] developed a biodegradable material able to release both bacteriophages and ciprofloxacin. This material was used to treat wounds infected with the bacteria *Staphylococcus aureus*. The patients developed the infection when being exposed to high levels of radiation. Firstly, they were treated with antibiotics but the infection remain in their bodies. One month later, they were treated with this new developed material. The wounds stop oozing fluids and the infection disappeared in one week.

2.4. - Biomedical applications of biodegradable polymers

2.4.1. - Fundamentals

Only during the last decades the development of the investigation about the biomedical applications of either biodegradable or biocompatible polymers has grown. Historically, the natural collagen was used for different purposes, but was during the Second World War when this research became important. For instance, the poly (methyl methacrylate) (PMMA) was one of the first biocompatible polymers that was used to repair the human cornea.

All materials used in biomedicine should fulfill some requirements and characteristics when they are designed:

- Degradation time should meet the purpose of the application.
- They should have adequate mechanical properties according to the function.
- They should not produce a continuous anti-inflammatory response
- Degradation products should be absorbable and excretable as well as being antiseptic, sterilizable and compatible with the receptor.
- The resulting products of the degradation cannot be mutagenic, carcinogenic, toxic or antigenic [35].

Some of the most common applications are the surgical sutures, which are the oldest one, orthopedic prosthesis, wound protection, and devices for drug delivery.

2.4.2. - Temporary scaffolds

The temporary scaffolds are one of the most important applications of biodegradable polymers. Temporary scaffold are used to replace a tissue of the human body that has been broken or weakened by an illness, injury or surgery. The main function of the scaffold is to serve as an artificial support during the time that the natural tissue is regenerated. Therefore, it should have the same shape and mechanical performance as the tissue to be replaced.

Temporary scaffolds are used in different situations [36]–[41]:

- As orthopedic fixation devices when the required mechanical performance is low. Those are interference screws for knee, wrist or ankle, bolts and tacks for ligament fixation or meniscus surgeries and pins and rods for fracture fixation. Nowadays they are not fully developed for applications where the mechanical performance required is higher.
- In odontology it is common to use polymeric particles to fill the cavity created when a dental piece is removed.

Currently the term scaffold is used to appeal the biodegradable and porous materials with tridimensional structure that are used for in vitro or in vivo culture growth. The aim of the scaffold is to replace a biological tissue or organ that has lost his functionality [36]–[41]. These scaffolds can be easily manufactured by the technique named electrospinning, which allows obtaining micro or nanofibers. This example is the basis of the tissue engineering, one of the fields in biomedicine with more growing interest [36], [40].

2.4.3. - Tissue engineering

These days the third generation of biomaterials is in use. Compared to the second one this generation has the particularity to not only be bioinert and bioactive but also has to interact with the body in a specific way. This is achieved through cellular and molecular stimuli as well as through the combination of the bioabsorbability and bioactivity of the material.

As mentioned previously, these materials are used to replace a human tissue or organ that has been injured but should also disappear during the healing process. Typically the employed species in tissue engineering are living cells and extracellular components which take part in the development of devices that

allow, stimulate or promote the healing or full recovery of the injured organ or tissue.

The most interesting materials for tissue engineering are the synthetic bioabsorbable polymers that can be degraded via hydrolysis in physiologic conditions within the human body and can be completely removed by metabolic processes. Consequently scaffolds could withstand the growing of the own organism avoiding infection problems or the fibrous tissue formation [39], [42]. The development of the tissue engineering would imply the decrease of the associated problems to other techniques [43], [44].

- Donor availability and rejection reaction to allografts.
- Infectious diseases transmission when a xenograft is done.
- Costly and painful interventions in the case of autografts.

Finally, a small schema about how the tissue engineering works is presented in Figure 2. 7. The standard procedure is described below [45]:

1. Cell extraction from human body.
2. In vitro cell growing.
3. Seed of cell in the scaffold.
4. Scaffold cell culture to increase cell number.
5. Regenerated tissue implant.

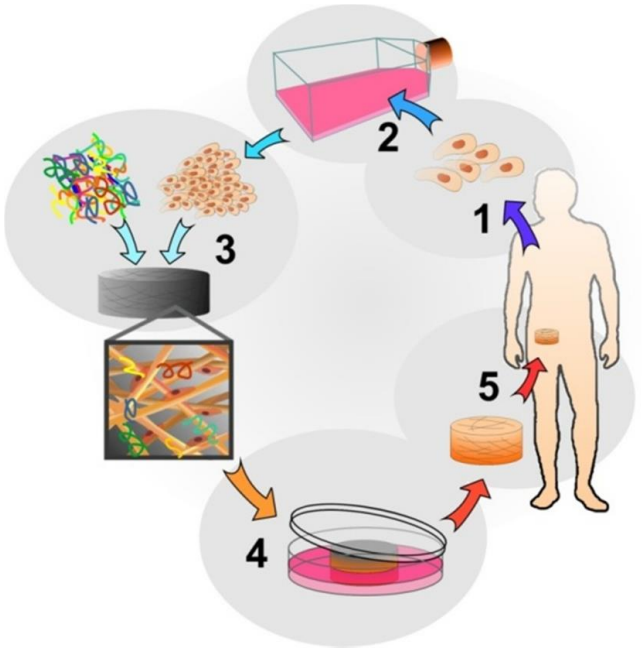

Figure 2. 7: Scaffold development for tissue engineering [46], [47].

2.5. - Electrospinning

2.5.1. - Introduction

During last decades synthetic fiber fabrication was achieved with extrusion machines. The typical diameters obtained are between 10 and 500 μm. [48].

Electrospinning is a technique that uses electric forces to obtain fibers. It is a relatively cheap and simple process that can produce a broad band of fiber diameters going from few nanometers to micrometers with polymers that can be either natural or synthetic [49]–[51].

2.5.2. - Technique principles

In 1228 Guillermo Gilberto described the interaction between fluids and electric and magnetic fields. But it was around the middle 1900 when Geoffrey Ingram Taylor presented a theoretical explanation of these interactions. He made a mathematical model to describe the structure of the cone formed by the fluid drop when was influenced by an electric field. Around the nineties, the method became popular. Nowadays the number of articles published about electrospinning is constantly increasing. This is due to the great interest on the

different applications of the micro/nanofibers in cosmetics, optical tests, textile industry or the medical field[50].

Basically, the technique is based on the application of an electrostatic field between two poles. One of these poles is the needle of the injection system and the other is the collector, where the fibers are deposited. The matrix obtained is porous and has a characteristic texture, color and density[47]–[51].

2.5.3. - Electrospinning set-up

In Figure 2. 8 is presented a schema of the electrospinning equipment. As it could be observed on the left side is placed the syringe with the polymer dissolution. The use of an infusion pump is necessary in order to control the flow rate of the dissolution. This pump is regulated to produce the same amount of pressure constantly during the whole process. The electrostatic field generates a polarization and a charge that produce the attraction of the jet to a grounded conductive surface. In the meantime, the solution reaches the collector, the solvent is evaporated and non-woven fibers are randomly collected.

The applied electrical field is able to break the surface tension of a drop produced in the needle tip. A kind of electrified cone, named as a Taylor cone, is subsequently formed due to a polarization-charge phenomenon. The charges induced into the fluid when it covers the separation distance between the two electrodes (needle and collector) lead to one orthogonal and one tangential force, forming thus the Taylor cone [8], [39], [48], [51], [52]. In Figure 2. 9 it could be observed the Taylor cone formation phenomenon.

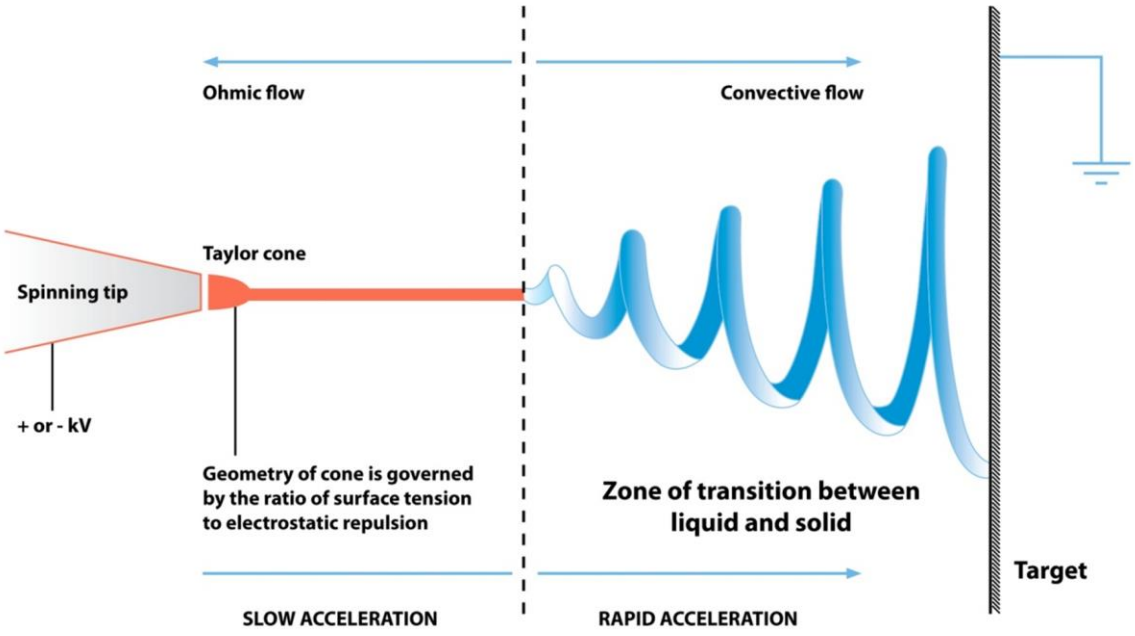

Figure 2. 8: Electrospinning scheme.

This process generates a great acceleration on the jet resulting in a decrease of its diameter. A fiber is obtained when the jet solidifies (i.e. when the solvent is evaporated). The electric current of this process is characterized by a high voltage and very low intensity [50].

Depending on the solution and processing parameters it is possible or not to obtain the proper fibers. These critical parameters are, for instance, the solvent used, the polymer concentration and operational parameters like flow rate, applied voltage and needle-collector distance. Electrospraying is a particular case where fibers are not obtained but regular nano or microspheres useful for encapsulation applications are produced.

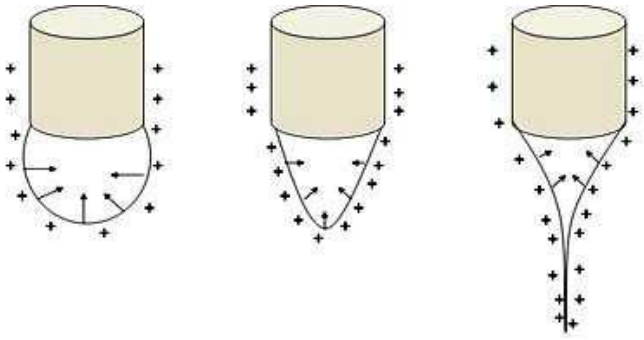

Figure 2. 9: Forces acting one against the other in the drop.

2.5.4. - Processing parameters

The electrospinning process is a simple process, however it has many different factors that affects somehow the properties of the obtained fibers. These parameters could be arranged in three main groups [37], [53].

- Solution properties:
  - Polymer type (molecular weight, structure)
  - Polymer concentration
  - Viscosity
  - Conductivity
  - Density of surface charge
  - Surface tension
  - Dielectric constant of the solvent

- Equipment variables
  - Flow rate
  - Electric potential
  - Distance between the needle tip ant the collector
  - Geometry
  - Type of collector

- External/ambient parameters
  - Humidity
  - Temperature of the solution
  - Air velocity in the electrospinning chamber

The following table describes shortly some of the effects of these previously named parameters in the characteristics of the obtained fibers. These parameters are described below ideally and separately, although during the process they have interrelations and therefore the modification of one of them suppose the change of others. For that reason many different experiments should be repeated to find the optimal parameters for each situation [50], [54].

Process parameters		Effects on fibers morphology
I	*Molecular weight*	An increase on the molecular weight produces the reduction of drops and beads. For this reason high molecular weight polymers are usually selected.

	Viscosity/concentration	These parameters are directly proportional. For each solution there is a min/max concentration where the fibers are produced with no agglomerates. The fiber diameter increases when the concentration is higher. Low viscosity promotes discontinuous fibers, and high viscosity makes impossible the flow of the fluid.
	Conductivity/charge density on the surface	A high conductivity is better to obtain more uniform fibers and avoid the presence of defects. Usually, high conductivity leads to small fiber diameters.
	Dipolar momentum/dielectric constant	A high dielectric constant of the solvent usually leads to good results in the electrospinning process.
II	*Flow rate*	The higher the flow rate is, the bigger the fiber diameter will be. Typical flow rates go from 0.5 to 10 mL/h.
	Electric potential	The more intense the electric field is the thinner the fibers will be The electric potential should be between 0 kV and 50 kV for the electrospinning process.
	Needle-collector distance	There are a min/max distance to form fibers and avoid the formation of drops or agglomerates. The usual range is between 5 and 30 cm.
	Collector type	The fiber geometry would vary depending on how the collector rotate or move and also of the disposition (e.g. horizontal or vertical) when a static collector is employed.
III	*Ambient parameters*	A low temperature means a high viscosity of the solution and therefore a big diameter fiber. As the relative humidity increases, the solidification process becomes slower, allowing elongation of the charged jet to continue longer and thereby to form thinner fibers.

Table 2. 1: Effects of the processing parameters in the electrospinning technique.

In order to be able to characterize the fibers there are three aspects to take into account when obtaining the optimal parameters [50].

- The surface fiber should not present defects such as bead formation.
- The fiber diameter should be representative and tunable.
- It should be possible to obtain isolated fiber without agglomerates for later studies.

2.5.5. - General applications

The application of the electrospinning is really broad. However taking into account the existing patents it must be said that approximately around the 66% of the applications are related with Medicine. The following list briefly presents the different singular applications depending on the field of use:

- Nanosensors
  - Thermal sensor
  - Piezoelectric sensor
  - Biochemical sensor
- Filters
  - Liquid filtration
  - Gas filtration
- Biomedical applications
  - Drug delivery
  - Hemostatic devices
  - Wound protection
- Skin mask
  - Cleaning
  - Healing
  - Medical therapy
- Protective clothes
  - Air zero impedance
  - Aerosol particle trapping efficiency
  - Anti-biochemical gases
- Tissue engineering
  - Porous scaffolds for the skin
  - Stents for veins and nerve regeneration
  - 3D structures for the bone and cartilage regeneration

- Other industrial applications
    - Nano/micro electronic devices
    - Electrostatic dissipation
    - Magnetic interference protection
    - Photovoltaic devices
    - LCD devices
    - Ultralightweight materials for aerospace industry
    - High efficiency and functionality catalyzers

2.5.6. - Biomedical applications

As mentioned previously, medicine is the field where electrospinning has more applications and, consequently, where more studies are carried out. The main explanation of this is that most of the human tissues are made up of nanofibers with a really high hierarchy as it happens in bones, cartilage, collagen or skin. [55]. On the following paragraphs the more common applications are presented:

- Medical prosthesis: this is the field where the highest number of studies have been done on the application of the electrospinning. The reason is that the mat obtained is suitable for any application where a soft tissue is needed. There are many different patents for applications such as veins, breast or vascular. These films could also be used as a coating to prevent the failure of the prosthesis. [56]–[58].

- Wound protection: wound could be healed with the help of a thin polymeric film. As the film is made of nanofibers it enhances the skin growth and hence avoids the scar apparition. This method is limited because the bone and the skin do not require the same type of fibers [59], [60].

- Scaffold for human tissue growing: this is probably, within the biomaterial field, the use where more future applications are expected. There are designs that try to imitate the extra cellular matrix and also to reproduce the structures as well as the biological functions. Hereafter, it is necessary that the fibers have lower fiber diameter than the cell diameter in order to enhance cell adhesion. [61]. The study around this topic has become more interesting for many researchers during the last years [59], [60].

- Drug delivery: how a drug acts inside the human body depends on its physical properties (e.g. solubility, partition or charge coefficient). Hence some drugs could act over non targeted tissues. Furthermore, it is possible that they are out of their therapeutic interval, or can even act in a non-desired way or have adverse effects [62], [63].

To avoid this, at the moment, drug delivery is carried out with some other substances that empower its action. Most of the times these are polymeric substances. There are two key methodologies to optimize the drug action:

- Modified release: it tries to dissipate or completely remove the secondary effects producing an optimal therapeutic concentration for the organism. Regularly, the main aim is to obtain a zero order releasing kinetic. This means that there are no drug concentration changes in the organism.

- Targeted release: it focuses on the drug to reach the target, ensuring thus the release in the required place at the same time that the drug is inactive somewhere else in the body.

The design of the drug delivery describes diverse types of response depending on the releasing rate or type, for instance can be constant or by impulses. Normally, the body drug absorption is better when the medicine is small and covered by a thin layer. In drug delivery there is a general rule which says that the greater the surface of the drug and its structure is the faster the dissolution velocity will be. Taking into account the nanofibers-drug link, the drug delivery could be performed in diverse ways [58].

- Drug particles are incorporated on the surface of the nanofibers which act as the matrix.
- Either the drug or the matrix are presented as nanofibers and the final product is presented as an interwoven mat.
- Drug and polymer mixture results in one single fiber.
- The matrix is formed in a kind of tubular way and the drug becomes trapped inside of these tubes.

CHAPTER III: OBJECTIVES

3.1. - General objectives

The present project has been developed having as a general purpose the preparation of PLA scaffolds that incorporate arginine or a polymer based on the arginine. These mats of microfibers are produced by the electrospinning process and are able to adsorb bacteriophages due to the cationic nature of the arginine units.

3.2. - Specific objectives

The following specific objectives are stablished on purpose of achieving the general objective of the project:

1. The establishment of the optimal conditions to prepare PLA electrospun fibers that incorporate the selected arginine compounds. Typically the solvents are optimized as well as the electrospinning operational parameters (e.g. collector distance, flow rate or voltage).

2. The characterization of the compounds (pure arginine and arginine based polymers) and the drug (PHMB) through the use of FTIR and NMR spectroscopies, DSC and TGA calorimetric analyses, and X-ray analysis. Additionally, molecular weight determination by GPC of the Arg-based polymers.

3. The morphologic characterization of the fibers obtained under the optimal conditions. Morphology is evaluated by SEM observation and diameters measured by further analyses.

4. To evaluate the hydrophobicity of the electrospun mats with all the range of solutions.

5. To prove the incorporation of PHMB and the different arginine containing compounds by FTIR and NRM spectroscopies..

6. To see the influence of the arginine compounds and PHMB in the thermal properties of the produced mats by DSC and TGA analysis.

7. To load the scaffolds with bacteriophages and analyze the antibacterial activity in comparison with PHMB loaded samples.

8. To tests the biocompatibility of the manufactured scaffolds.

9. The potential application of the PLA mats loaded with bacteriophages as temporary scaffolds for medical applications should be determined.

CHAPTER IV: MATERIALS AND METHODS

4.1. - Chemical products

The PLA used in this research is PLA 4032D from Natureworks® with 98% L-lactic isomer content.

L-Arginine (reagent grade ≥ 98%) purchased from Sigma-Aldrich.

The lyophilized PHMB is obtained from B. Braun Surgical S.A.

The bacteriophages are purchased to JSC BIOCHIMPFARM and had a minimum concentration of 10^5 phages per mL.

Different types of arginine-based and biodegradable poly(ester amide) (PEA), poly(ester urethane) (PEUR) and poly(ether ester urethane)s (PEEUR) are courtesy provided by Prof. *Ramaz Katsarava* from the Institute of Chemistry and Molecular Engineering of the Agricultural University of Georgia. This polymers are named as depicted in the following table for ease of use. The structural formulae and synthesis schemes are given in the following figures in order to understand the composition of each polymer. Note that synthesis is performed following a two-step process. The first one involved the preparation of a monomer containing the amino acid units whereas the second one correspond to the polymerization with a diacyl derivative.

Name	Polymer
PEA	Arg-HD-Arg-Se
PEUR	Arg-PD-Arg-EG
PEEUR-1	Arg-EG-Arg-EG_2
PEEUR-2	Arg-PD-Arg-EG_2
PEEUR-3	Arg-EG_2-Arg-EG_2
PEEUR-4	Arg-EG_4-Arg-EG_2

Table 4. 1: Arginine based polymers designation.

It should be pointed out that for PEEUR-1 and PEEUR-2 the ether bond is only present in the diacyl unit. However, in the PEEUR-3 and PEEUR-4, the ether is present in both the diol and diacyl unit.

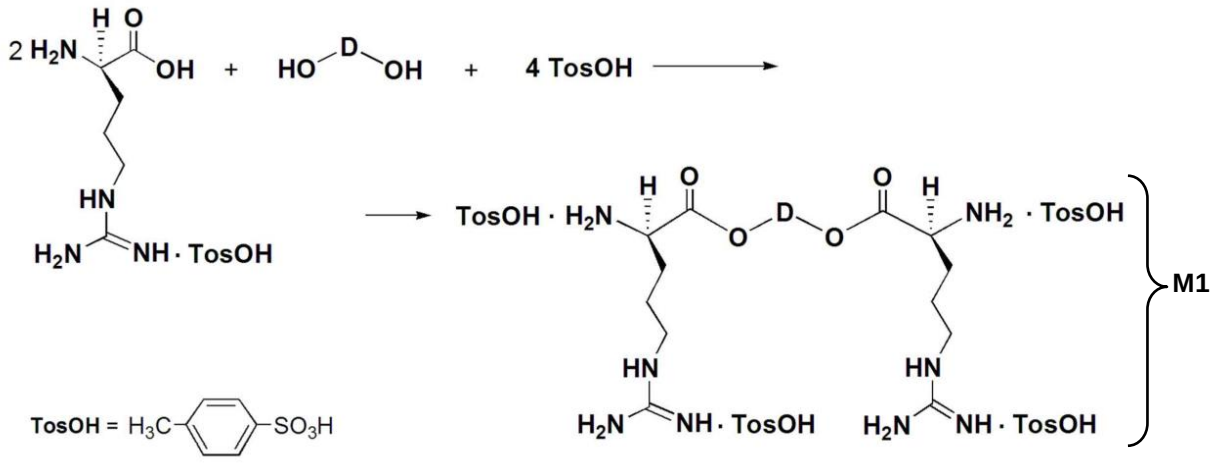

Figure 4. 1: "Scheme 1": The first step of synthesis of the Arg-based polymers: Synthesis of the monomers M1.

Where D has different assignations:

- D: -$(CH_2)_2$- →Coming from ethylene glycol (EG)
- D: -$(CH_2)_3$- →Coming from 1,3-propanediol (PD)
- D: -$(CH_2)_6$- →Coming from 1,6-Hexanediol (HD)
- D: -$(CH_2)_2$-O-$(CH_2)_2$- →Coming from diethylene glycol (EG_2)
- D: -$(CH_2)_2$-[O-$(CH_2)_2$]$_3$- →Coming from tetraethylene glycol (EG_4)

The followed process to obtain monomer M1 is described as explained in the supporting information of the article published by Memanishvili *et al* [17]:

"Typically, L-arginine (17.42 g, 0.1 mol), a diol (0.05 mol), *p*-toluenesulfonic acid monohydrate (38.1 g, 0.2 mol) and 270 mL of benzene are placed in a flask equipped with a Dean–Stark apparatus and a stirrer. The heterogeneous reaction mixture is refluxed for 24 h until 5.4 mL (0.3 mol) of water evolved.

The reaction mixture is then cooled to room temperature, benzene is decanted and a new portion of benzene (160 mL) is added to a viscous, tar-like mass obtained and refluxed again for 4 h, cooled to room temperature and left overnight. Benzene is decanted, the product is dried at r.t. in a vacuum and purified by reprecipitation from isopropanol solution into dry ethyl acetate for three times. The dried product is dissolved in 250 mL of hot isopropanol, filtered and 300 mL of dry ethyl acetate is added to the solution, the vessel with the precipitated white sticky mass is finally stored at 4 °C overnight.

Next day, the mixture of solvents is decanted and the reprecipitation procedure is repeated twice. The products are dried in a vacuum at 50 °C up to constant weight. White hygroscopic powders are obtained. The basic characteristics (yields, melting points) of M1 are summarized in Table 4. 2."

M1	**Empirical formula (Molecular weight, g/mol))**	**Yield (%)**	**Melting point [°C]**
Arg-EG-Arg	$C_{42}H_{62}N_8O_{16}S_4$ (1063.28)	70	66-69
Arg-PD-Arg	$C_{43}H_{64}N_8O_{16}S_4$ (1077.31)	75	67-71
Arg-HD-Arg	$C_{46}H_{70}N_8O_{16}S_4$ (1119.39)	71	73-76
Arg-EG_2-Arg	$C_{44}H_{66}N_8O_{17}S_4$ (1107.33)	63	72-75
Arg-EG_4Arg	$C_{48}H_{74}N_8O_{19}S_4$ (1195.45)	65	61-64

Table 4. 2: Basic characteristics of the monomer M1.

Monomer M1 has been reacted with different active diesters. Specifically, those derived from N-hydroxysuccinimide, indicated as the group Z in scheme 2.

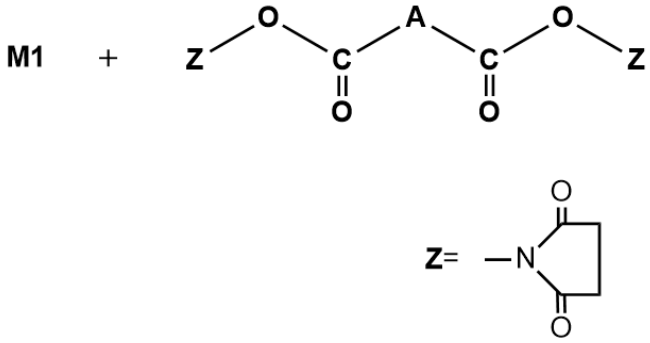

Figure 4. 2: "Scheme 2": Second step for the Arg-based polymer syntheses.

Where A could be:

- A: O-$(CH_2)_2$-O →Coming from etthylene glycol (EG)
- A: O-$(CH_2)_2$-O-$(CH_2)_2$-O →Coming from diethylene glycol (EG_2)
- A: -$(CH_2)_8$- →Coming from sebacic acid (Se)

The selected polymers are synthesized by polycondensation of arginine containing monomer M1 (1.0 mol), with activated diesters (1.0 mol) using Triethanolamine (TEA) (slight excess, 2.2 mol) as a *p*-toluenesulfonic acid acceptor. The reactions are carried out in DMSO.

The reaction mixture is stirred at 50-60 °C for 24 h. The obtained viscous solution is cooled to r.t., diluted with 8 mL of DMSO and poured drop-wise into dried acetone where the polymer precipitated as a gum-like sticky mass. The liquid phase (DMSO + acetone) is decanted and the obtained polymer washed for several times with fresh portions of chilled acetone. Then, 100 mL of dry acetone is added and refluxed for 2-3 h to remove low-molecular-weight fractions and impurities. The polymer is dried at 40-50 °C in a vacuum up to constant weight.

4.2. - Electrospinning

The following graph describes the display of the equipment used for the electrospinning process:

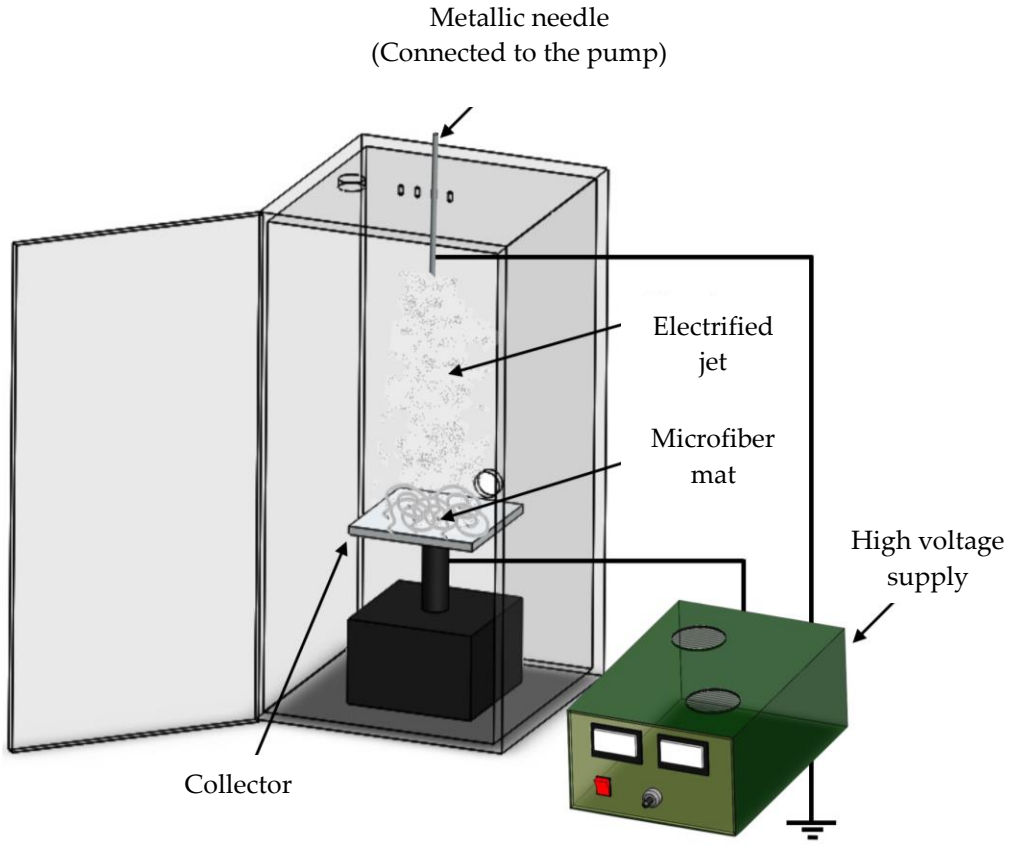

Figure 4. 3: Scheme of the electrospinning setup.

The electrospinning device is composed by the following elements:

- Collector: is the electric component where the fibers are accumulated. It could be adjusted in height and also changed in position inside the protective box. It is connected to one of the electrodes in order to produce the electric field. Due to the high voltage required the use of the security box is completely necessary.

- High voltage supply: is the device that produces the difference of potential between the needle and the collector that promotes the fiber formation and its deposition on the collector. The device is a *Gamma High Voltage Research* and could provide a voltage from 0 to 30 kV and an intensity from 0 to 750 mA.

- Pump: the electronic device which allows dosing and regulating the injection of the polymer solution to the needle at a constant rate defined by the user. The injection pump used is *Kd Scientific 120* of 230 V and 50/60 Hz.

- Syringe: is the place where the polymer is stored. It should be inert and do not cause anything to the nature of the contained polymer.

- Needle: part of the set-up where the solution flows. It is connected to the other electrode of the power supply device. It should be blunt in order to facilitate the creation of the Taylor's cone.

- Other required elements:
    - Aluminum film covering the collector to accumulate the electrospun fibers.
    - Coverslips and specimen holders to collect a small amount of fibers.
    - Optical microscope necessary to evaluate the quality of the produced fibers which are collected in the coverslips.

The polymer solution is prepared the day before at the desired concentration. Then, the solution is placed overnight in the orbital chamber at 37 °C. A plastic syringe of 10 mL is filled with the polymer solution and then electrospinning is carried out between the needle (18G) connected to the anode and the static

collector connected to the cathode. The direct current (DC voltage) is applied using a high voltage supply (ES30-5W model, Gamma High Voltage Research, USA). The flow is controlled using a KD120 infusion syringe pump (KD Scientific Inc., USA). The polymer jet is collected on an aluminum foil until a mat of 1gram is obtained. All electrospinning procedures are conducted at room temperature.

4.3. - Morphology and fiber diameter

Optical microscope uses light to create an augmented image. The simplest one, is the double convex image with a short focal distance. This kind of lenses could reach a magnification up to 15 times. Compound microscopes are the most used ones, these have diverse lenses available and therefore they could reach magnifications up to 2000X.

Compound microscope is made up of two lenses systems: the objective, and the eyepiece mounted in a close tube. Microscope lenses are arranged to have the objective in the focal point of the eyepiece. When looking through the eyepiece it is possible to see an augmented virtual image of the real image. The total magnification of the microscope depends on the distance between the lenses system. In this research 20X and 40X objectives are used. Morphological observations are carried out with a *Zeiss Axioskop 40* and the micrographs are taken with the digital camera *Zeiss AxiosCam MRc5.*

Figure 4. 4: Camera equipped optical microscope.

With the optical microscope it is easy to set the optimal parameters for the electrospinning process. For that, some fibers are collected in the coverslip which is placed in a specimen holder and afterwards observed in the optical

microscope. However, this process is inefficient to make a study of the fibers diameter because the light produces dispersion on the fibers and creates shadows. This involves an inaccurate measurement of the diameter. For that reason SEM observation is carried out for all the produced mats.

Electron microscopy is based on the usage of an electron beam in order to get images with a very high magnification. As the electrons travel much faster than the light, they have much more resolving power. Basically there are two types of electron microscopes depending on which phenomenon must be captured during the electron bombardment, the transmission electron microscope (TEM) and the scanning electron microscope (SEM).

In TEM observation the sample is trespassed by the electron beam and the internal structure is imaged. In the TEM, the objective lens physically performs the image formation thought:

- A Fourier transform analysis, which creates in the back focal plane of the objective lens the diffraction pattern of the object.
- An inverse Fourier transform which makes a real space image in the image plane with the interference of the diffracted beams.

Therefore the selection of the focus and the beams that pass through the objective's aperture is a critical point to be fitted in the TEM image formation.

Samples for TEM observation need to be prepared accordingly the following protocol:

- First of all, the grids need to be prepared with a plastic film. The grids are cleaned and with collodion, a thin plastic layer at the water/air surface is formed. Then, the grids are dried in paper taking into account that the water should not be dried so fast to avoid wrinkles.

- After that, a carbon coating is carried out on the grids after the thin film is formed. When the desired thickness is achieved the coating should be finished.

- A uranyl formate solution is prepared for negative stain electron microscopy. Two (20 μL) drops of the solution and two (25 μL) of distilled water are deposited on a piece of parafilm

- A glow-discharged grid is hold by an anti-capillary reverse forceps. 2 μL of the phage solution is applied to the glow discharged grid. After waiting for 30 seconds the sample is dried using filter paper. Then, the grid surface should touch the water drop. This process should be repeated with the second water drop. The surface grid must touch the stain solution briefly and be dried with the filter paper. Finally, the grid surface should touch the second drop of the stain solution for 20 seconds, and later the filter paper be dried with vacuum.

After the sample preparation, the TEM observation is carried out with a Philips TECNAI 10 at an accelerating voltage of 100 kV.

When the specimen is observed by SEM the image comes from the diffracted electron. Many different phenomenon occur when matter is bombarded with electrons. Within the phenomenon that can be captured by the SEM the most important are the backscattered electrons and the secondary electrons. The backscattered electrons are the electrons which come from the primary beam whose trajectory has been modified by the collision with atoms of the sample. The secondary electrons are produced by an inelastic interaction. Before the electron leaves the outermost part of the sample it leaves behind an ionized atom with positive charge. These electrons have low energy due to this easy attraction and thus, are easily detected in the images.

Some of the most meaningful properties of this kind of microscopy are:

- Three dimensional appearance of the images.
- Ease to focus.
- Easy sample preparation.

The device used for this study is a *Focus Ion Beam Zeiss Neon 40 instrument (Carl Zeiss, Germany)*. Sample preparation consists on applying a conductive layer. Samples are coated with a thin carbon film of around 5-7 nm thickness with a *Balzers SCD-004 Sputter-coater*. This coating prevents the electric charge formation in the sample due to the low conductivity of the polymer and the interaction of this charge with the incident ion beam. If this happens the images would become distorted. For that reason, this coating is essential for an optimal image acquisition. Moreover, this coating works as a protection since all polymers tend to melt when exposed to high voltage ion beams.

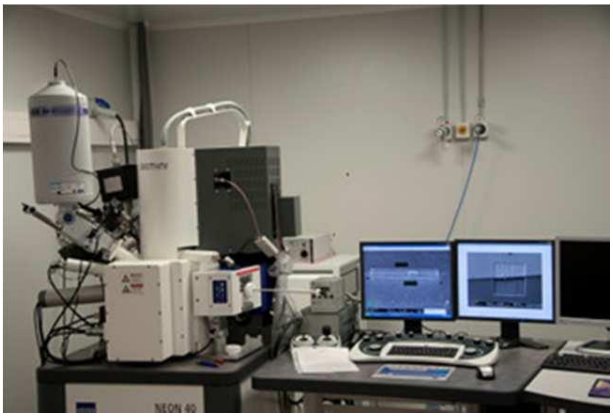

Figure 4. 5: Focus Ion Beam microscope used during the research.

4.4. - Infrared analysis

Infrared analysis allows to develop a qualitatively study of a polymer and determine its functional groups. The IR is a physicochemical technique based on the molecular vibration modes of excitement.

At higher temperatures than absolute zero, the chemical bonds between atoms are vibrating. This vibration could be of two types: stress or bending. Stretching vibrations produce a continuous interatomic distance change along the axis of the bond of two atoms. Bending vibrations suppose a change in the angle between the bonds. Within bending vibration it could be distinguish: scissoring, wagging, rocking and twisting. Furthermore, some vibrations (e.g. stretching vibration) could be symmetrical or asymmetrical (Figure 4. 6).

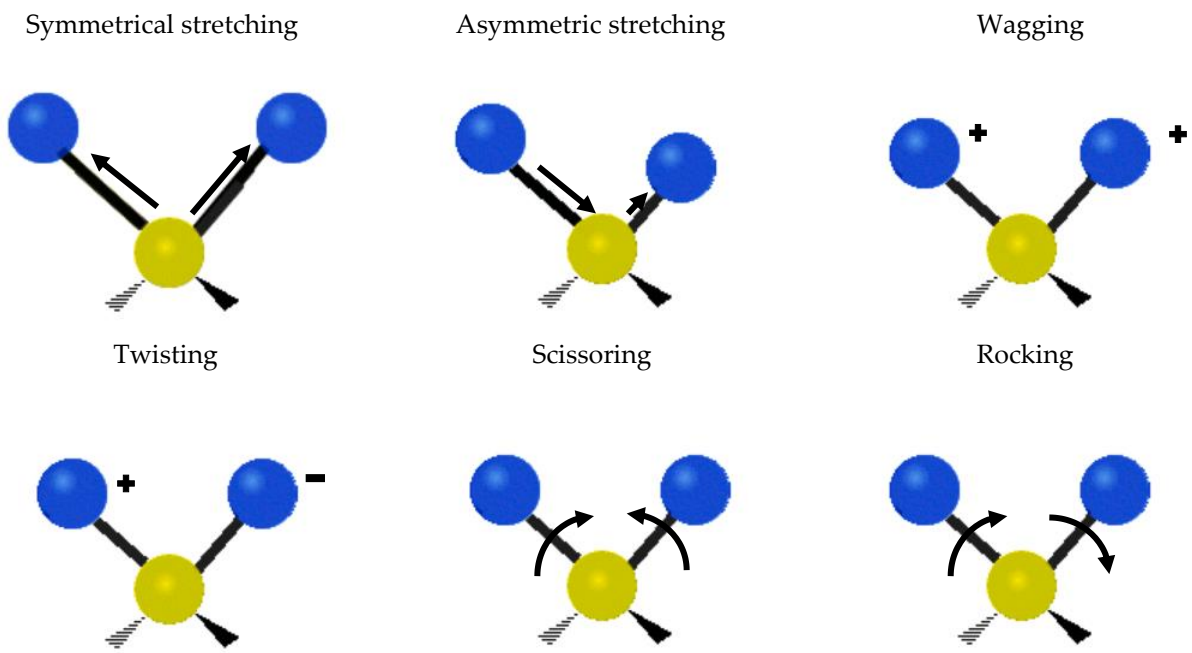

Figure 4. 6: Vibrational modes of molecules.

When any of these changes occur, a peak in the absorption spectra appears. IR light is in the same vibrating frequency as the bonds of the analyzed molecule. Thus, when an IR radiation is applied it absorbs all the frequencies that are the same as the bond frequency vibrations. Consequently, when an organic compound interacts with the IR radiation the chemical bonds suffer an excitation which results on an energy absorption of the specific wavelength for each bond.

In conclusion, the IR spectra of a material is just a graphic representation of the absorption that happens in the infrared region which depends on the radiation frequency. To be able to quantify the amount of absorbed radiation the transmittance is determined (T %). The functional group identification is carried out taking into account that each one has a characteristic absorption for a specific wavelength.

The existing spectrophotometers could be classified into two main groups. There are double beam spectrophotometers which analyze the different absorbed wavelengths and compare them with a reference, air usually. The differences between the two beams are represented through a peak or transmission band at a determined wavelength. The Fourier transform infrared spectrophotometers produce the incidence of the whole wavelength spectra in the sample several times. To obtain the spectra the transmitted radiation is collected as an

interference signal (interferogram) and the Fourier transform operation is applied.

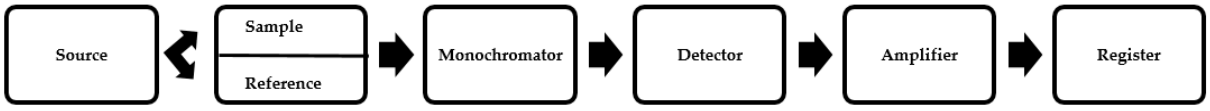

Figure 4. 7: Double beam spectrometer.

Figure 4. 8: Fourier transform infrared spectrometer.

For this study, the spectrophotometer used is a Fourier transform *Jasco FTIR 4100* which is able to operate in the range of 500-4000 cm^{-1}. A *Specac model MKII Golden Gate* attenuated total reflection (ATR) equipment with a heated Diamond ATR Top-Plate is also used. As all the samples to be tested are solid, a thin layer of the material is pressed in the window of the equipment in order to avoid the air accumulation that could lead to distorted results.

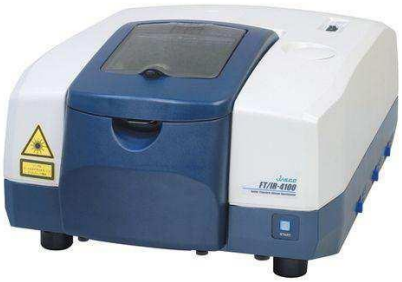

Figure 4. 9: *Jasco FTIR 4100.*

4.5. -Thermal analysis

Thermal gravimetric analysis (TGA) is a method of thermal analysis based on the physic or chemical changes of the tested material that occur during a heating process (dynamic analysis) or while it is submitted at a determined temperature (static analysis). These changes are measured in a dynamic analysis as a function of the increasing temperature while the sample is heated at a constant rate. This

analysis provides information about physical or chemical changes that happen in the sample such as for instance vaporization, second-order phase transformations, dehydration or decomposition. TGA is a method commonly used to determine the mass gain or loss due to decomposition, oxidation or loss of volatiles.

The degradation of some samples is studied at a heating rate of 20 °C/min with around 5 mg in a *Q50 thermogravimetric analyzer (TA Instruments)* in a range of temperatures from 30 °C to 600 °C.

The dynamic scanning calorimetry (DSC) is a technique to determine the heat flow of a material when its temperature becomes modified. As the heat flow is related with the physical or chemical changes of a substance this thermoanalytical technique allows to know the characteristic temperatures associated to the indicated changes. At the same time, it allows to quantify the amount of energy released or absorbed in these changes.

The sample pan and the reference pan (empty) are at the same temperature over the experiment. The fundamental is that when the sample suffers a physical change, such as a phase transformation, more heat flow will be needed in order to maintain both at the same temperature. Depending on the type of process, exothermic or endothermic, the sample needs more or less heat flow. For example, if a solid sample is melting it will take more heat flow to raise its temperature at the same rate than the empty pan. This is due to the heat absorption of the sample during the phase transformation from solid to liquid. On the contrary, if the sample experiment exothermic processes, such as crystallization, less heat will be needed to reach the desired temperature. For a polymeric material, the thermal transitions that could appear in a thermogram are: glass transition temperature (T_g), crystallization temperature (T_c) and melting temperature (T_m).

The glass transition and the melting temperature are visible when the temperature of a semicrystalline sample is increased and are associated to the amorphous and crystalline phases, respectively. The glass transition is presented as a step on the baseline of the registered DSC signal. What happens there is that the sample is only undergoing a change on its heat capacity due to the increased mobility of the polymeric chains.

When the temperature is increased, the amorphous solid would become less viscous. At some times, the molecules would have enough freedom to be

crystalline arranged by their own. This is expressed as a cold crystallization process and a crystallization temperature. This transformation from amorphous to crystalline is presented as an exothermic peak on the DSC curve. At higher temperatures the sample could reach the melting temperature if it is initially crystalline or if a cold crystallization process took place. This process is evidenced by extra exothermic peak in the DSC trace. The ability to determine these temperatures as well as the enthalpies of the processes makes the DSC an essential tool for the analysis of thermal processes.

Figure 4. 10: DSC *Q100 (TA Instruments)*.

All thermal analysis are carried out with a DSC *Q100 (TA Instruments)* equipped with a refrigerated cooling system. Experiments are conducted under a flow of dry nitrogen with a sample weight of approximately 5 mg. The calibration of the equipment is performed with indium.

4.6. - Nuclear magnetic resonance

Nuclear magnetic resonance is usually employed to complement the information obtained through IR analysis and therefore verify the chemical information of the molecule and the bonding disposition. Moreover, it allows determining terminal groups associated to the low molecular mass. This technique let the user to know the evolution of a determined reaction as for example if the polymerization reaction has finished.

The fundament is based on the determination of the absorption/emission at certain frequencies of electromagnetic radiation. The energy absorption is associated to an orientation change of the nuclear magnetic moment (nuclear spin) and is consequently characteristic of each type of nucleus. The external magnetic field causes a difference of energy between nuclei that are oriented parallel or antiparallel respect to this field. Absorption of electromagnetic energy allows to promote nuclei to an antiparallel orientation, while the radiation is subsequently emitted when nuclei come back to the low energy parallel orientation. These processes are carried out at atomic scale, and the energy emitted is quantified with specific values for magnetic forces and electromagnetic radiation frequencies. But not all nuclei are sensitive to the electric field application. For that reason in this research the analysis is made based on the ^{1}H nucleus.

In the ^{1}H-NMR spectra the hydrogen nuclei are differentiated according to the electronic environment (i.e. the electronegativity of atoms directly linked to the hydrogen atoms). As a consequence, protons can absorb/emit radiation at slightly different frequencies. A NMR spectra provide information about the chemical structure that involves the hydrogen atoms of the material studied. In the graph the following characteristics are examined:

- Number of signals: they correspond to the different types of hydrogens that each compound has.

- Relative area of the peaks (signals): the intensity of peaks is proportional to the number of hydrogens that are involved in the signal. These areas are important to corroborate the final formula and also to perform quantitative analyses.

- Signal coupling: it is the phenomenon produced by the magnetic influence of the hydrogens present in the adjacent atoms. This fact make that each peak in n+1 peaks signals, where n is the number of chemically equivalent protons linked to neighboring atoms. Hereby, it could appear triplets when there are two neighboring protons or quadruplets when there are three, etc. If the observed nucleus has neighboring protons different each other the coupling of both are multiplied.

For the spectra measurements, around 20 mg are dissolved in $CDCL_3$ and analyzed in the spectrometer. The equipment used for this research is a Fourier transform *Bruker AMX-300* working at 300.13 MHz.

4.7. - Synchrotron radiation

The electromagnetic radiation emitted by high speed electrons spiraling along the force lines of a magnetic field is called synchrotron radiation. Depending on some factors such as the energy of the electrons or the strength of the magnetic field the maximum intensity is presented as radio waves, visible light or X-rays. As the radiation is highly polarized and the intensity exceed significantly other sources the synchrotron radiation is a potent tool for all investigation fields.

For this project either small or wide angle X-ray diffraction (SAXS/WAXD) is used. With these techniques is possible to study the dynamics as well as the structure of the target material. Simultaneous SAXS/WAXD experiments allow investigating structural changes in real time. Two position-sensitive detectors are placed in different locations covering a wide angular range during the experiment. The scheme of the experimental setup is presented in Figure 4. 11. With the SAXS it is possible to detect heterogeneities in the electron density on a large scale, while with the WAXD it is possible to get information about the molecular and atomic ordering of the analyzed materials.

The collected data is processed differently depending on the diffraction angle. For WAXD the deconvolution is performed and hereby the crystallinity and the morphology is obtained. The software used to treat the data acquired from SAXS experiments is CORFUNC in order to perform a correlation function analysis. This correlation function allows getting morphological parameters such as the thicknesses of the amorphous and crystalline lamellar layers.

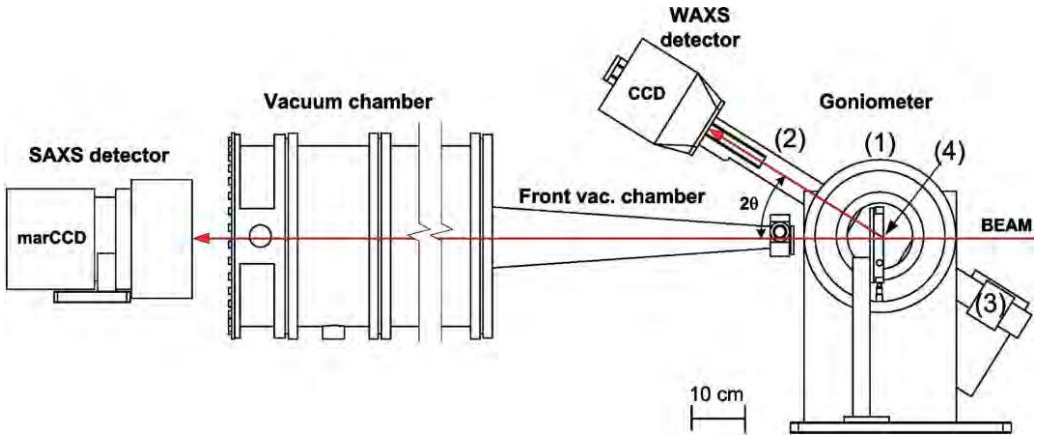

Figure 4. 11: Scheme of the experimental setup for simultaneous SAXS/WAXS experiments performed at the NCD beam line of synchrotron ALBA. The main parts of the goniometer are rotation unit (1), arm (2), counterweight (3), and hot stage (4). The vacuum chamber is made of cylindrical parts of different lengths and a square based truncated pyramid at the front [64].

The X-ray diffraction is based on the interaction of the electromagnetic radiation, which has a wavelength of around 10^{-7} and 10^{-11}, with materials with a certain order on its crystalline structure. Bragg studied this phenomenon and developed and equation which relates the crystallographic planes and the diffraction angle of the radiation.

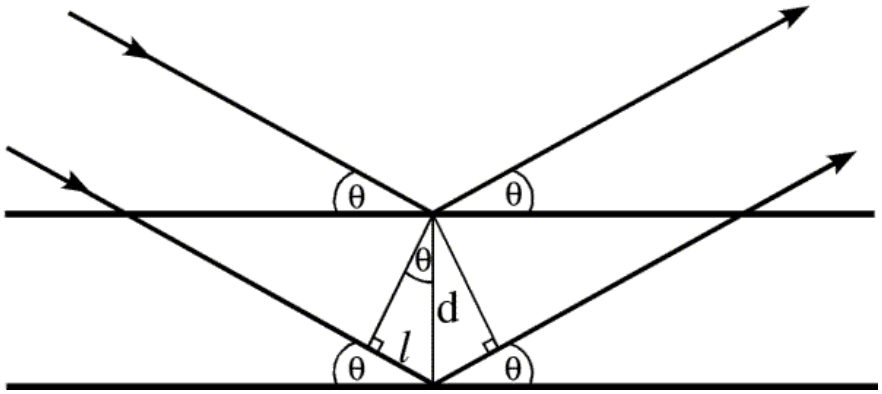

Figure 4. 12: Representative scheme of the different parameters that interfere in the Bragg's law.

The equation of the denominated Bragg's law is described as follows:

$$\lambda = 2 \cdot d_{hkl} \cdot sin(\theta)$$

where λ in the employed wavelength, d_{hkl} is the characteristic distance between Miller's planes of the crystal lattice with *hkl* indices. Finally, θ is the incident angle which is at the same time is the diffraction angle.

The X-ray diffraction of angles above 0.5° provides information about the lamellar crystal organization (SAXS). With higher angles than 2.5° (WAXD) it is possible to study the crystal lattice and the unitary cell from which it is formed. It is possible also to explain Bragg's law as a function of the dispersion vector. Its module is used to generate the temperature profiles. The WAXD profiles are recorded every 20 seconds with a heating rate of 10°C/min. The equipment used for this study is the particle accelerator *ALBA* from Parc Tecnològic del Vallès.

4.8. - Gel permeation chromatography

Gel permeation chromatography is a powerful separation technique which finds a great application in polymer science field around the sixties [65]. Nowadays

this method is commonly used for the separation of different analytes of polymer samples depending on their molecular sizes. It is a type of size exclusion chromatography. It uses the different penetrations of the macromolecules through the pores of a gel hosted in the chromatographic column. The usual materials that are hosted in the column are cross linked polystyrene and porous glass.

The chromatograph is of the same kind as the one used in the high efficiency liquid chromatography, being thus the column and the detector the two most important parts of the device. When a polymeric solution with different molecular weight distribution is forced to flow through the GPC column, a splitting of the different molecular weights occur. The molecules with greater size need less time to flow through the column because they are dragged with the solvent. On the contrary, the small analytes can enter in the pores more easily and therefore the retention time becomes larger. At the outlet of the column the variation of the refraction index of the pure solvent compared to the collected fraction is registered. To know the molecular weigth values is necessary to have calibration patterns. For this study the measurements are realized with the chromatograph *Waters model 510* equipped with columns of 10000 y 1000 Å *μ-Stiragel (Polymer Lab.)* of styrene-divinilbenzene thermostatically controlled at 35 ºC, with a refraction index detector (*RI 410*). The data obtained are treated with *Maxima 820* software. The calibration is carried out with low dispersion polystyrene. The eluent is 1,1,1,3,3,3-hexaflouroisopropanol. The flow rate is 0.5 mL/min and the total volume injected is 100 μL with a sample concentration of 2 mg/mL.

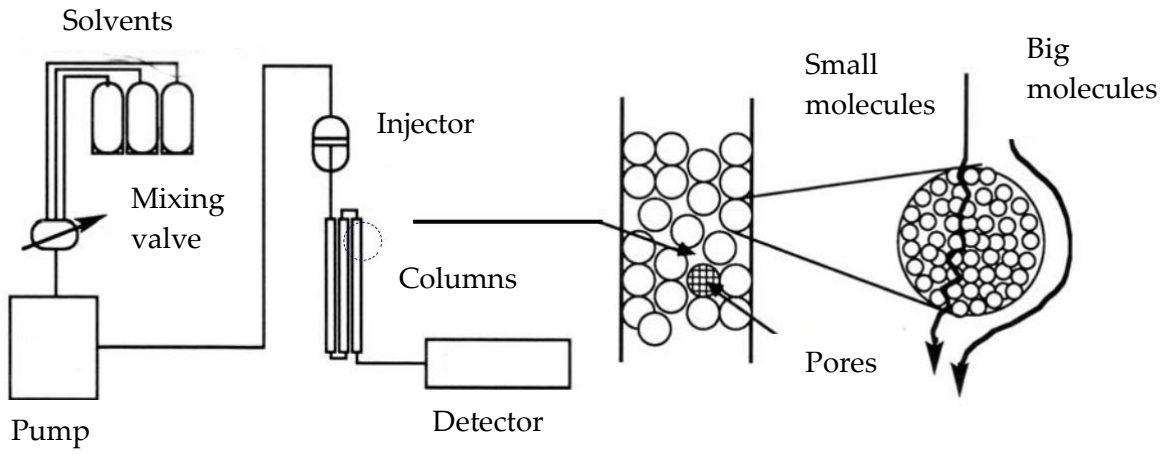

Figure 4. 13: Scheme of the GPC equipment and separation of molecular sizes.

4.9. - Contact angle

The equilibrium contact angle (solid/liquid/vapor) is typically used on interfacial analysis and it is generally considered as one of the most sensitive methods to provide information of the outer molecular layers. Contact angles are measured by the analysis of the shape of a drop. For this technique two hypotheses need to be considered:

- The drop is completely symmetric respect a vertical axis, being thus irrelevant the direction from where it is observed.
- The drop is stable and is not in movement making therefore viscosity and inertia two negligible factors. Hence the only forces that affect the drop shape are gravity and the interface tension.

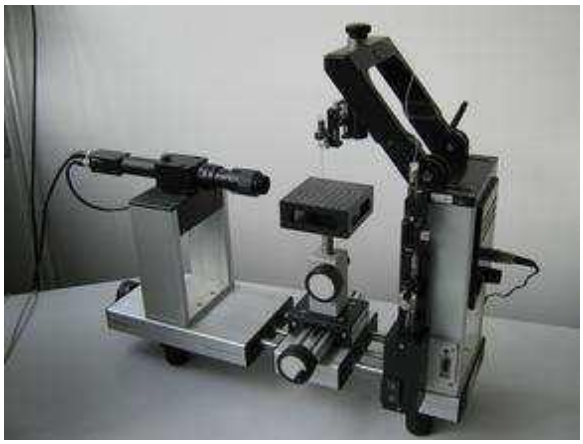

Figure 4. 14: Contact angle equipment used for measurements.

Contact angles are measured adjusting a mathematical expression to the shape of the drop and then calculating the angle between the tangent to the drop shape and the baseline previously determined.

Contact angles are measured at room temperature with sessile drops using an *OCA-15 PLUS Contact Angle Microscope (Dataphysics, USA)* and *SCA20* software. Contact angle values of the right and left sides of distilled water drops are measured and averaged. Measurements are performed 10 s after the drop (0.5 μL) is deposited on the sample surface. All CA data are an average of 15 measurements on different surface locations.

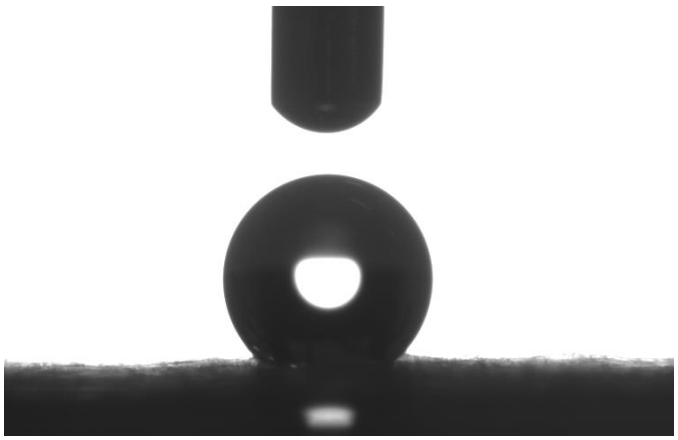

Figure 4. 15: Water drop dispensation in a sample.

4.10. - Bacterial culture growth inhibition

An assay in plate using the soft-agar overlay technique was performed in order to evaluate the potential antimicrobial capacity against *Staphylococcus aureus* of the manufactured polymeric scaffolds loaded with bacteriophages.

4.10.1. - Media preparation and bacterial strain

Brain-hearth infusion agar (BHI agar) and brain-hearth infusion broth (BHI) were each prepared by dissolving 37 g of BHI in powder form (Scharlab) in 1 L of distilled water. The medium was sterilized by an autoclave cycle at 121 ºC during 30 minutes. The infusion broth powder (BHI) is composed by the following formulation:

- Brain extract (12.5 g/L)
- Hearth extract (5 g/L)
- Dextrose (2 g/L)
- Peptone (10 g/L)
- Sodium chloride (5 g/L)
- Disodium phosphate (12.5 g/L)

The final pH was adjusted to 7.2-7.4 (by adding HCl or NaOH solutions) prior to perform the autoclave cycle. To prepare BHI agar, 15 g/L of bacteriological agar was added in the previously indicated medium. On the other hand, semisolid

BHI agar (BHI soft-agar) was made by dissolving the BHI medium (37 g) and the bacteriological agar (7 g) in 1 L of distilled water.

Staphylococcus aureus bacteria (*S.aureus*) ATCC# 25923 (The American Type Culture Collection (ATCC), Rockville, MD, USA) were used as bacterial host for bacteriophage.

4.10.2. - Bacteriophage

Commercial bacteriophage (Phagestaph™, JSC Biochimpharm, Tbilisi, Republic of Georgia) for medicinal use was applied in the experiments. This is a sterile liquid preparation for oral administration, local and external use. The preparation is a mixture of sterile filtrates of bacterial phagelysates of *S.aureus*, and 1 mL of the preparation contains *S.aureus* bacteria specific phages (*bacteriophagum Staphylococcus aureus*) not less than 10^5 pfu.

4.10.3. - Plaque assay of soft-agar overlay

The bacterial host for bacteriophage was grown by seeding 100 μL of *S.aureus* in 5 mL of BHI broth at 37 ºC overnight under orbital shaking (100 rpm). An aliquot of 100 μL of the overnight culture was then mixed with 100 μL of bacteriophage stock solution (10^5 pfu/mL). This mixture was incubated at 37 ºC for 30 min and was mixed with 4 mL of partially heated semisolid BHI soft-agar. The mixture was then poured onto a BHI agar plate and incubated at 37 ºC overnight. Bacteriophage growth was identified as a clear transparent plate in comparison with the cloudy control plate. This negative control was prepared in the same manner with 100 μL of *S.aureus* (bacterial host) without bacteriophage seeded onto the plate agar.

4.10.4. - Bacteriophage adsorption onto the fiber mats

For determination of the bacteriophage loading, 1x1x0.2 cm^3 pieces of scaffolds were prepared. Each mat was placed inside one eppendorf microtube and 1 mL of bacteriophage preparation was added. The microtubes were maintained at 37 ºC in an orbital shaker for 24 h to facilitate the bacteriophages adsorption. Then, the bacteriophage preparation was removed from microtube, and the mats were washed two times with 1 mL of sterile water, to remove the remaining liquid of the bacteriophage preparation as well as the non-specific bound compounds.

After washing, the scaffolds were air dried. Then, the scaffolds were placed again on clean eppendorfs with 500 μL of sodium chloride (0.9 %-*w*/*v*) overnight at 37 ºC and orbital shaked (100 rpm). The bacteriophages released in the sodium chloride were mixed with bacterial host and plated using the soft-agar overlay technique to determine the number of pfu formed. A negative control was prepared from mats without loaded bacteriophages. A positive control sample of bacteriophage mixed with only sodium chloride was used to normalize the data. The samples were assayed in triplicate.

4.11. - In-Vitro biocompatibility assays: cell adhesion and proliferation

Immortal cell culture (derived from tumors or cells transformed by viral elements) is a methodology that allows to have cells continuously. This cell cultures have some advantages, for instance, is not necessary neither the sacrifice of animals nor the cell isolation and purification. For this reason, first biocompatibility tests are performed using this kind of cells. The term *in-vitro* biocompatibility is applied when a material that not creates cell death by toxicity (cytotoxicity) behaves as a suitable medium for cell adhesion and proliferation.

Cellular adhesion and proliferation on electrospun scaffolds were determined with MDCK cells (Madin-Darby Canine Kidney, ATCC, Rockville, MD, USA). The MDCK cells is a cellular line of epithelial-like cells. These were cultured in Dulbecco's modified Eagle medium (DMEM) supplemented with 10% fetal bovine serum, 50 U/mL penicillin, 50 μg/mL streptomycin and 2 mM L-glutamine at 37 ºC in a humidified atmosphere with 5% CO2 and 95% air.

The culture medium was changed every two days and, for sub-culture, the cell monolayers were rinsed with phosphate buffer saline (PBS, pH 7.2) and detached by incubation with trypsin-EDTA (0.25 %) at 37 ºC for 2-5 min. Cell concentration was established by count with a Neubauer camera using 4% trypan-blue as dye vital. The detached cells with viability ≥ 95% were used for cultures the conditions for biocompatibility assays.

Electrospun samples were prepared by cutt-off square pieces of 1x1 cm^2 from mats collected (0.2 cm of thickness) on an aluminium foil. These samples were placed into the wells of a 24-well culture plate and sterilized by UV-radiation in a laminar flux cabinet for 15 min. To fix the samples in the well, a small drop of

silicone (Silbione® MED ADH 4300 RTV, Bluestar Silicones France SAS, Lyon, France) was used as adhesive. The samples were incubated with 1 mL of the culture medium in culture conditions for 30 min to equilibrate the material. Finally, the medium was aspired and the material was evaluated for cell adhesion and proliferation by exposing cells to direct contact with the material surface.

To assess cell adhesion, aliquots of 50-100 μL containing $5x10^4$ cells were seeded onto the electrospun samples in the wells. The plate was incubated in culture conditions for 30 min to allow cell attachment to the material surface. Then, 1 mL of the culture medium was added to each well and the plate was incubated for 24 h. Finally, cell viability was determined by the MTT assay. Controls were performed by cell culture on the polystyrene surface of the plate (TCPS).

Cell proliferation was evaluated by a similar procedure to the adhesion assay, but the aliquot of 50-100 μL contained $2x10^4$ cells. The cultures were maintained for 7 days to allow cell growth and adequate cell confluence in the well. The media were renewed every two days. Finally, viability was determined by the MTT assay.

The MTT [3-(4,5-dimethylthiazol-2-yl)-2,5-diphenyltetrazolium bromide] assay was carried out after 24 h and 7 days of culture. For this purpose, 50 μL of MTT solution (5 mg/ml in PBS) was added to each well. This assay measures the ability of a mitochondrial dehydrogenase enzyme from viable cells to cleave the tetrazolium rings of the pale yellow MTT and form dark-blue formazan crystals. The latter are largely impermeable to cell membranes resulting in its accumulation within healthy cells. Thus, the number of surviving cells is directly proportional to the level of the formazan product created. After 3 h of incubation with MTT, the wells were washed two times with PBS. Then, each electrospun sample was moved away of the well and placed in a clean well. The formazan crystals were solubilized by adding 200 μL of DMSO/methanol/water (5v:3v:2v) mixture , and 15 min later the absorbance at 570 nm was measured using an ELISA reader (Figure 4. 16).

Accordingly, the cellular viability on the electrospun sample was determined as the difference between the viability remainder in the well that contained sample and the viability of the well control (without material or plate, TCPS). The cellular adhesion and proliferation were evaluated at three independent experiments. The viability or absorbance values were normalised by cm^2 of material area. The results are expressed as the average absorbance values of four

replicates and graphically represented. The statistical analysis was performed by one-way ANOVA to compare the means of all groups; Tukey Test was then applied to determine a statistically significant difference between two studied groups. The tests were performed with a confidence level of 95% ($p < 0.05$).

To obtain SEM images, samples from adhesion and proliferation assays were processed as follows. First, they were fixed in 2.5% glutaraldehyde-PBS overnight at 4 ºC, and then dehydrated by washing in an alcohol battery (30º, 50º, 70º, 90º, 95º and 100º) at 4 ºC for a minimum of 30 min per step. Finally, the samples were dried and covered by carbon sputtering for SEM examination.

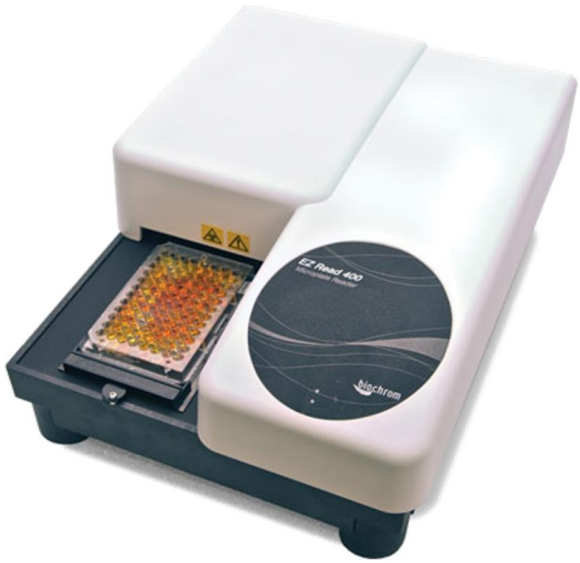

Figure 4. 16: Automatic microplate reader *EZ-READ 400 ELISA*.

CHAPTER V: RESULTS AND DISCUSSION

5.1. - Characterization of the Arg-based polymers

5.1.1. - Thermal analysis

The thermal analysis of the different Arg-based polymers is divided in two different tests. First of all, a differential scanning calorimetric study was carried out to get information about the glass transition temperature of the polymers. The thermal gravimetric analysis was also performed to get in this case information on degradation of polymers and how it was influenced by the incorporation of cationic compounds.

The protocol followed for DSC analysis was always the same for the six considered samples. This protocol consists on: A first heating scan from -50 °C to 200 °C, one cooling scan from the melt state and finally a second heating to 150 °C. The characteristic temperatures of the different polymers after analyzing the data obtained by the equipment are presented in Table 5.1.

Material	T_g **[°C]**
PEA	67.7
PEUR	59.9
PEEUR-1	66.3
PEEUR-2	64.1
PEEUR-3	49.5
PEEUR-4	54.4

Table 5. 1: Glass transition temperatures of the different Arg-based polymers.

Except PEEUR-3, all the polymers showed a very similar behavior having a T_g at around 60 °C. No melting and crystallization peaks were detected confirming the completely amorphous nature of the different copolymers. This feature in consistent with the highly complicated chemical repeat unit that precludes an effective arrangement. In fact, an amorphous character is usual in similar amino acid based PEAs despite strong intermolecular hydrogen bond interactions can be established between the constitutive amide urethane groups. The presence of these interactions can justify the high glass transition temperature as well as the presence of relatively voluminous lateral groups.

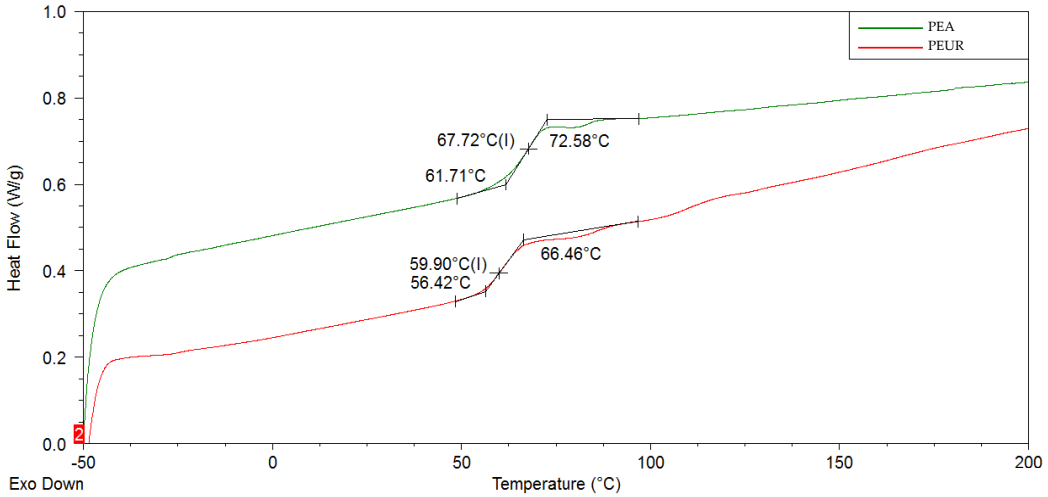

Figure 5. 1: Example for glass transition temperature determination of the PEA and PEUR.

TGAs showed also an analogous behavior for all polymers. In Table 5. 2 measurements of different weight percentages loss are given. All the samples present comparable degradations, although the PEEUR-3 degrades at slightly lower temperature. Depending on bibliography consulted the degradation temperature of a polymer is reported to a concrete value of weight loss. It is important to remark that a 25% of the total weight loss is considered usually an important amount of material degraded, and this weight loss occur for all the samples at a temperature around 325 °C.

Material	Weigth Loss	10%	25%	50%	75%
PEA	**Temperature [°C]**	313.0	342.3	384.9	422.7
PEUR		277.8	328.4	373.7	423.3
PEEUR-1		279.4	325.2	375.3	413.7
PEEUR-2		289.5	323.6	370.5	408. 9
PEEUR-3		282.6	314.6	365.2	398.2
PEEUR-4		264.0	314.1	372.1	407.3

Table 5. 2: Degradation temperature for Arg-based polymers.

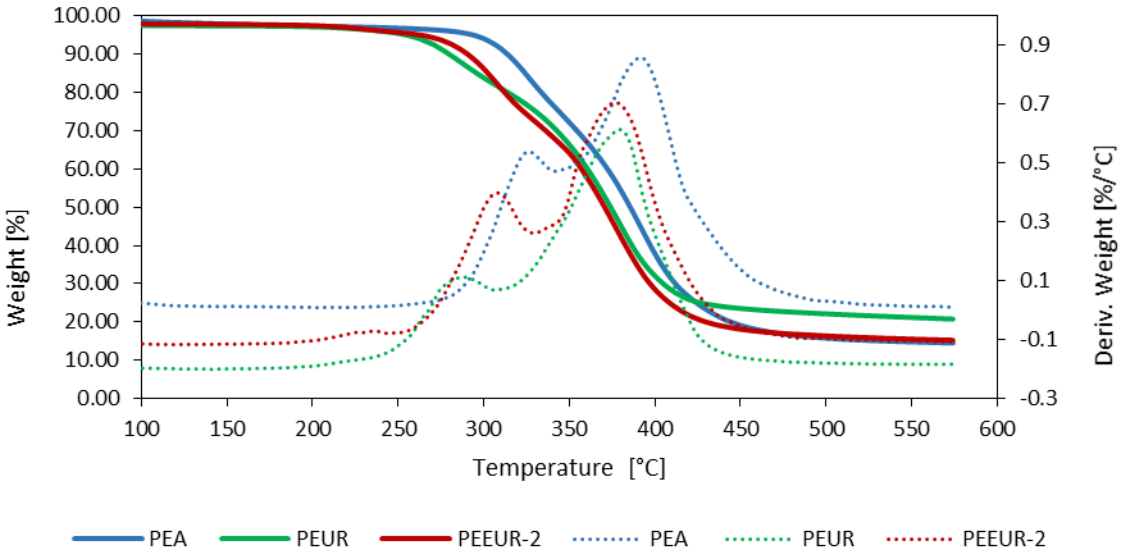

Figure 5. 2: Weight and derivative weight loss of a representative group of samples of Arg-based polymers.

5.1.2. - Infrared analysis

Through the infrared analysis is possible to determine the different groups of the polymers. The characteristic groups that are presented in all polymers are visible in all spectra.

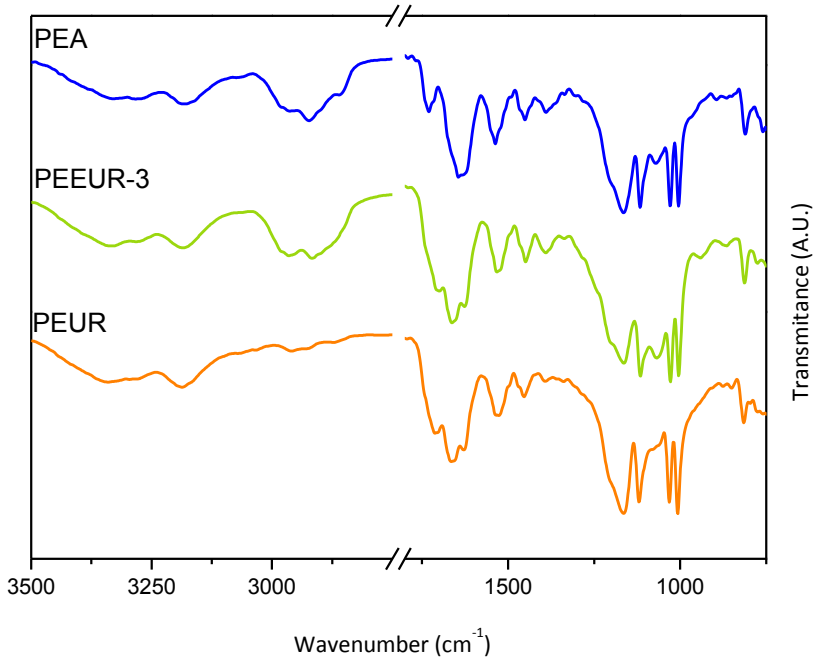

Figure 5. 3: Comparison between the FTIR spectra of PEA, PEUR and PEEUR-3 samples.

The main identification that could be done to these polymers is the following: around 1100 cm^{-1} there is a C-O stretching that could correspond either to ester, ether and urethane groups [-CH_2-O-X-, being X a C=O, or a CH_2 group]; at 1550 cm^{-1} can be detected the Amide II band associated to 60% N–H bend and 40% C–N stretching; at 1650 cm^{-1} the typical amide I band [-NH-C(O)-O-] that is mainly associated to the C=O stretching is observed; the peak observed at 1750 cm^{-1} [-C(O)-O-] notifies the characteristic CO stretching of the ester group; between 3000-3500 cm^{-1} a series of bands associated to different kinds of NH groups [e.g. NH-C(O) & NHC(=NH)NH_2.HOTos] are observed. High wavenumbers correspond to free NH groups whereas those forming strong intermolecular interactions shift to lower values (e.g. Amide A detected as a well-defined peak around 3200 cm^{-1} and the Amide B detected as a small should be around 3030 cm^{-1}). In Figure 5. 4 the Amide A, Amide I, Amide II and the C-O stretching are pointed out.

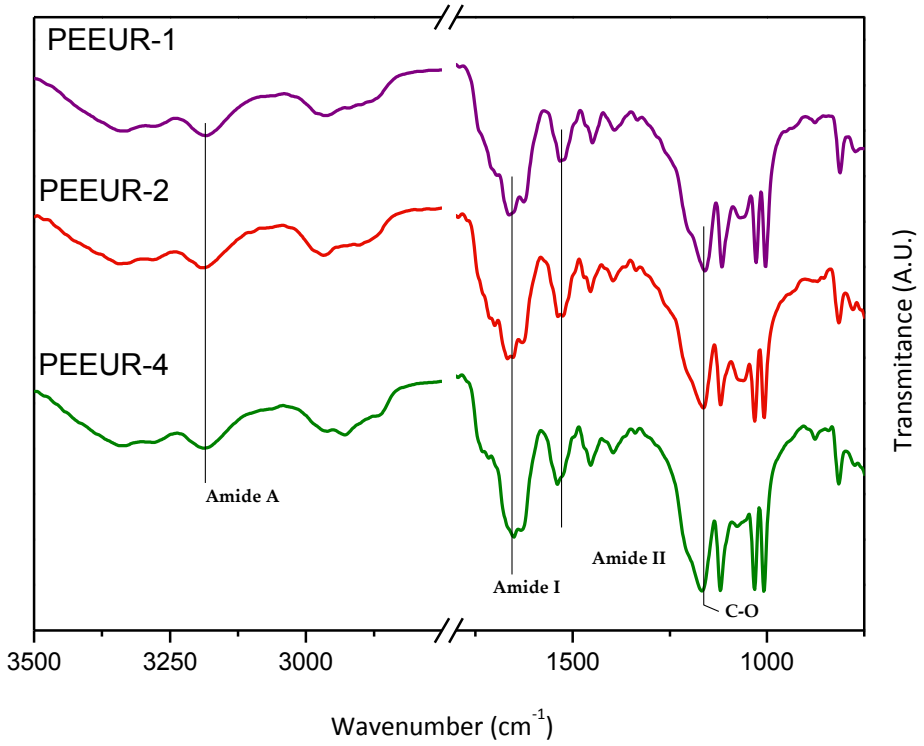

Figure 5. 4: FTIR spectra of different PEEUR's show no significant differences.

5.1.3. - Nuclear magnetic resonance

All the Arg-based polymers were analyzed by the nuclear magnetic resonance technique. Again here all spectra showed the same characteristic peaks. Obviously, depending on the diol or diacyl units some differences were detected since the number of methylene groups varied. Next is presented the full identification of peaks for PEEUR-2 (chemical shifts δ in ppm) as a representative example. Please, note that: "m" means multiplet, "s" singulet and "br." broad.

PEEUR-2 (Arg-PD-Arg-EG_2): 1.53-1.91 (8H, m, CH$\underline{CH_2CH_2}$); 2.3 (2H, s, $OCH_2\underline{CH_2}CH_2O$); 2.51 (6H, m, $\underline{CH_3}C_6H_4$); 3.35 (4H, br, $NHCH_2$); 3.59 (4H, m, CH_2OCH_2); 4.08 (2H, br, CH); 7.42 (4H, m, C_6H_2-CH_3-$\underline{H_2}HOSO_2$) 7.76 (4H, m, $HOSO_2$-$\underline{H_2}C_6H_2$-CH_3).

The two peaks present around 7.5 ppm correspond to aromatic protons of the *p*-toluenesulfonic group that is present in all arginine containing polymers. The singular peak of this polymer is at 2.3 ppm and corresponds to the PD

(Propanodiol). Below is presented a graph of the most representative peaks of the PEEUR-2

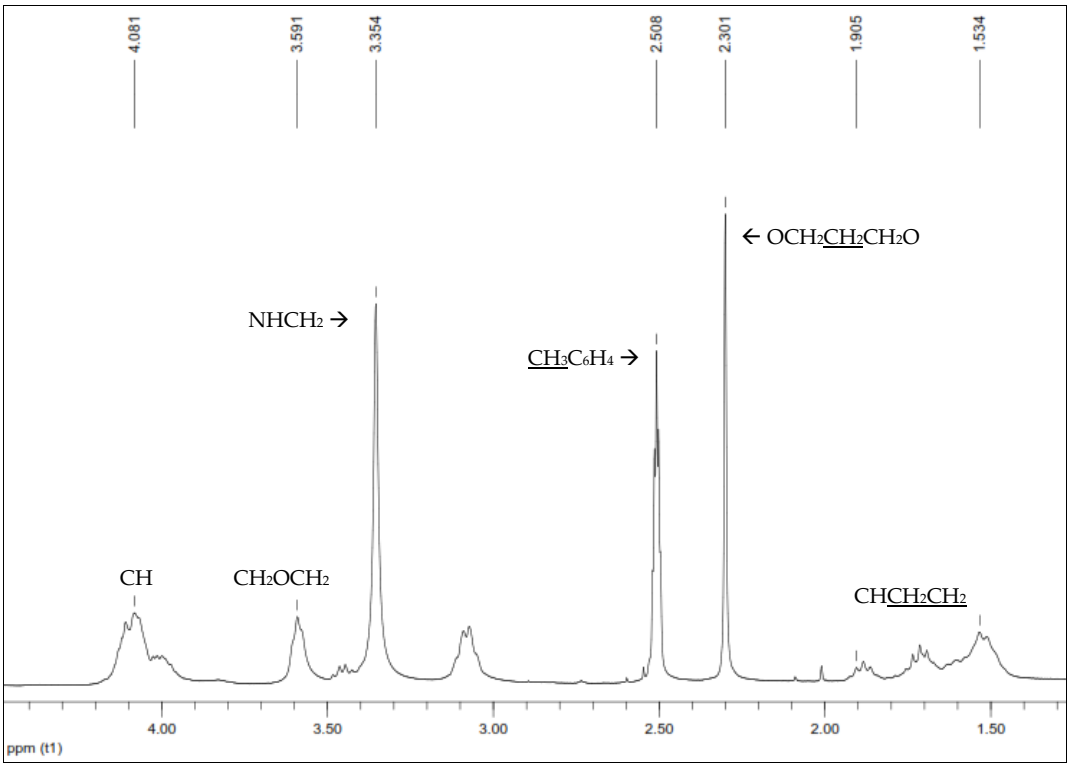

Figure 5. 5: Part of the NMR spectra of the PEEUR-2 sample.

5.1.4. - Synchrotron radiation

Through the X-rays analysis it is possible to determine that all of the Arg-based polymers are completely amorphous as deduced also from DSC data. A broad scattering peak is observed with minimum changes between samples (Figure 5. 7). Thus, average distances between constitutive atoms are practically identical. The image of a typical crystalline sample (e.g. pure Arginine) is presented in Figure 5. 6 where typical and well-defined Bragg reflections are observed.

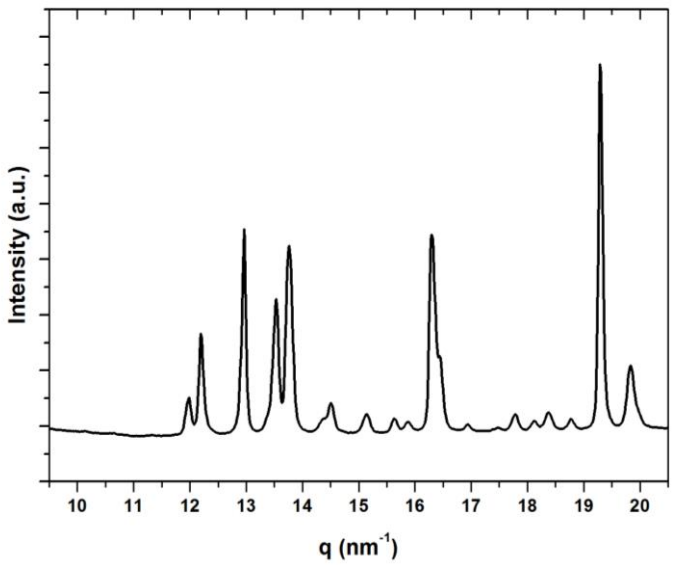

Figure 5. 6: Crystalline peaks of arginine.

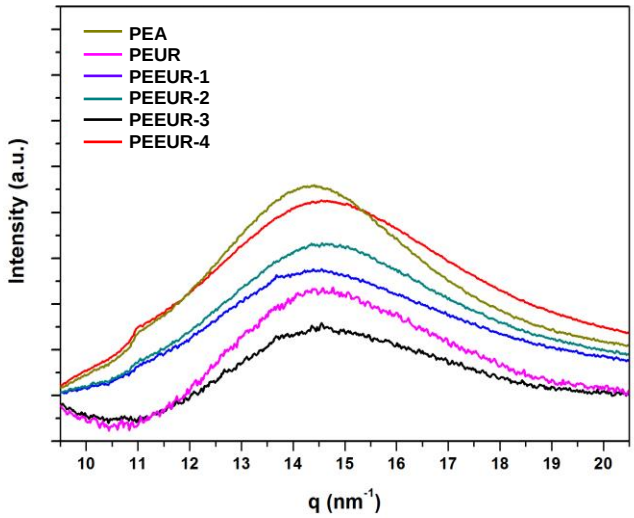

Figure 5. 7: X-rays analysis of the Arg-based polymers.

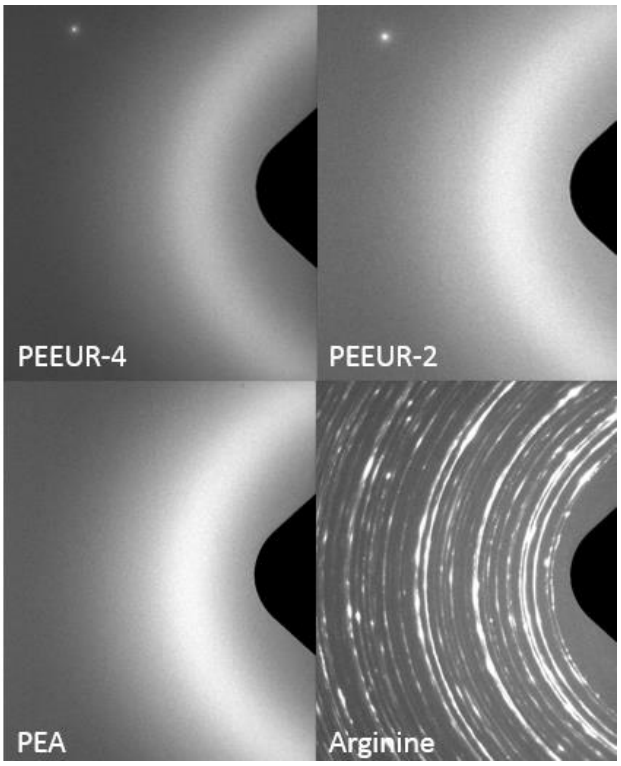

Figure 5. 8: Amorphous and crystalline halos for different polymers and pure arginine.

5.1.5. - Gel permeation chromatography

In Table 5. 3 the values of the mean molecular weight and dispersity index of the different received Arg-based polymers are summarized:

Material	M_n [g/mol]	M_w [g/mol]	Dispersity
PEA	7209	17533	2.43
PEUR	5500	12362	2.25
PEEUR-1	4327	7515	1.73
PEEUR-2	3996	6902	1.72
PEEUR-3	3571	6926	1.94
PEEUR-4	2609	7210	2.76

Table 5. 3: Molecular weight and dispersity index.

In the picture below it could be observed a typical molecular weight distribution curve of a cationic representative polymer.

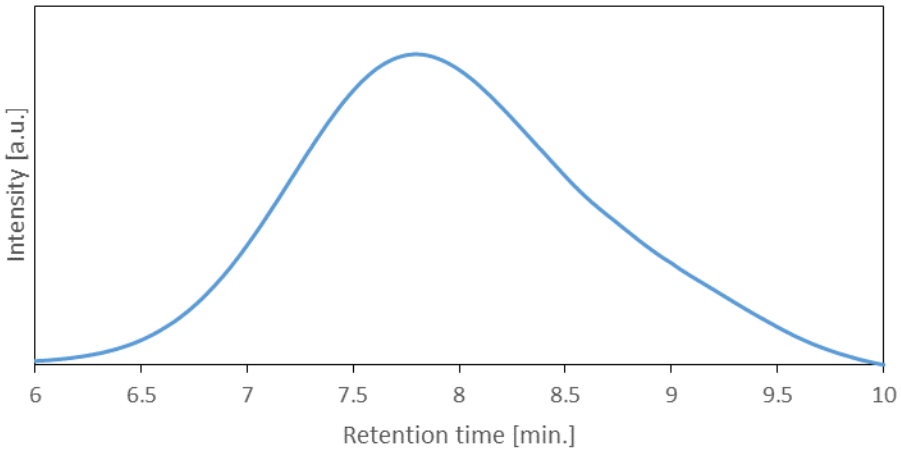

Figure 5. 9: GPC distribution curve the studied PEA.

5.2. - Optimal preparation of electrospinnable polymer solutions

Depending on the compatibility of the polymers with the available solvents the solutions for the electrospinning were prepared in different ways. In the following table is resumed the solubility tests performed with the different materials used during the development of this project.

Material / Solvent	PLA	PHMB	Arginine	Arg-based polymers
Water	Insoluble	Soluble	Soluble	Insoluble
$CHCL_3$-C_3H_6O 2:1 (*v*/*v*)	Soluble	Insoluble	Insoluble	Insoluble
Formic Acid	Soluble	Soluble	Soluble	Soluble
DCM	Soluble	-	-	Insoluble
DMF	Insoluble	-	-	Soluble

Table 5. 4: Solubility tests for solvent selection.

The solvent used to get PLA mats was a mixture 2:1 *v*/*v* of chloroform ($CHCL_3$) and acetone (C_3H_6O). The polymer concentration selected was 10% *w*/*v* of PLA. Therefore, for the reference material 1 g of PLA was dissolved in 10 mL of $CHCL_3$-C_3H_6O 2:1 (*v*/*v*) for 24 hours at 37 °C. The inclusion of different modifiers to that base was additive. To have the sample of PLA with 0.25% (w/v) of PHMB, 25 µg of PHMB were dissolved in 100 µL of formic acid and added to the previous solution of PLA 10% (*w*/*v*).

The arginine containing mats were produced by adding different amounts of arginine to the final solution. Firstly, the arginine was dissolved in formic acid as performed for PHMB loaded samples. Mats of different concentrations (*w*/*w*) were produced. For instance, to prepare a mat with 10% (*w*/*w*) of arginine, 111 mg of arginine were dissolved in 200 μL of formic acid.

The samples with different mixtures of Arg-based polymers were produced using as solvent a 1:1 (*v*/*v*) mixture of dichloromethane and dimethylformamide. First trials were developed using formic acid to dissolve the arginine containing polymer but it precipitated when mixing with PLA dissolved in $CHCL_3$-C_3H_6O 2:1 (*v*/*v*). For that reason this solvent was discarded.

Final procedure was as follows: 1 g of PLA was dissolved in 5 mL of DCM for 24 hours at 37 °C, and the Arg-based polymer in 5 mL of DMF. After mixing in a vortex, no precipitation or phase separation was observed. If more quantity of DMF was added a phase separation occurred. Table 5. 5 summarizes the different mats produced and the solvents and concentrations elected.

Material	Base	Amount [mg]	Solvent of the base	Amount [μL]	Second element	Amount [mg]	Solvent of the second element	Amount [μL]
PLA	PLA 10% (*w*/*v*)	1000	$CHCL_3$-C_3H_6O 2:1 (*v*/*v*)	10000	-	-	-	-
PLA-0.25% PHMB	PLA 10% (*w*/*v*)	1000	$CHCL_3$-C_3H_6O 2:1 (*v*/*v*)	10000	PHMB 0.25% (*w*/*v*)	25	Formic acid	100
PLA-5%Arg	PLA 10% (*w*/*v*)	1000	$CHCL_3$-C_3H_6O 2:1 (*v*/*v*)	10000	Arginine 5% (*w*/*w*)	53	Formic acid	100
PLA-10%Arg	PLA 10% (*w*/*v*)	1000	$CHCL_3$-C_3H_6O 2:1 (*v*/*v*)	10000	Arginine 10% (*w*/*w*)	111	Formic acid	200
PLA-20%Arg	PLA 10% (*w*/*v*)	1000	$CHCL_3$-C_3H_6O 2:1 (*v*/*v*)	10000	Arginine 20% (*w*/*w*)	250	Formic acid	400
PLA*	PLA 10% (*w*/*v*)	1000	DCM-DMF 1:1 (*v*/*v*)	10000	-	-	-	-
PLA-PEA	PLA 10% (*w*/*v*)	1000	DCM	5000	Arg-HD-Arg-Se 20% (*w*/*w*)	250	DMF	5000
PLA-PEUR	PLA 10% (*w*/*v*)	1000	DCM	5000	Arg-PD-Arg-EG20% (*w*/*w*)	250	DMF	5000
PLA-PEEUR-1	PLA 10% (*w*/*v*)	1000	DCM	5000	Arg-EG-Arg-EG_2-20% (*w*/*w*)	250	DMF	5000
PLA-PEEUR-2	PLA 10% (*w*/*v*)	1000	DCM	5000	Arg-PD-Arg-EG_2-20% (*w*/*w*)	250	DMF	5000
PLA-PEEUR-3	PLA 10% (*w*/*v*)	1000	DCM	5000	Arg-EG_2-Arg-EG_2-20% (*w*/*w*)	250	DMF	5000
PLA-PEEUR-4	PLA 10% (*w*/*v*)	1000	DCM	5000	Arg-EG_4-Arg-EG_2-20% (*w*/*w*)	250	DMF	5000

Table 5. 5: Complete description of the required materials for the manufacture of the produced mats.

5.3. - Optimization of the electrospinning conditions

As mentioned in the previous chapter, the optimal conditions for the electrospinning process are difficult to achieve as they depend on many factors such as, for instance, the ambient conditions. Before obtaining the desired mat, diverse parameters were changed in order to achieve the best conditions. These parameters are the needle-collector height distance, the applied voltage and the flow rate. An example of the optimization process is presented below where the operational parameters were fitted to achieve the most uniform fiber diameter and the lower number of possible imperfections.

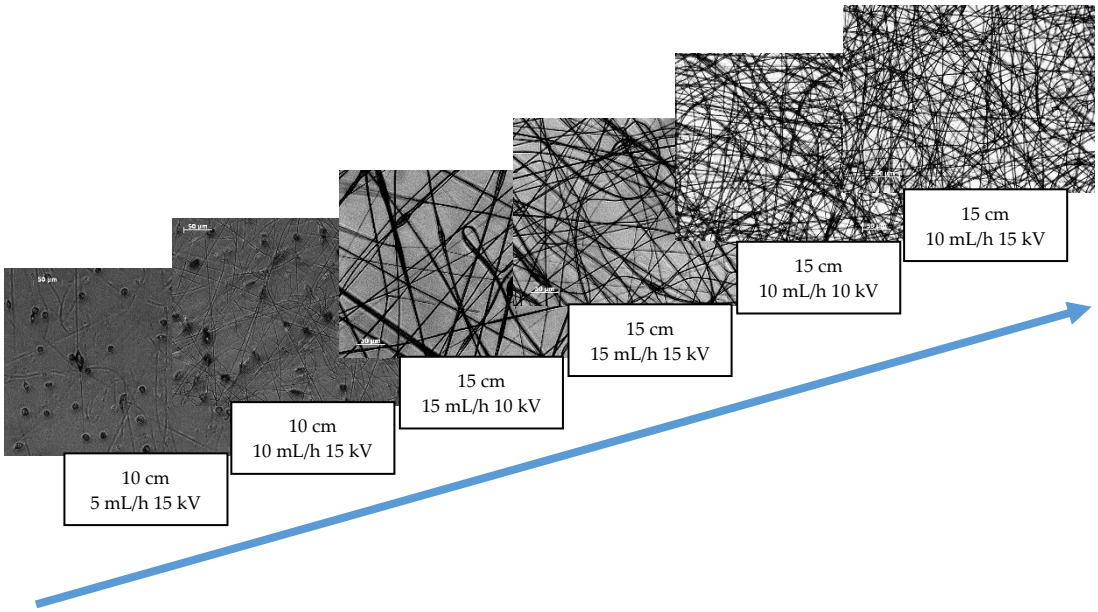

Figure 5. 10: Example of the electrospinning optimization process.

In Table 5. 6 the optimal operational parameters to electrospun each sample are listed. The optimal parameters were very similar for the PLA mats and the samples that contain pure arginine as well as PHMB, except for the sample with the highest arginine content (i.e. 20%). When the solution was prepared with DCM:DMF instead of chloroform and acetone the final viscosity decreased and therefore the flow rate needed to be tuned. As it happens in the mat of 20% of pure arginine, for the samples with a 20% of the Arg-based polymer the distance to the collector was increased as a consequence of the increase of the need electrostatic charges. Therefore to achieve a uniform mat of continuous and regular nanofibers was a difficult task. Even though the solutions were stored at a constant temperature of 37 °C, the electrospinning room temperature and the ambient humidity were variables that could not be controlled, for that reason sometimes small changes in the processing parameters were done (e.g. for the PLA-PEEUR-3 sample the flow rate needed to be decreased since room temperature was higher during the period at which these essays were performed).

Sample	Distance [cm]	Flow Rate [mL/h]	Voltage [V]
PLA	15	10	15
PLA-0.25%PHMB	15	10	15
PLA-5%Arg	15	10	15
PLA-10%Arg	15	10	15
PLA-20%Arg	18	5	20

PLA*	15	1	20
PLA-PEA	18	1	20
PLA-PEUR	18	1	20
PLA-PEEUR-1	18	1	22
PLA-PEEUR-2	18	1	20
PLA-PEEUR-3	18	0.75	20
PLA-PEEUR-4	18	1	20

Table 5. 6: Optimal electrospinning parameters for each sample produced.

5.4. - Fiber characterization

5.4.1. - Optical microscope analysis

The optical microscope is not a good technique for a quantitative characterization of the fibers due to its reduced size in addition to its birefringent border produced by the light dispersion. These two factors make impossible to measure accurately the diameter of the electrospinned fibers. However, the OM is a technique that perfectly match for *in situ* and initial characterization. Thus, the decision in the optimization of the electrospinning parameters are taken faster. Figure 5. 11 shows different images of the optimal conditions for different compounds.

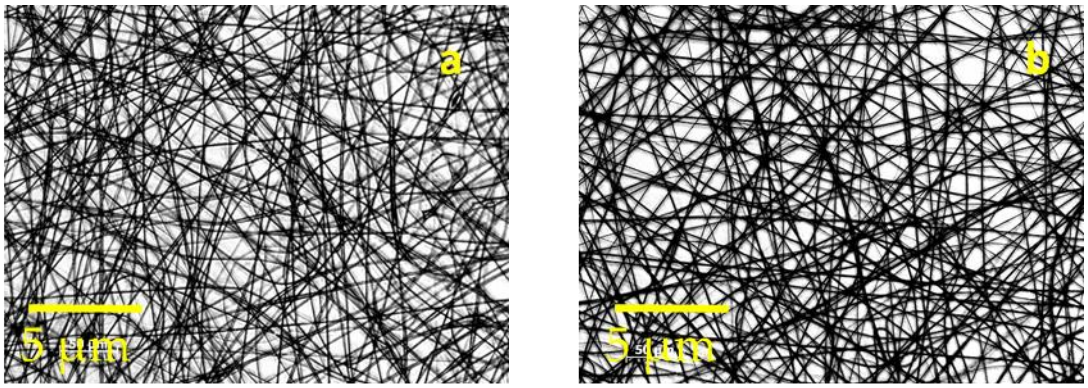

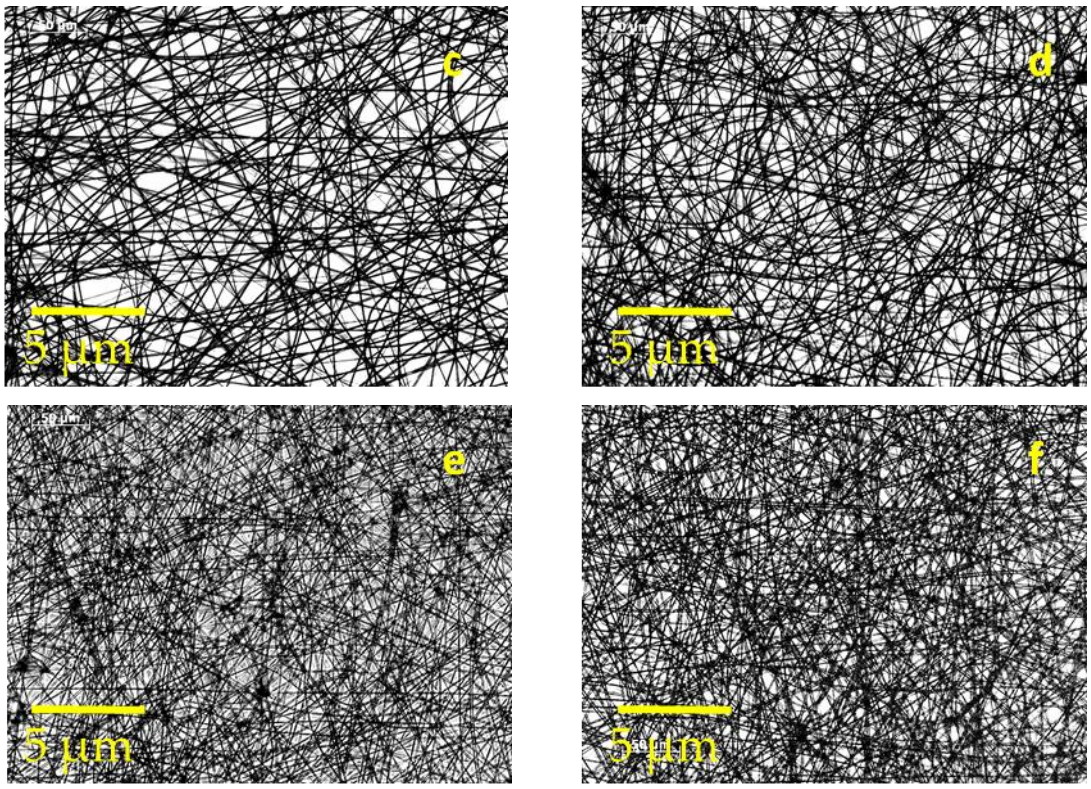

Figure 5. 11: Different captions (20X) of the optimal electrospinning conditions: a) PLA; b) PLA-0.25%PHMB; c) PLA-10%Arg; d) PLA-20%Arg., e)PLA-PEA, f) PLA-PEEUR-1

5.4.2. - SEM morphology

For the morphologic study of the electrospinned fibers SEM was used. This allows obtaining more magnified images of the fibers and therefore to observe characteristics such as the roughness, the porosity or the presence of cracks. Figure 5. 12 shows detailed SEM micrographs of all the fibers produced by electrospinning. It could be observed as the mats prepared with PLA present a rough surface with some pores as it is typically described in the bibliography [49], [54], [66] The sample loaded with PHMB present a smooth surface as it was also expected [67]. All the scaffolds prepared with different percentages of arginine (5, 10 and 20%) present smoother fibers than the mats prepared with only PLA as it could be observed in Figure 5. 12-c). Finally, it is important to note that the inclusion of the Arg-based polymers in the produced mats let to a less rough fiber surface. The diameter of those fibers made up with mixtures of PLA and an Arg-based polymer is more irregular along its length as it could be observed in Figure 5. 12-d).

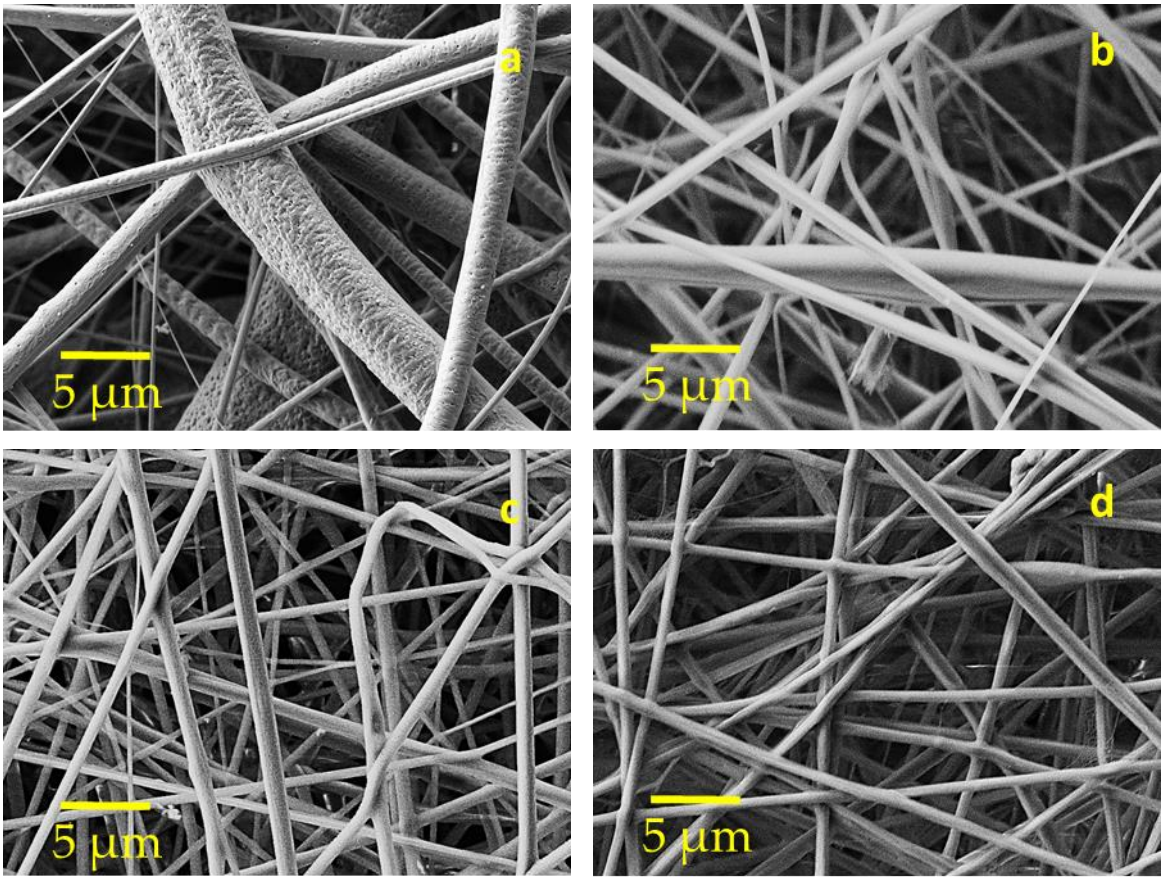

Figure 5. 12: SEM micrographs (10.000 X) of: a) PLA; b) PLA-0.25%PHMB; c) PLA-20%Arg; d) PLA-PEEUR-4

5.4.3. - Fiber diameter

SEM images were also used for quantitative purposes and specifically to determine the fiber diameter distribution. The mean diameter of the fiber is a measurement that expresses the homogeneity of the fibers in the scaffold for each compound. For that purpose diameter measurements were repeated several times for each sample. Around 70 measurements were taken avoiding the measurement of the same fiber and from pictures of different zones of the mat.

In this research the program *Smart Tiff* was used for the diameter measurement. All the obtained data was treated with O*RIGIN 8 PRO.* This program let the user to analyze the diameter distribution as well as to represent graphically these distributions.

In Figure 5. 13 different micrographs of the fibers are presented together with the graphs of the fiber diameter distribution. There it could be observed that all the manufactured mats showed a unimodal distribution, which lead to think that all the samples where produced under optimal conditions. The high fluidity and the high charge of the solution polymer cause a broad diameter distribution because of the more limited conditions and the higher difficulty to obtain fibers. This phenomenon happens in the PLA-20%Arg due to the high electrostatic charge generated in the jet during the electrospinning process.

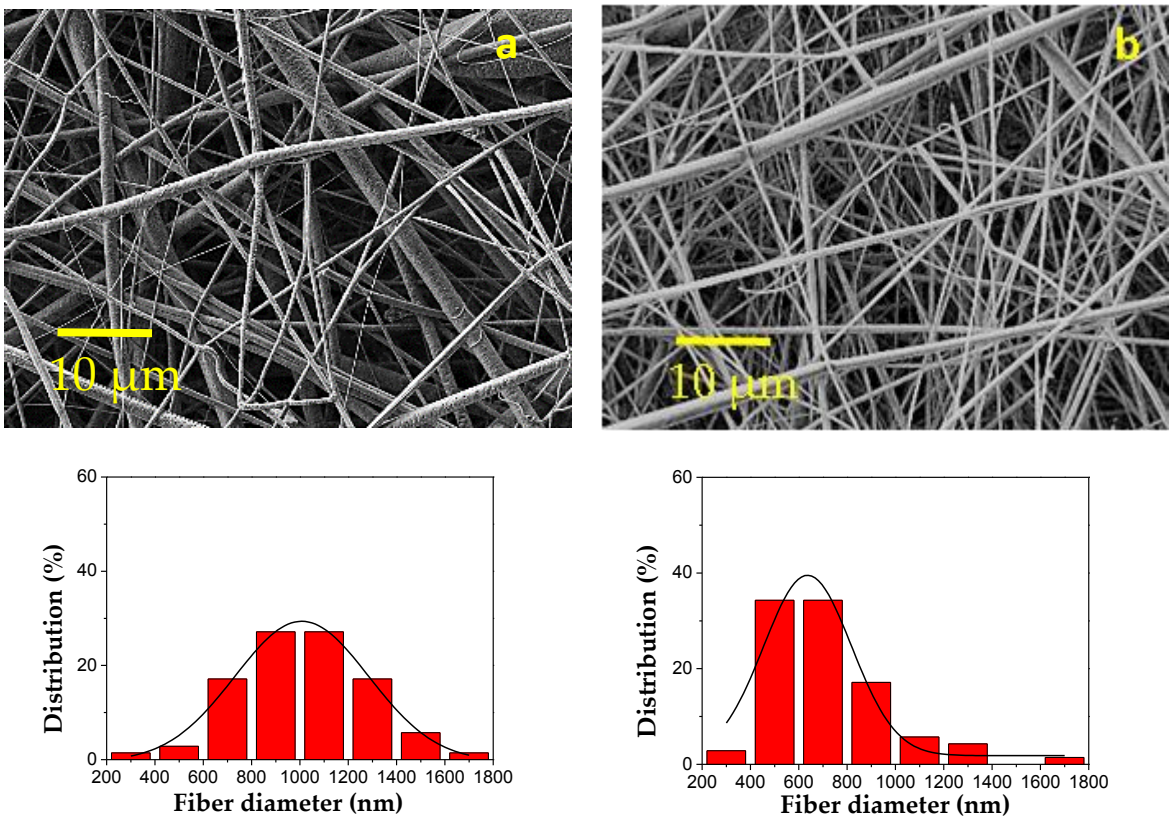

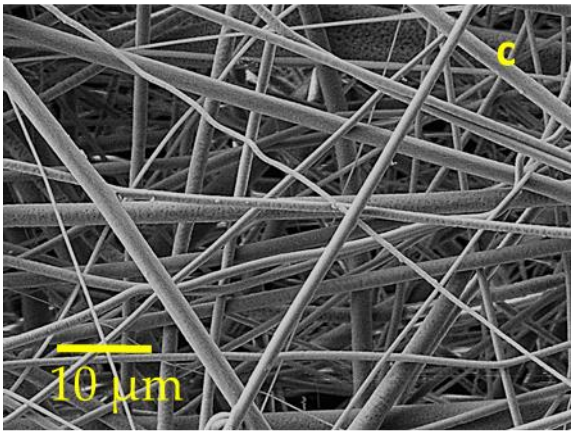
c
10 µm

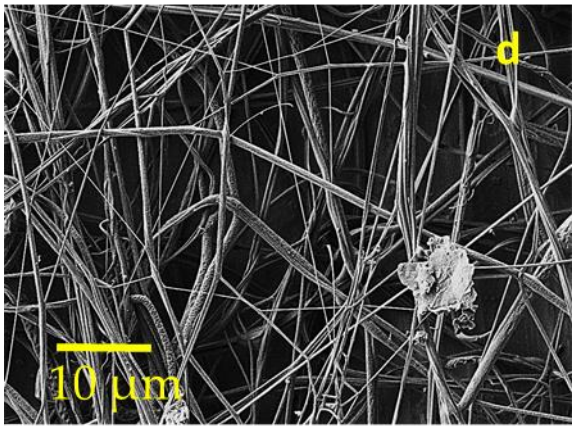
d
10 µm

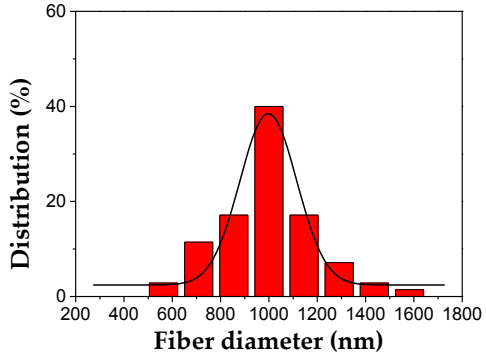
Distribution (%)
0
20
40
60
200 400 600 800 1000 1200 1400 1600 1800
Fiber diameter (nm)

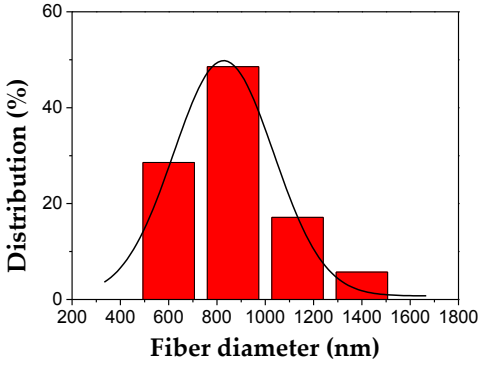
Distribution (%)
0
20
40
60
200 400 600 800 1000 1200 1400 1600 1800
Fiber diameter (nm)

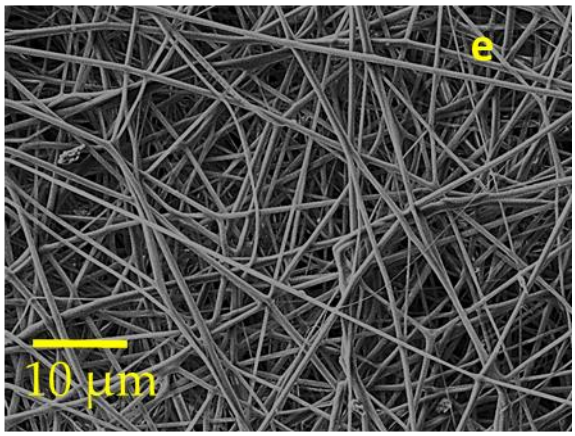
e
10 µm

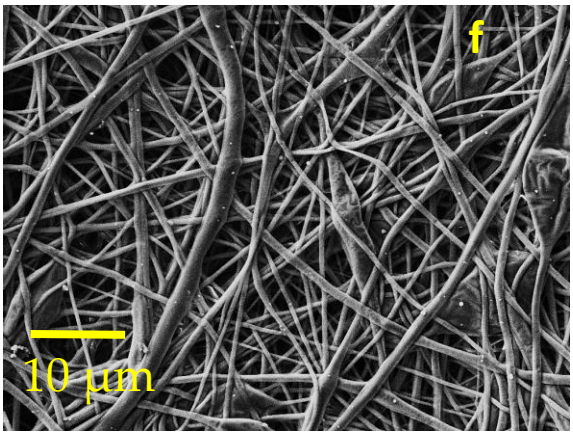
f
10 µm

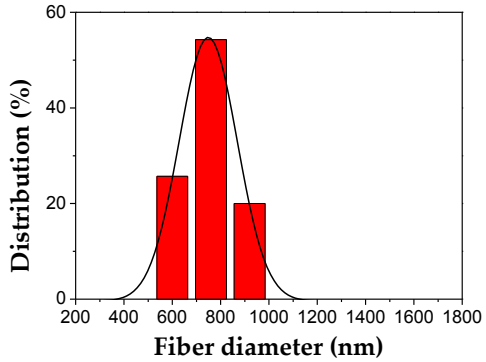
Distribution (%)
0
20
40
60
200 400 600 800 1000 1200 1400 1600 1800
Fiber diameter (nm)

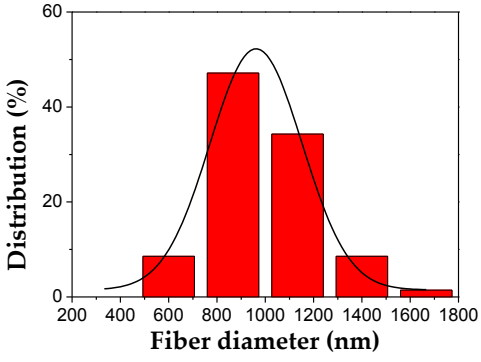
Distribution (%)
0
20
40
60
200 400 600 800 1000 1200 1400 1600 1800
Fiber diameter (nm)

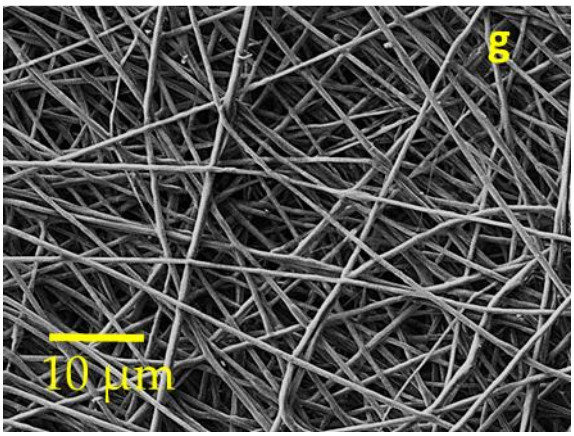
g
10 μm

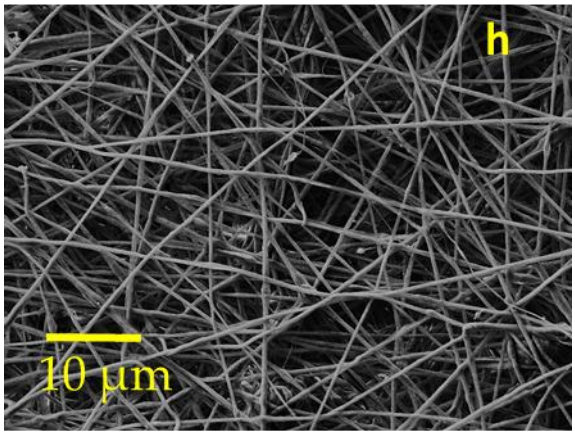
h
10 μm

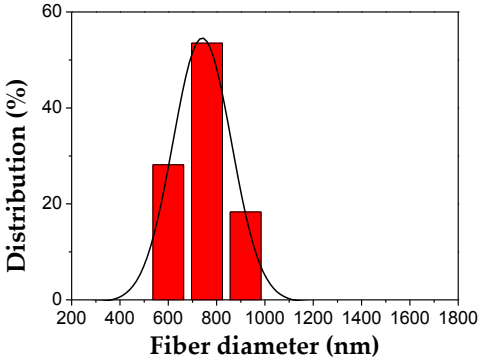
Distribution (%)
0
20
40
60
200 400 600 800 1000 1200 1400 1600 1800
Fiber diameter (nm)

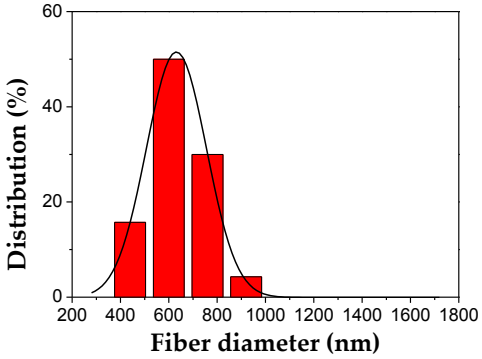
Distribution (%)
0
20
40
60
200 400 600 800 1000 1200 1400 1600 1800
Fiber diameter (nm)

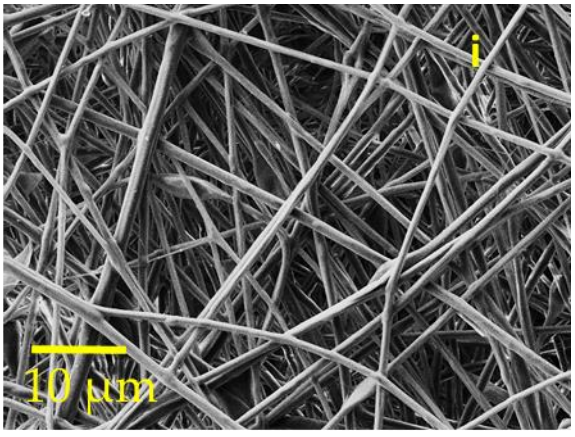
i
10 μm

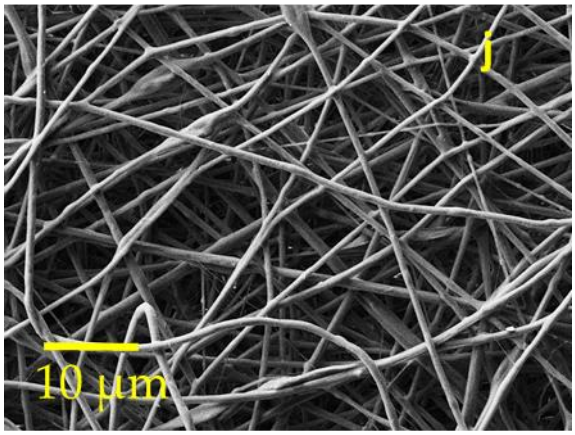
j
10 μm

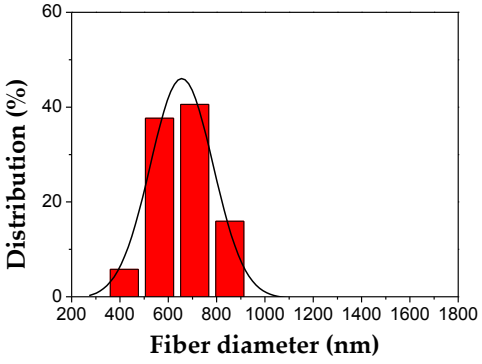
Distribution (%)
0
20
40
60
200 400 600 800 1000 1200 1400 1600 1800
Fiber diameter (nm)

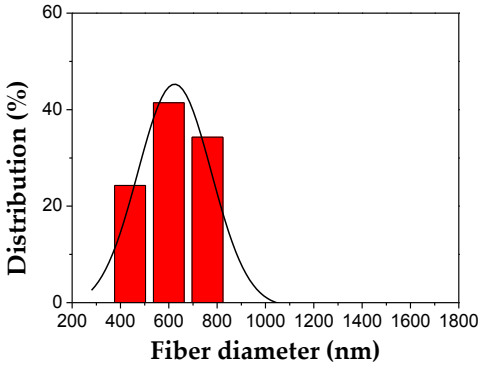
Distribution (%)
0
20
40
60
200 400 600 800 1000 1200 1400 1600 1800
Fiber diameter (nm)

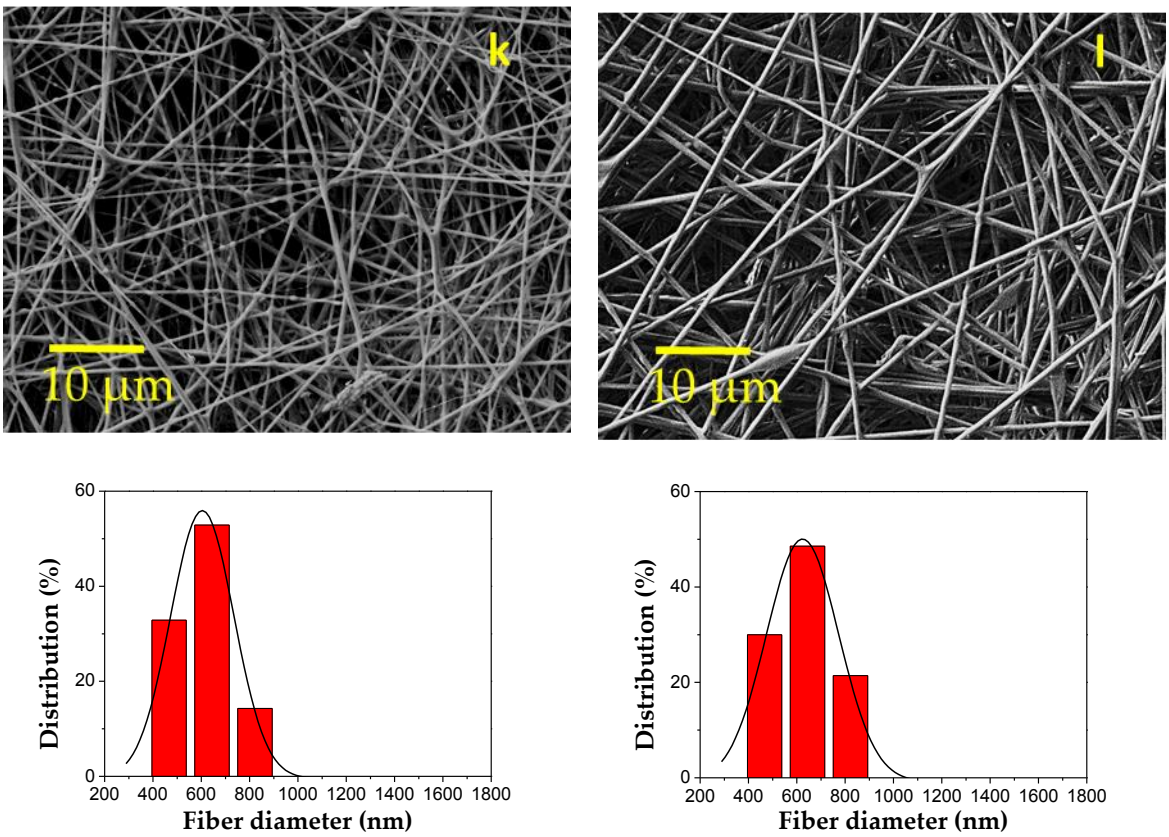

Figure 5. 13: Diameter distribution and SEM micrographs of (5.000 X): a), PLA, b) PLA-0.25%PHMB, c) PLA-5%Arg, d) PLA-10%Arg, e) PLA-20%Arg, f) PLA*, g) PLA-PEA, h) PLA-PEUR, i) PLA-PEEUR-1, j) PLA- PEEUR-2, k) PLA- PEEUR-3, l) PLA- PEEUR-4.

First thing to comment locking at Figure 5. 13 is the observation that the addition of PHMB reduced significantly the diameter of the fiber. This phenomena was expected due to the high quantity of the PHMB added, and also because this feature was already observed in other studies [67]. The addition of pure arginine did not influence the diameter while the amount of loaded compound was, however when the quantity of arginine increased a higher quantity of formic acid was required to get a good solution. Therefore, the added formic acid changed the surface tension of the drop when forming the Taylor's cone leading to a significant diameter variations [50].

For the second block of mats (i.e. those produced from DCM:DMF mixtures) the operational parameters were completely different and therefore possible changes in the fiber diameters could be expected. The addition of any of the cationic Arg-based polymers produced a decrease in the diameter of the fiber, which was a consequence of the increase of the charge.

As the solution was highly charged with the application of the same voltage the fiber pulled the jet more quickly and therefore the final diameter decreased.

Sample	Ø [nm]	Tukey's test
PLA	1007 ± 32	
PLA-0.25%PHMB	636 ± 28	a
PLA-5%Arg	997 ± 23	b
PLA-10%Arg	827 ± 27	a, b, c
PLA-20%Arg	748 ± 11	a, c, d
PLA-*	961 ± 23	d, h
PLA-PEA	740 ± 12	a, c, d, e
PLA-PEUR	631 ± 13	a, c, d, e, f, g
PLA-PEEUR-1	655 ± 12	a, c, d, e, f, g
PLA-PEEUR-2	624 ± 14	a, c, d, e, f, g
PLA-PEEUR-3	604 ± 11	a, c, d, e, f, g
PLA-PEEUR-4	623 ± 13	a, c, d, e, f, g

Table 5. 7: Obtained fiber diameter (Data: $\bar{X}$ ± SEM). Tukey's test: a, p < 0.05 VS PLA; b, p < 0.05 VS PLA-0.25%PHMB; c, p < 0.05 VS PLA-5%Arg; d, p < 0.05 VS PLA-10%Arg; e, p < 0.05 VS PLA*; f, p < 0.05 VS PLA-PE; g, p < 0.05 VS PLA-20%Arg.

Interestingly, it is possible to observe that the quantity of pure arginine added plays an important role on the fiber diameter but the type of Arg-based polymer added does not play any role. This could be because all the family of the arginine containing polymers have the same number of arginine groups on its structure and the quantity added was always the same.

5.4.4. - Infrared analysis

Through the use of the Fourier Transform Infrared spectroscopy (FTIR) it is easy to see the composition of the mats in a qualitative way. Depending on the peaks that are observed in the spectra it is possible to identify the incorporated compounds, for instance PHMB or arginine.

First of all, a spectrum of a PLA mat was obtained. In Figure 5. 14 it can be observed the characteristic bands of PLA. The band at 1753 cm^{-1} corresponds to the stretching ν(C=O). The one at 1452 cm^{-1} is associated to the asymmetrical bending δas(CH_3) [68]. The peak that appears at 1182 cm^{-1} is associated with the asymmetrical vibration of the bond C-O-C, and the band at 1086 cm^{-1} corresponds to the symmetrical vibration of C-O-C [69], [70].

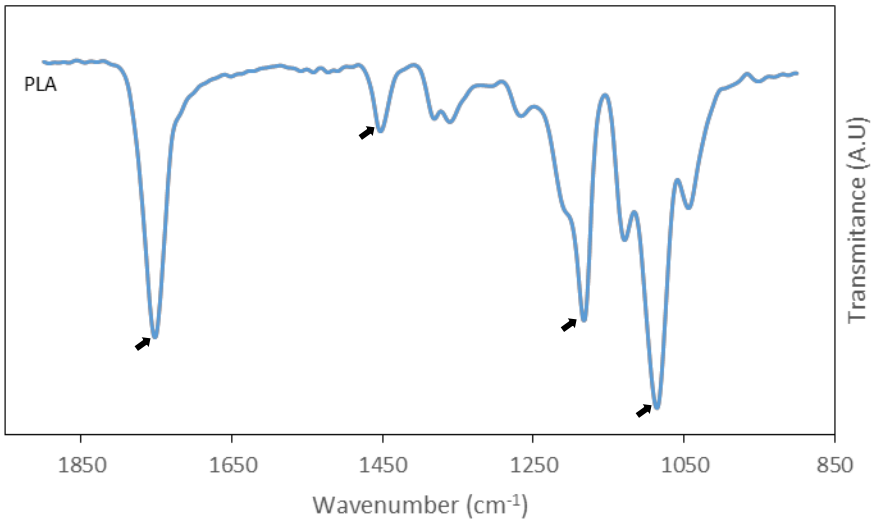

Figure 5. 14: Typical peaks observed in the PLA mat.

The PHMB was examined isolated first and later in the mat made up with PLA and 0.25% of PHMB. Observing the spectrum of the pure PHMB powder (Figure 5. 15), it can be pointed out the typical bands that correspond to the amines of the biguanide are visible. Specifically, the CN bond is depicted at 1490 cm^{-1} [71], whereas the band at 1537 cm^{-1} represents the NH bond [72]. It is not possible to observe these characteristic peaks of amine groups in the FTIR spectra of the loaded samples (see for example Figure 5. 16), probably as a consequence of the low sensitivity of the infrared spectrum and the reduced drug concentration (i.e. 0.25%).

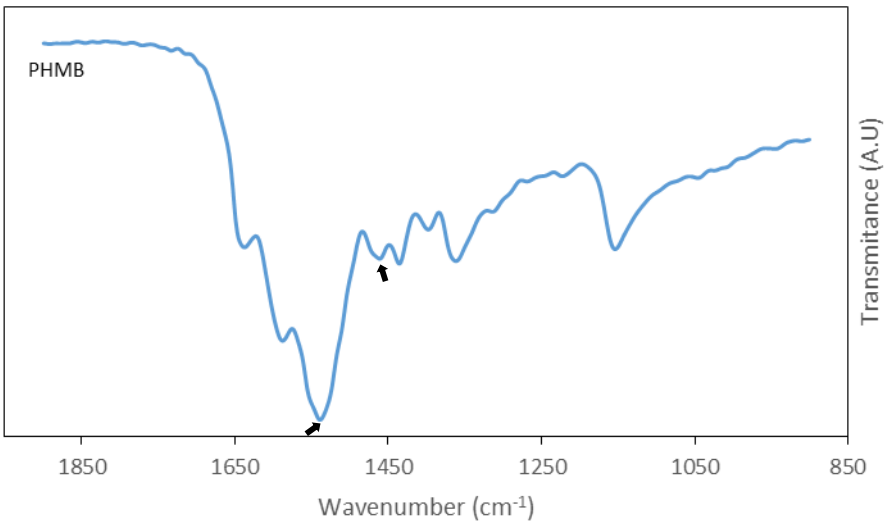

Figure 5. 15: FTIR spectra of the pure PHMB powder.

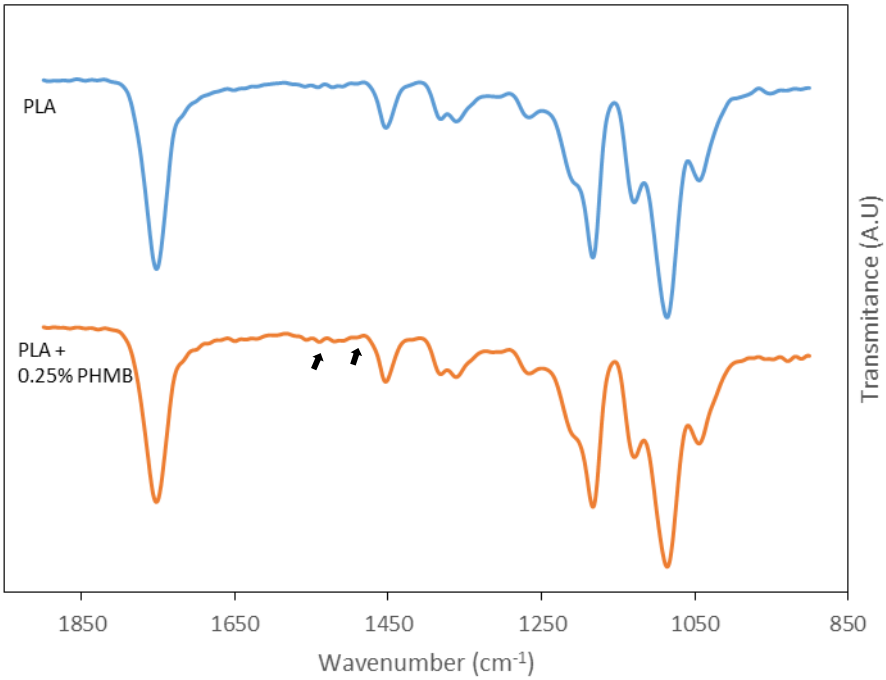

Figure 5. 16: Effect of the addition a 0.25% of PHMB to the PLA compared with the pure PLA sample.

The same process was done when arginine was incorporated. After obtaining the spectrum of pure arginine, the FTIR analysis was done to the different percentage of arginine loaded scaffolds. In Figure 5. 17 the characteristic peaks of the arginine are shown. The band at 1409 cm^{-1} corresponds to the symmetrical bending of the CH_3 bond. Another important band of the arginine is the one at 1674 cm^{-1}, which indicates the bending of the NH_2 bond. The bending of the OH bond is depicted at 1545 cm^{-1} [73].

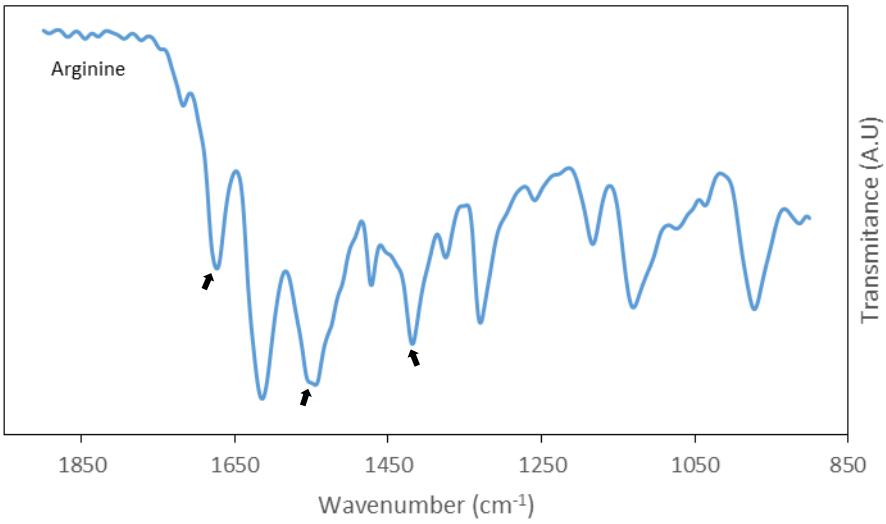

Figure 5. 17: Typical peaks observed in an arginine FTIR spectrum.

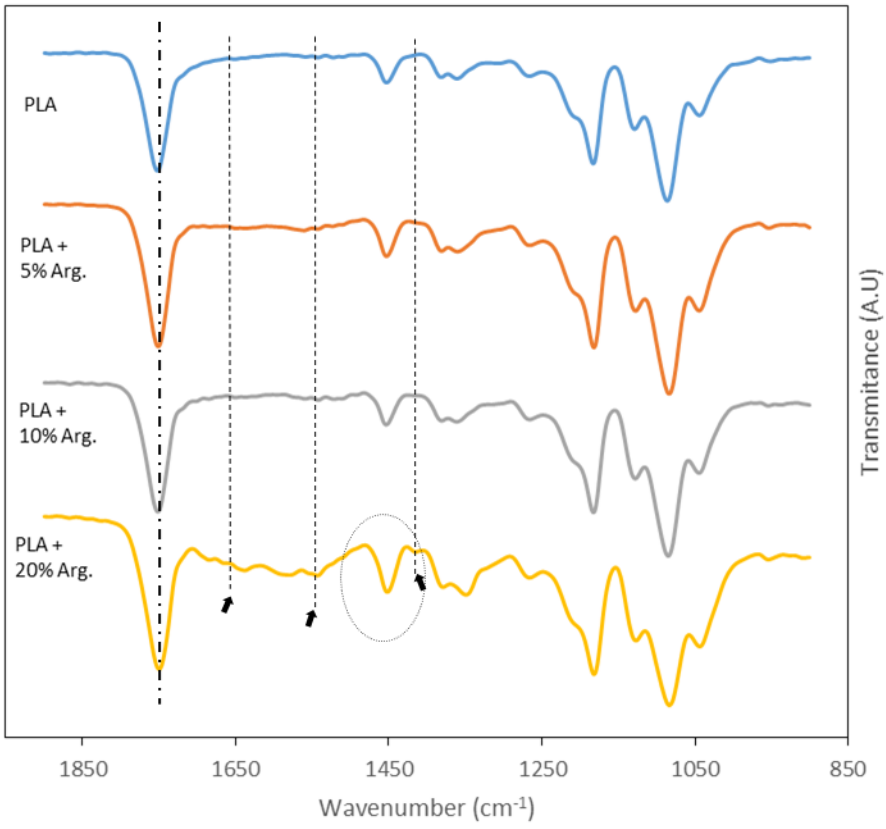

Figure 5. 18: Comparison of different percentages of arginine samples.

Figure 5. 18 shows the comparison of the different spectra of mats loaded with different percentages of arginine. Depending on how much arginine the mat has, the effect of the arginine is easier to see. For instance, in the PLA-20%Arg the

characteristic bands previously described can still be observed. This incorporation is also noticeable from the changes in the relative intensity of some other bands, such as that appearing after the band at 1409 cm^{-1}.

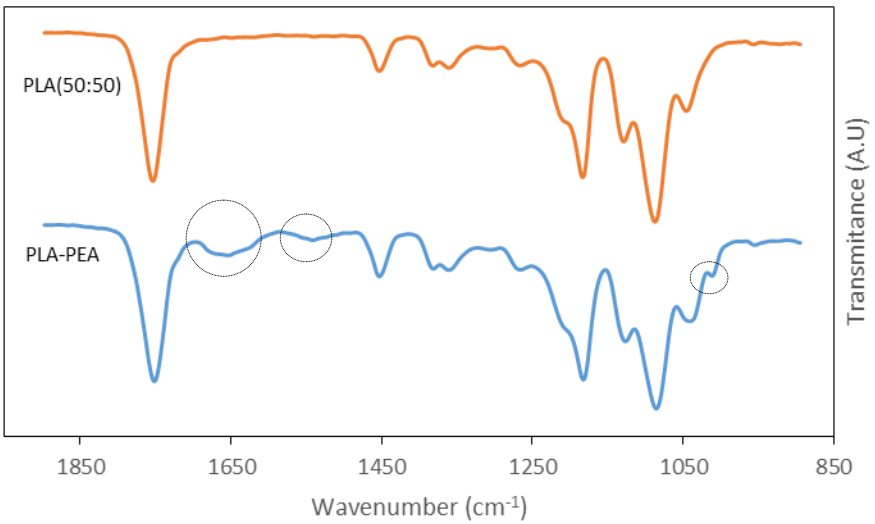

Figure 5. 19: Comparison of the FTIR spectra between PLA* and PLA-PEA.

Figure 5. 19 shows the effect of mixing the pure PLA with one representative Arg-based polymer (i.e. PEA). In all the samples is possible to observe the same effects. Around 1650 cm^{-1} is possible to observe the CO stretching which corresponds to the Amide I. At 1550 $cm^{-1}$is visible a peak that should be assigned with the Amide II. Finally, the CN stretching (characteristic of aliphatic amines) is noticeable at around 1010 cm^{-1} [74].

5.4.5. - Thermal analysis

The thermal properties of the different materials produced were tested by a differential scanning calorimeter and, when necessary with a thermal gravimetric analysis to know the degradation temperatures of the samples. In the DSC analysis the protocol was the same for all the samples. The protocol consists of four different scans. In the first scan the information about the melting of the electrospun mat is obtained. Thus, in this first heating made at 20 °C/min the crystallinity of the mat can be calculated. The endothermic peak represents the melting with a regular and gradual step up, depending on the sample nature. After this rise there is a drop until the recovery of the baseline.

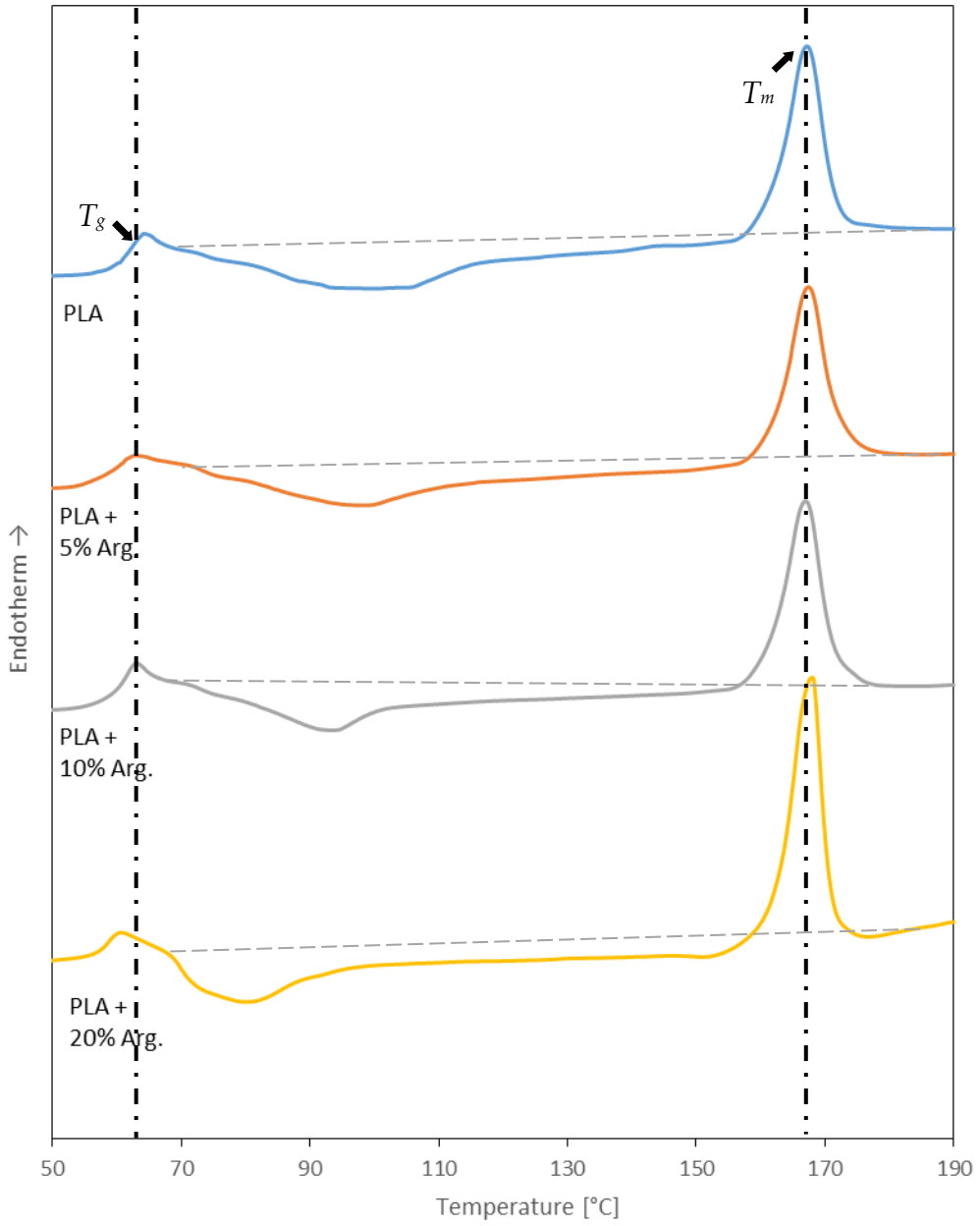

Figure 5. 20: Effects produced in the characteristic temperatures of the electrospun samples containing arginine.

The recovery and maintenance of the baseline means that the polymer is stable during the fusion and also at a bit higher temperatures. This is an important characteristic that means that the material could be easily processed once melted. On the contrary, if other different peaks appear, the polymer is not capable to be processed at higher temperatures than the melting point because it suffers decomposition or it is not stable. Spectra show also a glass temperature transition

at temperatures close to 65 ºC that has an appearance of n exothermic peak as a consequence of a relaxation process that is typical of PLA samples.

After the first fusion, a cooling down is done at 10 °C/min in order to see the crystallization of the material. This scan has the purpose of obtaining the exothermic peaks that appear when the crystallization happens. The area of this peak indicates the percentage of the polymer that can non-isothermally crystallize from the melt state.

The following scans, third and fourth correspond to the hating runs of the previously crystallized sample and of a melt quenched sample- The last is carried out to obtain information about the glass transition temperature of the different materials. Depending on the mixtures the temperatures of the scans vary, but usually they go from -50 °C or 0 °C to a temperature around 200 °C. This maximum temperature depends on the degradation temperature of the material. Through the thermal gravimetric analysis the exact degradation temperature of the materials was accurately obtained.

The addition of the arginine to the PLA in the mats produces some changes that are clearly visible in Figure 5. 20. First of all, the cold crystallization suffers a shift to the left. This means that the more arginine the mat has, the lower the crystallization temperature is. It is observable as well that the relaxation peak appears in some cases only some degrees before crystallization took place. The glass transition temperature seemed to slightly decrease with the addition of the small Arg molecules (i.e. a maximum shift of 2.5 ºC was observed at the maximum load). Calorimetric traces also showed that the melting point was not affected by the addition of arginine, which means that it was not effectively incorporated in the crystalline PLA phase

Nevertheless, it is important to point out that the PLA-20%Arg electrospun sample presents some areas that are richer in arginine (i.e. a content close to 30%) than others and, therefore, the results of the DSC were different. To prove that, an NMR of the sample was carried out in different zones. Therefore, the NRM spectra were obtained from different mat regions. Specifically, a content of 29% was found in some scarce regions were arginine aggregates were formed. In this case, the DSC curve (Figure 5. 21) presents two different melting points and two separated crystallizations also. The red dashed line which represent the supposed crystallization of arginine. This second crystallization process is complex since the melting of PLA is also produced, interfering in the shape of the crystallization peak.

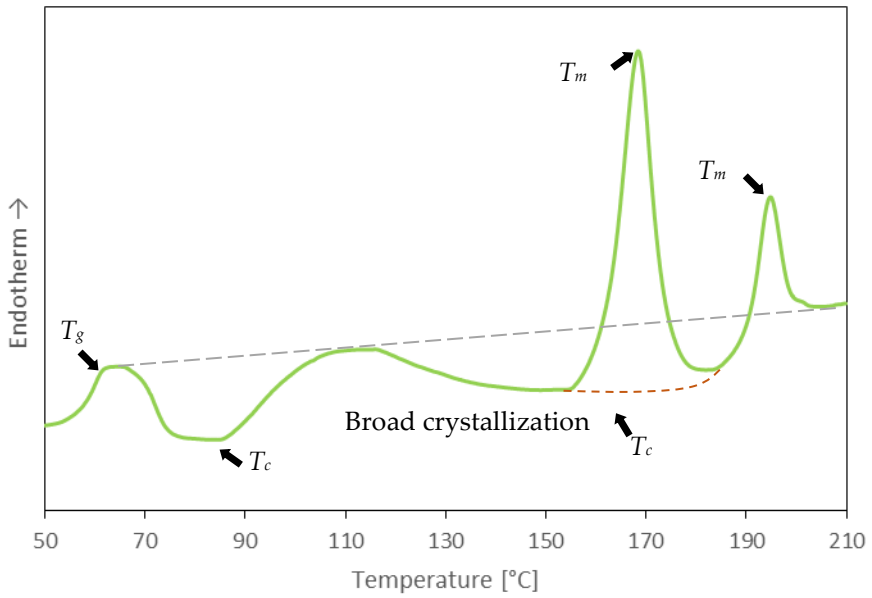

Figure 5. 21: DSC analysis of an arginine rich zone of the PLA-20%Arg sample.

Table 5. 8 summarized the main thermal parameters deduced from the different studied mats. It could be observed that the addition of Arg has no effect on the melting temperature (T_m). The glass transition temperature (T_g) becomes lower at the same time that the amount of arginine increases. This happens as well in the crystallization temperature but there is a higher difference (around 20 °C). At lower values of arginine the variation of the crystallization enthalpy is almost insignificant compared with the pure PLA sample, but nevertheless in the PLA-20%Arg sample the ΔH_c is increased more notoriously. The melting enthalpy was consequently increased as the arginine quantity did, suggesting a nucleation effect, a feature that is in agreement with the observed decrease on the cold crystallization temperature. These phenomena could be better explained by taking into account the diameter of the electrospun fibers. As mentioned previously, the higher the content of arginine is, the lower the diameter of the fiber will be. This variation is zero for the PLA-5%Arg sample but it is much more noticeable for the PLA-20%Arg. Therefore, as the fibers are thinner they could be more oriented and thus it is easier for the polymer to crystallize. Finally, in the table could be observed that the crystallinity, as it was expected, increases as well with the addition of arginine.

Material	T_g [°C]	ΔC_p [J/g°C]	T_c [°C]	T_m [°C]	ΔH_c [J/g]	ΔH_m [J/g]	ΔH_m - ΔH_c [J/g]
PLA	62.3	0.9	101.5	167.1	31.7	32.4	0.7
PLA 5%Arg	61.0	0.8	98.3	167.5	31.2	33.2	2.0
PLA 10%Arg	61.7	0.7	92.8	166.9	31.7	34.6	2.9
PLA 20%Arg	58.6	0.5	80.3	168.0	35.4	42.0	6.6

Table 5. 8: Thermal properties of the samples loaded with arginine.

In the following table all data obtained from the DSC analysis of the scaffolds prepared with the Arg-based polymers are summarized. At first sight, the only noticeable change is the reduction of the crystallization temperature when 20% of an Arg-based polymer is added. It could be observed that both the glass transition temperature and the melting temperature remain at the same values with variations of less than around one degree. Finally, the crystallinity variation of the analyzed polymers can also be considered as negligible.

Material	T_g [°C]	ΔC_p [J/g°C]	T_c [°C]	T_m [°C]	ΔH_c [J/g]	ΔH_m [J/g]	ΔH_m - ΔH_c [J/g]
PLA*	62.2	0.7	105.9	159.8	31.8	32.5	0.7
PLA-PEA	61.8	0.9	83.1	167.4	29.8	31.9	2.1
PLA-PEUR	62.3	0.9	81.4	167.9	29.9	31.0	1.1
PLA-PEEUR-1	61.9	0.8	86.3	166.6	29.9	31.0	1.1
PLA-PEEUR-2	60.6	0.8	83.2	167.1	30.1	31.5	1.4
PLA-PEEUR-3	61.3	0.7	83.2	166.5	31.6	32.7	1.1
PLA-PEEUR-4	60.2	1.0	80.3	166.7	29.9	31.7	1.8

Table 5. 9: Thermal properties of electrospun samples loaded with the different Arg-based polymers.

5.4.6. - Contact angle

Hydrophobicity of the prepared mats was tested by the contact angle analysis. In these tests a distilled water drop of 0.5 μL was released in the surface of the mat. The angle between the drop and the surface was measured. The results obtained are presented in the graphs below. It is interesting that the incorporation of the PHMB increased the contact angle. The expected result would be to be lower because of the hydrophilic behavior of the PHMB. Also, it is commonly known

that the smaller the fiber diameter is the lower the roughness results and therefore the lower contact angle will be. As the diameter of the PLA-PHMB sample is much lower compared to the pure PLA sample (around a 40%) the expected result would be to have a higher hydrophilicity. But surprisingly the results of the measurements show just the opposite. The explanation of this phenomenon is that the addition of the biguanide groups to the system produce the establishment of hydrogen bonding interactions with the polylactide ester groups.

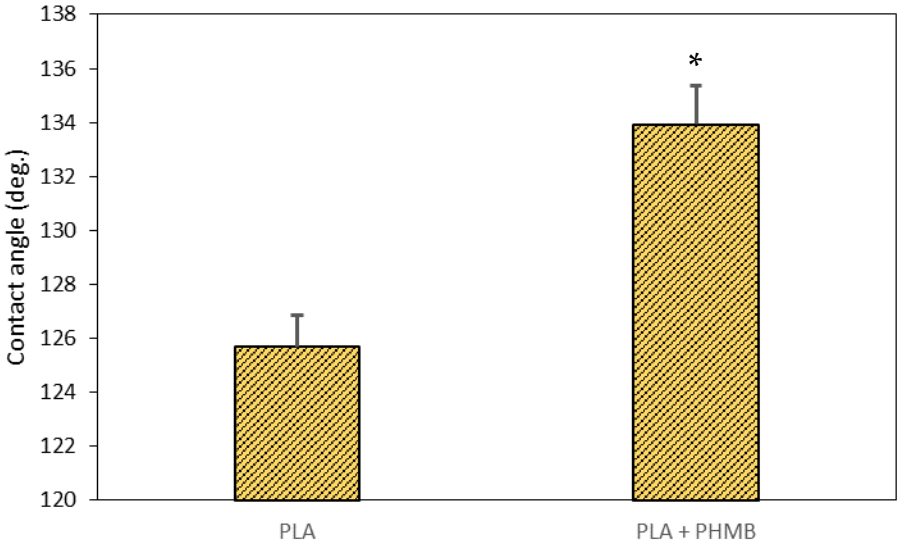

Figure 5. 22: Comparison of the contact angle measured in the PLA and PLA + 0.25%PHMB. Tukey's test: *, $p < 0.05$ VS PLA.

The same effect of having higher contact angle was observed in the samples that contain different percentages of arginine. The expected result should be again to have a more hydrophilic surfaces due to the positive charge of the arginine. It is important to point out that being the diameter of the PLA-5%Arg sample approximately the same as the pure PLA sample, the contact angle is much higher. Here the availability of many hydrogens in the lateral group of the arginine make easier the hydrogen bonding interaction with the polylactide ester groups. It could be observed that an increase of the amount of arginine contained in the mat let to a decrease of the contact angle. Here the diameter, and consequently the roughness, really plays an important role because of the direct relation between of the arginine and the fiber diameter.

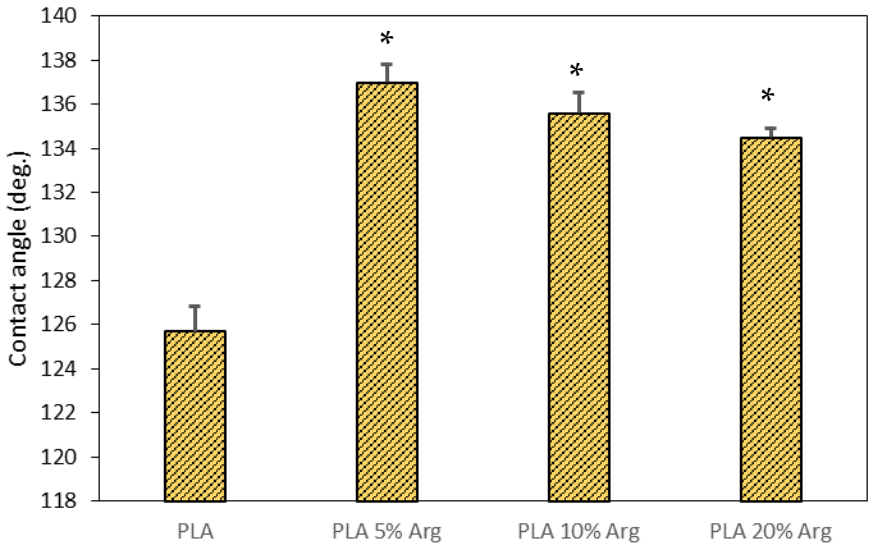

Figure 5. 23: Influence of the quantity of arginine on the contact angle. Tukey's test: *, $p < 0.05$ VS PLA.

All samples produced with the different types of Arg-based polymers showed the same behavior. Just after leaving the drop in contact with the mat it was absorbed by the scaffold. The explanation for this behavior could be the low roughness of the samples due to the small diameter of the fibers. This phenomenon happens in all the samples tested and in different regions of the mats therefore it can be concluded that all the scaffolds prepared that included whichever of the Arg-based polymers are completely hydrophilic.

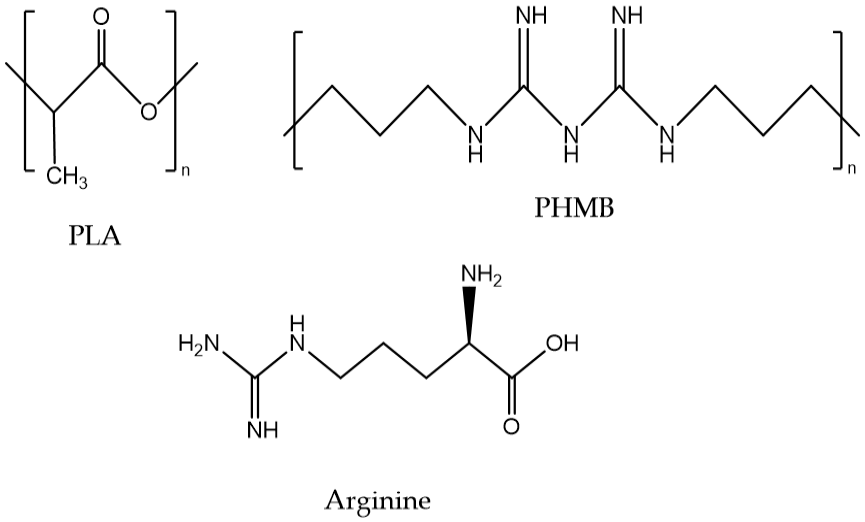

Figure 5. 24: Structural formula of the PLA, PHMB and arginine.

5.4.7. - Synchrotron radiation

The WAXD profiles of PLA scaffolds loaded with cationic polymers showed only an amorphous halo at low temperatures. Thus, PLA was unable to crystallize during the electrospinning process. Nevertheless, crystallization occurs during the subsequent heating as deduced from the apparition of typical PLA reflections. This crystallization begins at around 85°C and has its maximum at 145 °C. At 165 °C the sample completely melts. This behavior is observed in all the Arg-based polymers. It is meaningful that PLA is able to crystallize after being electrospun since this treatment leads to a significant molecular orientation. Note that PLA crystallize with difficulty when it is slowly cooled from the melt state where chains are completely disordered.

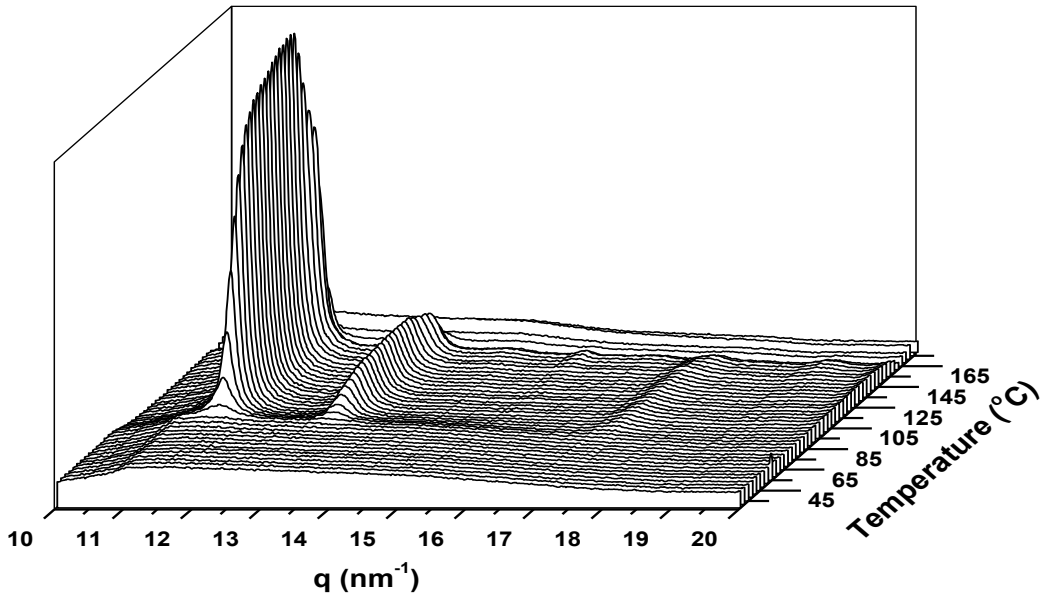

Figure 5. 25: Representative example of WAXD analysis at different temperatures carried out with a PLA scaffold loaded with an Arg-based polymer.

5.5. - Observation of phages by TEM

Through the observation of TEM images of samples prepared following the protocol described in the Materials and method section some comments are possible about the phages used in this research. TEM micrographs reveal, at the

morphological level, that all bacteriophages of the suspension characterized so far belong to the group called *Caudovirales*. More precisely, the two main groups observed were the *Myoviridae* and the *Siphoviridae*. The *Myoviridae* phages are characterized by a contractile tail, an icosahedral capsid and for being nonenveloped virus. The characteristics of the *Siphoviridae* phage are an icosahedral capsid and a long non-contractile tail. Furthermore the *Siphoviridae* phage is also a nonenveloped virus [75]. In the following image it is possible to observe the differences between the two types of bacteriophages.

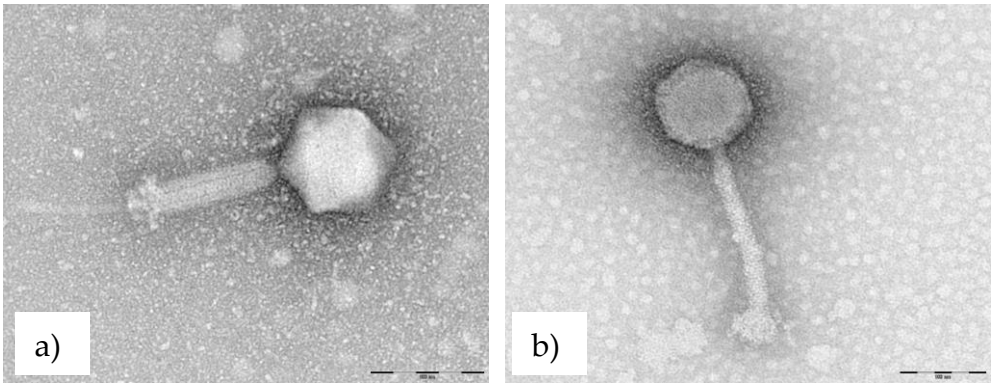

Figure 5. 26: TEM images of bacteriophages. a) *Siphoviridae* phage with non-contractile tail. b) *Myoviridae* phage with its characteristics contractile tail.

5.6. - Bacterial growth inhibition

The adsorption of bacteriophages in the electrospun mats did not make any change on the fibers characteristics. Both the size and the distribution remain constant. To determine the adsorption of the phages a lytic study was carried out using as hostage bacteria the *S. aureus.* Results are presented in Figure 5. 27. , where it is easily possible to see that the number of adsorbed phages on the scaffolds was quite low. The range of adsorbed phages was 10^2-10^3 pfu/g of mat compared to the quantity of phages (10^5 pfu/ml) at which the mats were exposed by direct contact. However, different observations could be developed from these results:

1. The scaffolds prepared with the PLA homopolymers do not show any lytic activity. This fact shows the low tendency of the phages to be non-specifically bound to these fibers. This result could also be interpreted as the experimental design used was the optimal due to the fact that non-specific interactions occur.

2. The antibacterial activity of the mat loaded with PHMB cannot be assessed because the releasing of the PHMB is too high and gives consequently rise to a significant antibacterial effect on the hostage bacteria of the phages.

3. In testing conditions, the scaffolds loaded with arginine present the same capacity to adsorb phages (with values of $2.3x10^2$-$3x10^2$ pfu/g of mat) independently of the percentage of arginine.

4. The scaffold of PLA-PEA and PLA-PEEUR1 show the worse results of bacteriophage adsorption, $7x10^1$ pfu/g of mat.

5. Finally, the mat produced with PLA and PEUR shows the higher bacteriophage adsorption. The PLA-PEUR scaffold also shows a high variation on the loaded amount when different experiments are compared.

This results suggest that the presence of positive charges derived from the incorporation of arginine has a limited effect on the surface of the fibers. In fact, the distribution of either the aminoacic or the Arg-based polymer is uniform over the fibers as it was previously evidenced from calorimetric analysis as well as the X-ray diffraction. There is a partly modification of the fibers surface as it is proved by the contact angle analysis. However, this modification appears not to be great enough to promote a high phage load on the surface of the fibers.

Then, the addition of the positive charges on the fibers may have an asymmetrical distribution encouraging their distribution onto the surface to make easier the phage adsorption.

This observation lead to further studies on new scaffolds for phage adsorption (e.g. a core shell fiber where the shell corresponds to the cationic domain given by the arginine). Other proposal could be the preparation scaffolds where the fibers are superficially modified by the incorporation of coating polymers or by decoration with arginine compounds.

Sample	Phage activity (PFU/g)		
	Mean Count	Min. Count	Max. Count
PLA	0	---	---
PLA-PHMB	---	---	---
PLA-5%Arg	$2.3x10^2$	$2x10^2$	$3x10^2$
PLA-10%Arg	$3x10^2$	$1x10^2$	$6x10^2$
PLA-20%Arg	$3.7x10^2$	$3x10^2$	$4x10^2$
PLA*	0	---	---
PLA-PEA	$7x10^1$	0	$1x10^2$
PLA-PEUR	$6x10^2$	$1x10^2$	$1.1x10^3$
PLA-PEEUR1	$7x10^1$	0	$1x10^2$
PLA-PEEUR2	$1x10^2$	0	$2x10^2$
PLA-PEEUR3	$2x10^2$	0	$2x10^2$
PLA-PEEUR4	$3.7x10^2$	$2x10^2$	$5x10^2$

Figure 5. 27: Lytic activity of bacteriophage adsorbed in the electrospun samples.

5.7. - In-Vitro biocompatibility assay: cell adhesion and proliferation

Cellular adhesion and proliferation assays on electrospun scaffolds were determined with MDCK cells, which are epithelial-like cells. Cellular adhesion was determined 24 h after the culture began while the proliferation assay was evaluated after 7 days.

Cell adhesion results are shown in Figure 5. 28. It is easily observed that either the pure arginine or the Arg-based loaded mats have no early cytotoxic effects when are put in direct contact with the cells (Figure 5. 28 a,b). About the adhesion assay on the electrospun scaffolds (Figure 5. 28 c,d)., it should be pointed out that the mats loaded with arginine load show a decrease on the number of cells attached. Being clearly meaningful ($p<0.05$) this decrease of the number of cells in the scaffold prepared with 5% and 20% of arginine when compared to the control or the PLA mat.

When analyzing the PLA-PEA and PLA-PEUR mats, it is possible to observe a significant decrease ($p<0.05$) compared to the control. Furthermore, the scaffolds

with different types of PEEURs show an increase in the number of cells attached related to the spacing of the arginine residues. Although no significant differences are observed between the control, the PLA and the PEEUR mats, it is possible to see differences on the scaffolds of PLA-PEA and PLA-PEUR (Figure 5. 28 d).

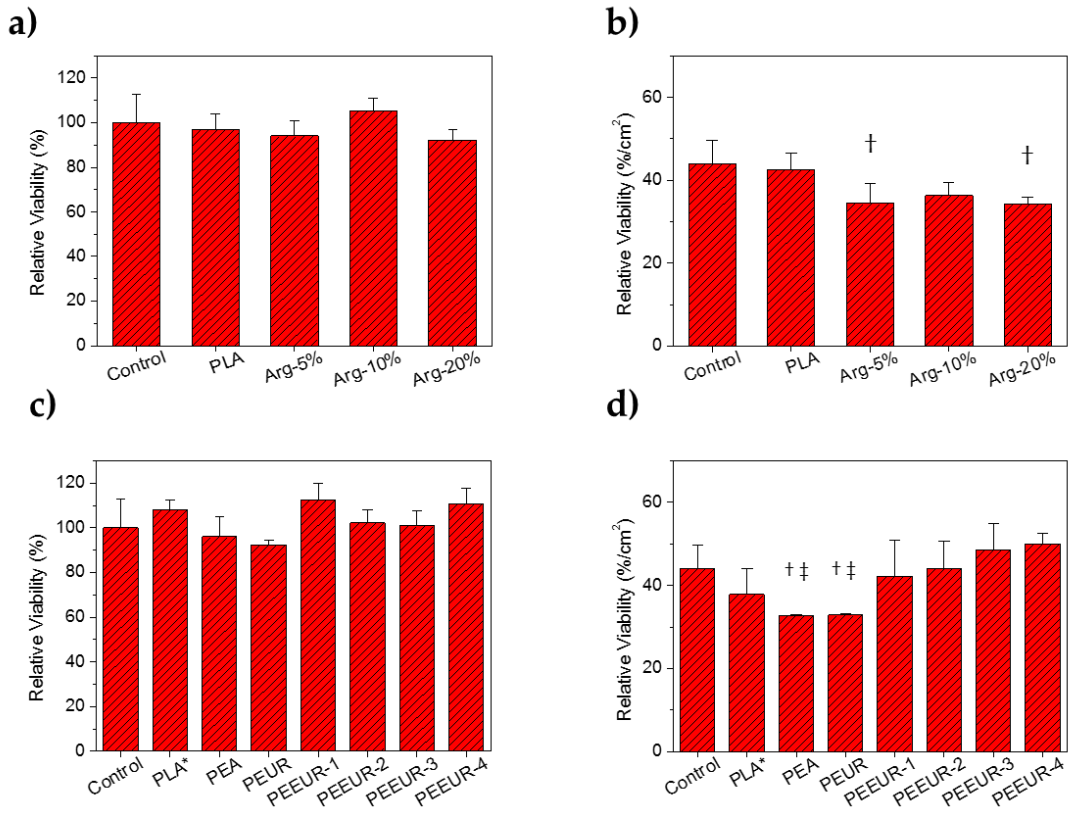

Figure 5. 28: Cellular adhesion onto electrospun scaffolds loaded with Arg (a,b) or prepared from mixtures of PLA and PEA, PEUR or PEEUR (c,d). Total viability to evaluate the cytotoxic effects (a,c). Viability normalized by electrospun surfaces (b,d). Tukey test, †p <0.05 vs PLA; ‡p<0.05 vs PEEUR3 and 4.

Proliferation assay results are shown in Figure 5. 29. Cell culture of MDCK cells show that either the PLA scaffolds loaded with arginine (Figure 5. 29 a) or the Arg-based polymer scaffolds are completely biocompatible (Figure 5. 29 c).The culture time of 7 days was enough to correct the cellular decrease observed in the adhesion assay of the mats loaded with arginine. However, the PLA-PEEUR3 and PLA-PEEUR4 mats show significant ($p<0.05$) increase of the number of cells compared to the control and the PLA scaffold. The higher increase could be again related to the spacing between the arginine residues.

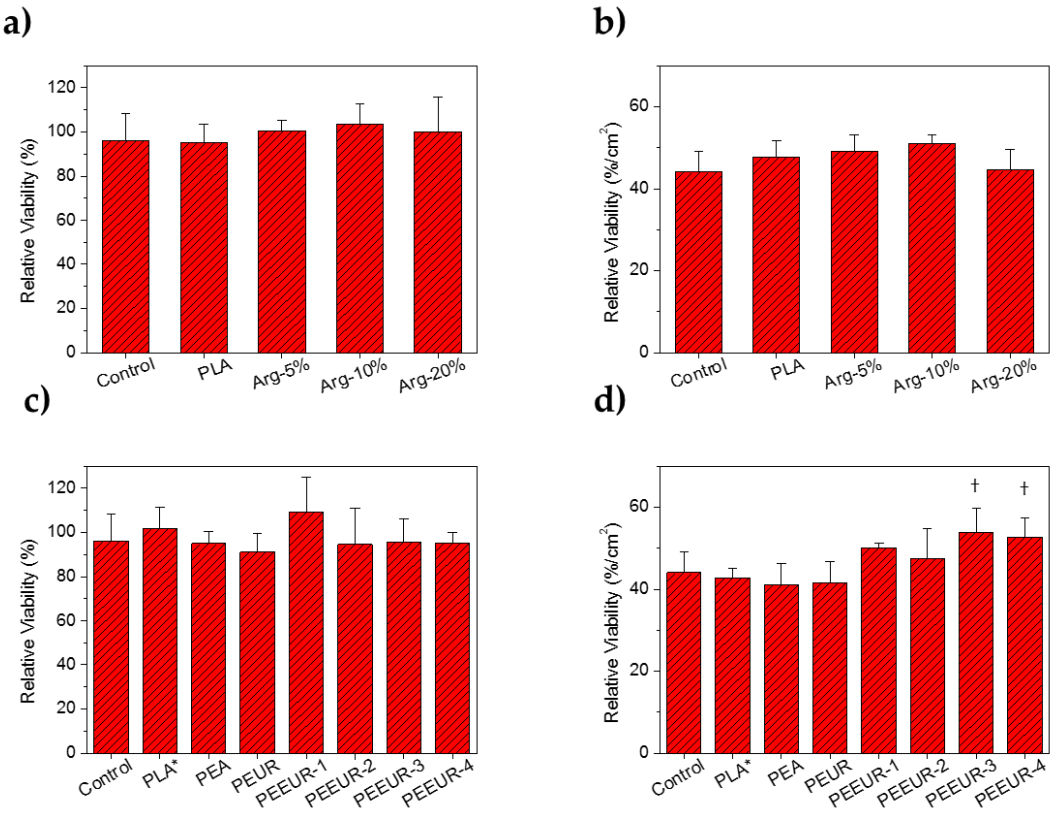

Figure 5. 29: Cellular proliferation onto electrospun mats loaded with Arg (a,b) or prepared from mixtures of PLA and PEA, PEUR or PEEUR (c,d). Total viability to evaluate the cytotoxic effects (a,c). Viability normalized by electrospun surfaces (b,d). Tukey test, †p <0.05 vs control and PLA matrix

Finally, from the biocompatibility results it could be pointed out that the scaffolds with different cationic arginine compounds are completely biocompatible and the PEEURs with higher spacing between the arginine residues promote the cellular proliferation.

In Figure 5. 30 SEM micrographs are presented showing qualitatively the cellular proliferation. Figure 5. 30 a) and b) are the micrographs of the MCDK cells proliferation control on the PLA fibers. It is observable that the cells are completely stretched forming the typical uniform cell monolayer. A similar proliferation was observed in all the studied scaffolds. The cellular spreading is guided by the fibers, being this a clear indicative of the biocompatibility and cell colonization on the fiber mats (e.g. Figure 5. 30 d) and j) detailed of the extensions such as lamellipodia).

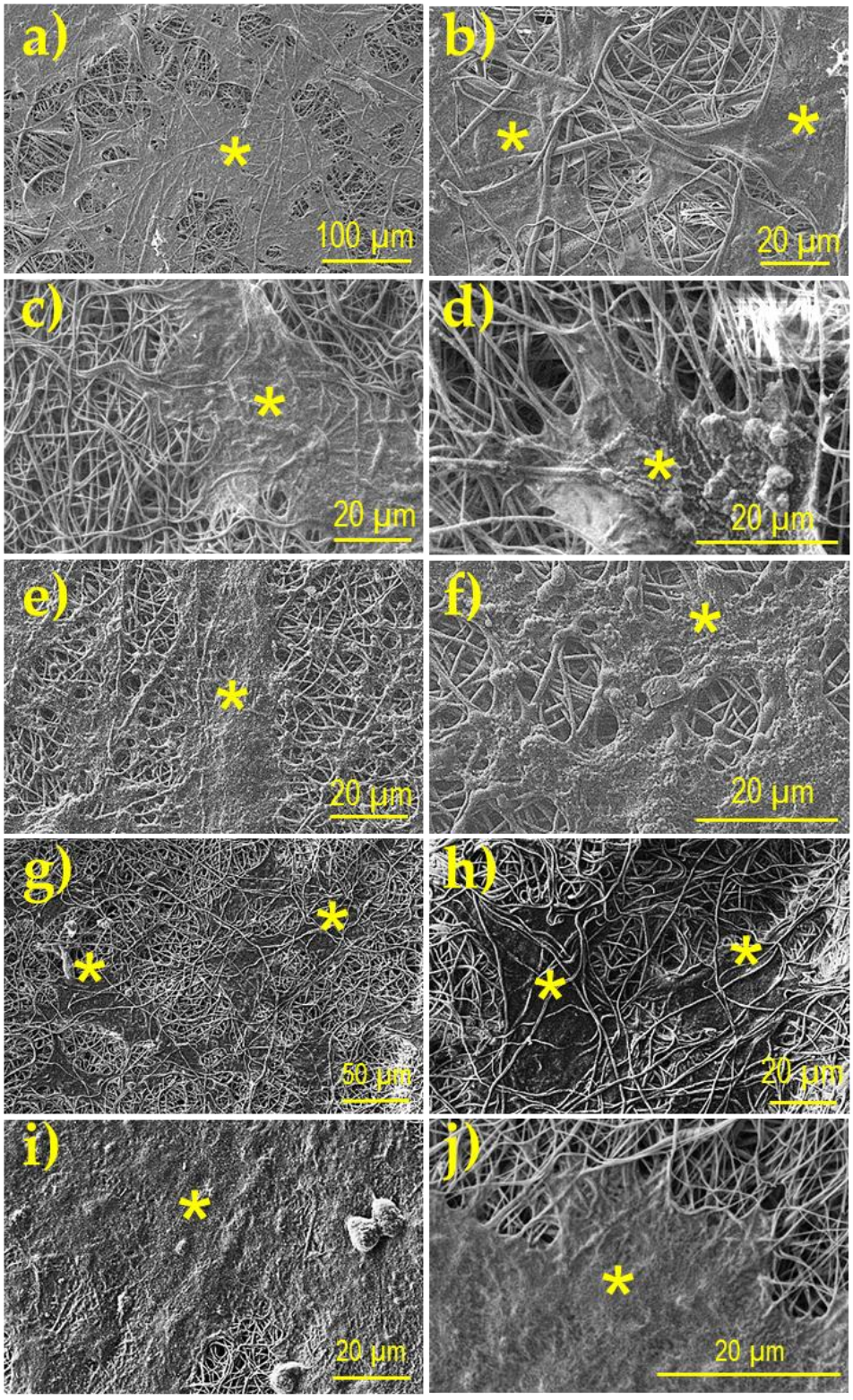

Figure 5. 30: Different micrographs of some representative scaffolds. a) and b) PLA mat; c) and d) PLA-20%Arg; e) and f) PLA-PEA; g) and h) PLA-PEUR; i) and j) PLA-PEEUR2

CHAPTER VI: CONCLUSIONS AND RECOMMENDATIONS

Once the study is finished and the results have been analyzed, the following conclusions could be formulated:

1. The characteristic temperatures and thermal properties of the arginine containing polymers are very similar. All these new synthetized biodegradable polymers are completely amorphous and present close molecular distributions.

2. The operational parameters for the electrospinning process change considerably in function of the polymer solution. The polymer solution also needs to be precisely tuned precisely to obtain the proper quality for the electrospinnable solution.

3. The PLA scaffolds always show a typical rough fiber surface independently of the solvent employed. On the contrary, the addition of any of the arginine compounds to the PLA solution leads to a smother fiber surface.

4. The addition of either PHMB or pure arginine decrease the fiber diameter. On one hand, the increase of the amount of pure arginine loaded into the fiber caused proportional decrease of the fiber diameter. On the other hand, the type of the arginine polymer derivative added to the PLA solution does not play any significant role in the fiber diameter.

5. In the FTIR analysis is easy to see the addition of high percentages of pure arginine (e.g. 20%). However, the addition of either PHMB or the Arg-based polymers is more difficult to be appreciated.

6. The thermal properties of the scaffolds do not suffer any great variations with the incorporation of any of the studied compounds (pure arginine or arginine-based polymers). Only the T_C decreases when any of the compounds is added.

7. Contrary to expectations, when either PHMB or pure arginine is loaded to the PLA scaffold the contact angle increases. The decrease of the fiber diameter should leads to lower contact angles. Furthermore, the inclusion of any of the new synthetized biodegradable polymers should make the surface of the scaffolds more hydrophilic. Therefore, the observed deviations must be a consequence of the establishment of new interactions between PLA and the added compounds (note for example the high ability to form hydrogen bond interactions).

8. The loading of bacteriophages in the scaffolds by adsorption is feasible. Best results are obtained from the scaffolds containing arginine cationic compounds .The antibacterial activity of the scaffold loaded with bacteriophages shows good results in the double layer agar test being more effective those scaffolds with higher cationic charges.

9. The scaffolds produced are completely biocompatible as shown on the adhesion and proliferation cellular assays. PEEURs with higher spacing between the arginine residues promote the cellular proliferation. All the produced scaffolds loaded with cationic arginine compounds show the same behavior when the uniform cell monolayer was observed in the micrographs.

10. The potential application of the loaded fibers with bacteriophages seems to have more promising results and further studies should be carried out in this opened gap in the field off biomedicine and tissue engineering.

CHAPTER VII: SUSTAINABILITY OF THE PROJECT

The development of new biodegradable polymeric materials indicates sustainability on itself. It is possible to get realized of this just considering some present industries: packaging, textile or biomedicine. These industries promote the development of the polymer industry either because the creation of new polymer or the modifications developed to the existing ones.

The polymers studied in this master thesis are PLA and arginine containing polymers. Both are groups of polymers that are considered really important the science field due to its biodegradable properties. This biodegradable properties refer to the capacity of the polymer to degrade by ester bond hydrolysis.

Nowadays, the biodegradable polymers show different advantages for the environmental protection. The main advantages compared to conventional polymers are described in the following table:

Conventional polymers	Biodegradable polymers
Use non-renewable resources	Sustainable production from agroindustry subproducts
Cumulated in the ambient	Easily degraded by microorganisms action
Its recycling could generate toxic residues	Its degradation generates O_2 and H_2O

Table 7. 1: Environmental impact comparison between conventional and biodegradable polymers.

This sustainability study includes the ambient and healthy impact, the social impact, as well as the economic impact related to the project. The objectives of this study are presented below:

1. To identify, describe and evaluate the effects of the development of this project and its consequences on the ambient factors (healthy, natural resources and the environment.
2. The potential effects on the society (or part of it) if the project is developed and the environmental impact during its whole cycle life.
3. To evaluate the total cost of the project using a budget as a tool.

7.1. - Environmental, health and social impact evaluation

First of all, an evaluation of the danger that some substances involve is carried out. For that the applicable law in the European Union (EU) is the REACH (registration, evaluation, authorization and restriction of chemicals).

On 18th December 2006 this REACH regulation was approved, CE Regulation n 1907/2006 of the European parliament and the council. This regulation imply a total modification of the legal framework about chemicals in the EU. Its objective is to guarantee a high level of protection of the human health and environment.

Two years later, the regulation CE n 1227/2008 of the commission of the 18th December 2008 offers a set of criteria about the risk of the chemicals. This regulation is about the classification, labeling and packaging of substances and mixtures (CLP). The main objective is to ensure the human healthy as well as the environment protection, identifying all the physicochemical, toxic and Eco-toxic properties of the substances and mixtures.

To perform this part, the data of the mentioned section are used, hereby the healthy and environmental risk of the chemicals used in this investigation project are known. For this, the following table is formulated:

Substance	Type of hazard
Acetone	H225,H319, EUH066, H336
Chloroform	H302, H351, H373
Dichloromethane	H351
Dimethylformamide	H312, H319, H332, H360
Ethanol	H225
Formic acid	H314
Hexafluoroisopropanol	H302, H312, H314, H332
PEA	n/d
PEEUR	n/d
PHMB	H319
PLA	n/d

Table 7. 2: Chemical products and their class of hazard.

Statement	Type of hazard
EUH066	Continuous exposure may cause dryness and cracking on the skin.
H225	Liquid and vapor very flammable.
H302	Intake harmful.
H312	Skin contact harmful.
H314	May cause skin burn and severe ocular injuries
H319	Cause severe ocular irritation.
H332	Inhalation harmful.
H336	May cause drowsiness or vertigo.
H351	It is suspected to cause cancer.
H360	May harm the fertility or the fetus.
H373	Could cause injure to the organs over continuous or repeated exposure.

Table 7. 3: Hazard statements.

In reference of the environmental impact of the biopolymer used the PLA is not a harmful substance according to Directive 67/548/CEE.

The CE n 1272/2008 (CLP) regulation replace the Directive 67/548/CEE of the council of 27th June 1967, concerning to the legal, regulatory and administrative dispositions about the classification, labeling and packaging of dangerous substances and the Directive 1999/45/CE of the European Parliament and the council of 31st May 1999, concerning to the legal, regulatory and administrative dispositions of the estates members about the classification, labeling and packaging of dangerous preparations. This two regulations will be derogated on 1st June 2015.

Additionally, it is also interesting to study the social impact of this project if it is deeply developed in the near future. More specifically, in these people who would need the regeneration/substitution of the damaged tissue. The benefit that this people would have is that they don't need to suffer a surgery in order to extract the scaffold because it is biodegradable therefore achieving less pain and less risk due to the surgery.

It is important to say that, on the whole life cycle of these scaffolds the environmental impact is almost negligible due to its biodegradability.

In this section are included all of which are considered good practices by the institution: waste processing, waste-water and residues. The company responsible of the chemical waste generated by the ETSEIB laboratories is ECOCAT in collaboration with CST (*centre per la sostenibilitat territorial*).

The containers for storing special wastes are all made of high density polyethylene (HDPE) being hermetic those used for biohazard wastes. Some of the containers used are presented on Figure 7. 1.

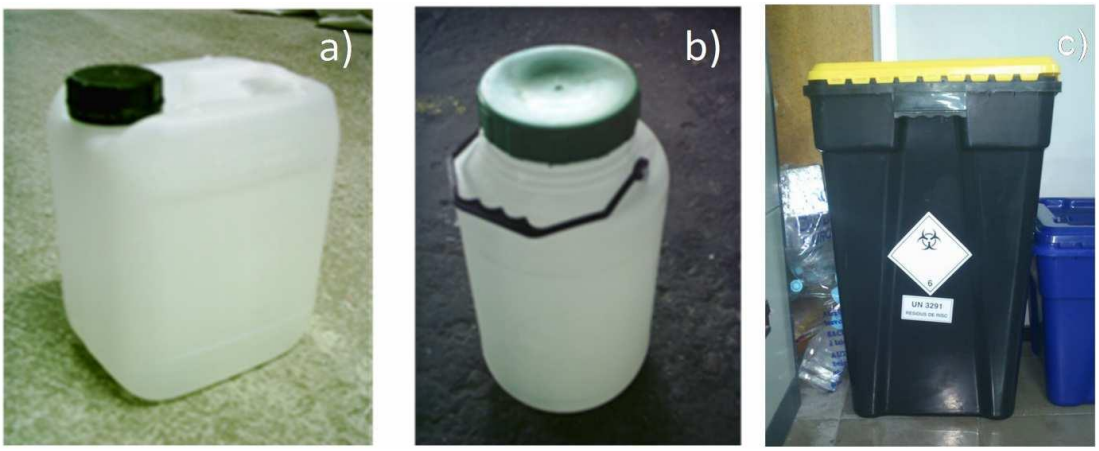

Figure 7. 1: Special waste storage: a) container for liquids, b) solids container, c) container for biohazard wastes.

7.2. - Economic evaluation of the project

In order to take decisions about the viability of the project it is necessary apart from the environmental evaluation to carry out an economical evaluation of the project. A bad evaluation in either the environmental study or the economic study could lead to the decision of not continue with a project even being this of high level.

To evaluate the total cost of the project is divided in four differentiated parts:

1. Cost of the solvents and chemical products required for the fiber mats manufacturing and for the cellular study. The price of these solvents as well as the chemical products are obtained from the supplier catalogue.
2. Personnel costs.

3. Equipment costs, taking into account amortization, the number of users that share the machine, an annual interest rate of 3% and the duration of the master thesis around 10 months.
4. Other costs.

In the following table the different costs are presented as well as the global cost that involve the development of this project.

Description				*Total (€)*
Solvents and chemicals costs				
Solvents	Quantity			
Acetone	2L			19.25
Chloroform	1L			81.15
Dichloromethane	1L			34.21
Dimetylformamide	1L			121.00
Ethanol	0.5L			4.26
Formic acid	0.5L			13.56
Subtotal solvents				273.43
Chemical products	Quantity			
PLA	Donated by Natureworks			0.00
PHMB	Donated by B.Braun			0.00
Bacteriophages	1			88.00
Subtotal chemical products				88.00
Others (+40% solvens and chemical products)				144.57
Total solvents and chemicals				**506.00**
Personnel costs				
Description	Quantity (h)	Price (€/h)		
Previous study and literature research	90	15		1350.00
Experimental	700	15		10500.00
Result analysis	240	15		3600.00
Total personnel costs				**15450.00**
Equipments costs				
Equipment	Price (€)	Amortization (years)	N. users	
Contact angle	3500	10	4	75.10
Electrospinning	3000	5	6	85.83
Optical microscope	12000	15	7	98.10

Camera O.M.	7800	5	7	191.29
SEM	210000	15	10	1201.67
DSC	62000	10	6	886.94
FTIR	24000	10	10	206.00
RMN	240000	25	10	824.00
UV	12000	10	12	85.83
GPC	28000	10	10	240.33
Synchrotron (external test)	375€/h	2 h use	-	750.00
Total equipment				**4645.10**
Activity budget				**20601.10**
Other costs				
+10% of the budget (cost of the supplies)				2060.11
Subtotal project				**22661.21**
Unforeseen expenses (+3% over the subtotal project)				679.84
Overhead (+21% over the subtotal project)				4758.85
TOTAL PROJECT				**28099.90**

REFERENCES

[1] R. Chandra and R. Rustgi, "BIODEGRADABLE POLYMERS," *Prog. Polym. Sci.*, vol. 23, no. 97, pp. 1273–1335, 1998.

[2] V. Bellon-Maruel, A. Calmon-Decriaud, and F. Ivestre, "Blockcopolymers - Polyelectrolytes - Biodegradation," *Adv. Polym. Sci.*, vol. 135, May 1998.

[3] M. Blanco, "Liberación de Triclosan a partir de hilos de sutura monofilares.," Etseib, UPC, 2007.

[4] a. J. C. Langford, J.I. and Wilson, "Seherrer after Sixty Years: A Survey and Some New Results in the Determination of Crystallite Size," *J. Appl. Cryst.*, vol. 11, pp. 102–113, 1978.

[5] L. S. Nair and C. T. Laurencin, "Biodegradable polymers as biomaterials," *Prog. Polym. Sci.*, vol. 32, no. 8–9, pp. 762–798, 2007.

[6] R. Moriana, "Desarrollo y caracterización de biocomposites enfibrados procedentes de recursos renovables. Estudio de su degradación en tierra.," UPV, 2010.

[7] T. Y. Cho and G. Strobl, "Temperature dependent variations in the lamellar structure of poly(l-lactide)," *Polymer (Guildf).*, vol. 47, no. 4, pp. 1036–1043, 2006.

[8] T. J. Sill and H. A. von Recum, "Electrospinning: applications in drug delivery and tissue engineering.," *Biomaterials*, vol. 29, no. 13, pp. 1989–2006, May 2008.

[9] R. A. Rodríguez Galán, M. L. Franco García, and J. Puiggalí Bellalta, "Biodegradable Poly(Ester Amide)s: Synthesis and Applications," G. P. Felton, Ed. Nova Science, 2011.

[10] A. Rodriguez-Galan, L. Franco, and J. Puiggali, "Degradable poly(ester amide)s for biomedical applications," *Polymers (Basel).*, vol. 3, no. 1, pp. 65–99, 2011.

[11] W. J. Pangman, "United States Patent Office," 1958.

[12] P. Alves, P. Ferreira, and M. H. Gil, "BIOMEDICAL POLYURETHANES-BASED MATERIALS," in *Chapter 1*, pp. 1–25.

[13] A. Gugerell, J. Kober, T. Laube, T. Walter, S. Nürnberger, E. Grönniger, S. Brönneke, R. Wyrwa, M. Schnabelrauch, and M. Keck, "Electrospun poly(ester-urethane)- and poly(ester-urethane-urea) fleeces as promising tissue engineering scaffolds for adipose-derived stem cells," *PLoS One*, vol. 9, no. 3, pp. 1–14, 2014.

[14] P. Alves, J. F. J. Coelho, J. Haack, A. Rota, A. Bruinink, and M. H. Gil, "Surface modification and characterization of thermoplastic polyurethane," *Eur. Polym. J.*, vol. 45, no. 5, pp. 1412–1419, 2009.

[15] X. Gao, K.-S. Kim, and D. Liu, "Nonviral gene delivery: what we know and what is next.," *AAPS J.*, vol. 9, no. 1, pp. E92–E104, 2007.

[16] A. Díaz, L. J. del Valle, D. Tugushi, R. Katsarava, and J. Puiggalí, "New poly(ester urea) derived from l-leucine: Electrospun scaffolds loaded with antibacterial drugs and enzymes," *Mater. Sci. Eng. C*, vol. 46, pp. 450–462, 2015.

[17] T. Memanishvili, N. Zavradashvili, N. Kupatadze, D. Tugushi, M. Gverdtsiteli, V. P. Torchilin, C. Wandrey, L. Baldi, S. S. Manoli, and R. Katsarava, "Arginine-based biodegradable ether-ester polymers with low cytotoxicity as potential gene carriers," *Biomacromolecules*, vol. 15, no. 8, pp. 2839–2848, 2014.

[18] T. Koburger, N. O. Hübner, M. Braun, J. Siebert, and a. Kramer, "Standardized comparison of antiseptic efficacy of triclosan, PVP-iodine, octenidine dihydrochloride, polyhexanide and chlorhexidine digluconate," *J. Antimicrob. Chemother.*, vol. 65, no. 8, pp. 1712–1719, 2010.

[19] K. Kaehn, "Polihexanide: A safe and highly effective biocide," *Skin Pharmacol. Physiol.*, vol. 23, no. SUPPL. 1, pp. 7–16, 2010.

[20] L. P. O'Malley, C. H. Shaw, and a. N. Collins, "Microbial degradation of the biocide polyhexamethylene biguanide: Isolation and characterization of enrichment consortia and determination of degradation by measurement of stable isotope incorporation into DNA," *J. Appl. Microbiol.*, vol. 103, no. 4, pp. 1158–1169, 2007.

[21] F. L. Rose and G. Swain, "Polymeric Diguanides. Great Britain Patent 702.," 1954.

[22] O. Lebel, T. Maris, and J. D. Wuest, "Hydrogen-bonded networks in crystals built from bis(biguanides) and their salts," *Can. J. Chem.*, vol. 84, no. 10, pp. 1426–1433, 2006.

[23] H. a. Pearson, G. S. Sahukhal, M. O. Elasri, and M. W. Urban, "Phage-bacterium war on polymeric surfaces: Can surface-anchored bacteriophages eliminate microbial infections?," *Biomacromolecules*, vol. 14, no. 5, pp. 1257–1261, 2013.

[24] Z. Golkar, O. Bagasra, and D. Gene Pace, "Bacteriophage therapy: A potential solution for the antibiotic resistance crisis," *J. Infect. Dev. Ctries.*, vol. 8, no. 2, pp. 129–136, 2014.

[25] F. L. Nobrega, A. R. Costa, L. D. Kluskens, and J. Azeredo, "Revisiting phage therapy: new applications for old resources," *Trends Microbiol.*, vol. 23, no. 4, pp. 185–191, 2015.

[26] G. Verbeken, J. P. Pirnay, R. Lavigne, S. Jennes, D. De Vos, M. Casteels, and I. Huys, "Call for a dedicated European legal framework for bacteriophage therapy," *Arch. Immunol. Ther. Exp. (Warsz).*, vol. 62, no. 2, pp. 117–129, 2014.

[27] M. Deghorain and L. Van Melderen, "The staphylococci phages family: An overview," *Viruses*, vol. 4, no. 12, pp. 3316–3335, 2012.

[28] A. Sulakvelidze, "The challenges of bacteriophage therapy," *Ind. Pharm.*, vol. 45, no. 31, pp. 14–18, 2011.

[29] D. Jikia, N. Chkhaidze, E. Imedashvili, I. Mgaloblishvili, G. Tsitlanadze, R. Katsarava, J. G. Morris, and A. Sulakvelidze, "The use of a novel biodegradable preparation capable of the sustained release of bacteriophages and ciprofloxacin, in the complex treatment of multidrug-resistant Staphylococcus aureus-infected local radiation injuries caused by exposure to Sr90," *Clin. Exp. Dermatol.*, vol. 30, no. 1, pp. 23–26, 2005.

[30] M. Kutateladze and R. Adamia, "Bacteriophages as potential new therapeutics to replace or supplement antibiotics," *Trends Biotechnol.*, vol. 28, no. 12, pp. 591–595, 2010.

[31] E. T. Pimienta-rodríguez, "Tratamiento con bacteriófagos como una alternativa antimicrobiana potencial," *Rev. CENIC Ciencias Biológicas*, vol. 44, no. 2, 2013.

[32] R. Capparelli, M. Parlato, G. Borriello, P. Salvatore, and D. Iannelli, "Experimental phage therapy against Staphylococcus aureus in mice," *Antimicrob. Agents Chemother.*, vol. 51, no. 8, pp. 2765–2773, 2007.

[33] E. Morello, E. Saussereau, D. Maura, M. Huerre, and L. Touqui, "Pulmonary Bacteriophage Therapy on Pseudomonas aeruginosa Cystic Fibrosis Strains : First Steps Towards Treatment and Prevention," vol. 6, no. 2, 2011.

[34] K. Markoishvili, G. Tsitlanadze, R. Katsarava, J. G. Morris, and A. Sulakvelidze, "A novel sustained-release matrix based on biodegradable poly(ester amide)s and impregnated with bacteriophages and an antibiotic shows promise in management of infected venous stasis ulcers and other poorly healing wounds," *Int. J. Dermatol.*, vol. 41, no. 7, pp. 453–458, 2002.

[35] B. Ulery, L. Nair, and C. Laurencin, "Biomedical applications of biodegradable polymers," *J. Polym. Sci. Part B Polym. Phys.*, vol. 49, no. 12, pp. 832–864, 2011.

[36] J. Pachence and J. Kohn, "Principles of tissue engineering," *New York, Acad. Press. R. Lanza*, 1997.

[37] J. Kohn and R. Langer, "Bioresorbable and bioredible materials.," *New York, Biomater. Sci. Acad. Press. B. Ratner*, pp. 64–72, 1996.

[38] K. Rezwan, Q. Z. Chen, J. J. Blaker, and A. R. Boccaccini, "Biodegradable and bioactive porous polymer/inorganic composite scaffolds for bone tissue engineering," *Biomaterials*, vol. 27, no. 18, pp. 3413–3431, 2006.

[39] A. Frenot and I. Chronakis, "Polymer nanofibers assembled by electrospinning.," *Curr. Opin. Colloid Interface Sci.*, vol. 8, pp. 64–65, 2003.

[40] J. C. Middleton and a J. Tipton, "Synthetic biodegradable polymers as orthopedic devices.," *Biomaterials*, vol. 21, no. 23, pp. 2335–2346, 2000.

[41] L. J. del Valle, a. Díaz, M. Royo, a. Rodríguez-Galán, and J. Puiggalí, "Biodegradable polyesters reinforced with triclosan loaded polylactide micro/nanofibers: Properties, release and biocompatibility," *Express Polym. Lett.*, vol. 6, no. 4, pp. 266–282, 2012.

[42] A. G. Mikos and J. S. Temenoff, "Formation of highly porous biodegradable scaffolds for tissue engineering," *Electron. J. Biotechnol.*, vol. 3, no. 2, pp. 114–119, 2000.

[43] A. G. M. R. C. Thomson, M. C. Wake, M. J. Yaszemski, "Biodegradable polymer scaffolds to regenerate organs.," *Adv. Polym. Sci.*, vol. 122, pp. 245–274, 1995.

[44] V. Maquet and R. Jerome, "Design of Macroporous Biodegradable Polymer Scaffolds for Cell Transplantation," in *Materials Science Forum*, 1997, vol. 250, pp. 15–42.

[45] L. J. Del Valle, R. Camps, A. Díaz, L. Franco, A. Rodríguez-Galán, and J. Puiggalí, "Electrospinning of polylactide and polycaprolactone mixtures for preparation of materials with tunable drug release properties," *J. Polym. Res.*, vol. 18, pp. 1903–1917, 2011.

[46] U. a Stock and J. P. Vacanti, "TISSUE E NGINEERING : Current State and Prospects," no. 1, 2001.

[47] J. H. S. George, "Engineering of Fibrous Scaffolds for use in Regenerative Medicine," Imperial College London, 2011.

[48] Y. M. Shin, M. M. Hohman, M. P. Brenner, and G. C. Rutledge, "Experimental characterization of electrospinning: the electrically forced jet and instabilities," *Polymer (Guildf).*, vol. 42, no. 25, pp. 09955–09967, 2001.

[49] M. Bognitzki, W. Czado, T. Frese, A. Schaper, M. Hellwig, M. Steinhart, A. Greiner, and J. H. Wendorff, "Nanostructured fibers via electrospinning," *Adv. Mater.*, vol. 13, no. 1, pp. 70–72, 2001.

[50] N. Bhardwaj and S. C. Kundu, "Electrospinning: A fascinating fiber fabrication technique," *Biotechnol. Adv.*, vol. 28, no. 3, pp. 325–347, 2010.

[51] Z. G. Wang, L. S. Wan, Z. M. Liu, X. J. Huang, and Z. K. Xu, "Enzyme immobilization on electrospun polymer nanofibers: An overview," *J. Mol. Catal. B Enzym.*, vol. 56, no. 4, pp. 189–195, 2009.

[52] C. Burger, B. S. Hsiao, and B. Chu, "Nanofibrous Materials and Their Applications," *Annu. Rev. Mater. Res.*, vol. 36, no. 1, pp. 333–368, 2006.

[53] M. M. Hohman, M. Shin, G. Rutledge, and M. P. Brenner, "Electrospinning and electrically forced jets. II. Applications," *Phys. Fluids*, vol. 13, no. 8, pp. 2221–2236, 2001.

[54] Z. M. Huang, Y. Z. Zhang, M. Kotaki, and S. Ramakrishna, "A review on polymer nanofibers by electrospinning and their applications in nanocomposites," *Compos. Sci. Technol.*, vol. 63, no. 15, pp. 2223–2253, 2003.

[55] T. Hayashi, "Biodegradable polymers for biomedical uses," *Prog. Polym. Sci.*, vol. 19, no. 4, pp. 663–702, Jan. 1994.

[56] C. J. Buchko, K. M. Kozloff, and D. C. Martin, "Surface characterization of porous, biocompatible protein polymer thin films," *Biomaterials*, vol. 22, no. 11, pp. 1289–1300, 2001.

[57] C. J. Buchko, M. J. Slattery, K. M. Kozloff, and D. C. Martin, "Mechanical properties of biocompatible protein polymer thin films," *J. Mater. Res.*, vol. 15, no. 1, pp. 231–242, 2000.

[58] C. J. Buchko, L. C. Chen, Y. Shen, and D. C. Martin, "Processing and microstructural characterization of porous biocompatible protein polymer thin films," *Polymer (Guildf).*, vol. 40, no. 26, pp. 7397–7407, 1999.

[59] C. M. Agrawal and R. B. Ray, "Biodegradable polymeric scaffolds for musculoskeletal tissue engineering," *J. Biomed. Mater. Res.*, vol. 55, no. 2, pp. 141–150, 2001.

[60] G. Buschle-Diller, J. Cooper, Z. Xie, Y. Wu, J. Waldrup, and X. Ren, "Release of antibiotics from electrospun bicomponent fibers," *Cellulose*, vol. 14, no. 6, pp. 553–562, 2007.

[61] C. T. Laurencin, A. M. A. Ambrosio, M. D. Borden, and J. A. Cooper, "Tissue Engineering: Orthopedic Applications," *Annu. Rev. Biomed. Eng.*, vol. 1, no. 1, pp. 19–46, Aug. 1999.

[62] R. Jain, N. H. Shah, A. W. Malick, and C. T. Rhodes, "Controlled drug delivery by biodegradable poly(ester) devices: different preparative approaches.," *Drug Dev. Ind. Pharm.*, vol. 24, no. 8, pp. 703–27, Aug. 1998.

[63] I. Imaz, J. Hernando, D. Ruiz-Molina, and D. Maspoch, "Metal-organic spheres as functional systems for guest encapsulation.," *Angew. Chem. Int. Ed. Engl.*, vol. 48, no. 13, pp. 2325–2329, 2009.

[64] D. R. Rueda, M. C. García-Gutiérrez, A. Nogales, M. J. Capitán, T. A. Ezquerra, A. Labrador, E. Fraga, D. Beltrán, J. Juanhuix, J. F. Herranz, and J. Bordas, "Versatile wide angle diffraction setup for simultaneous wide and small angle x-ray scattering measurements with synchrotron radiation," *Rev. Sci. Instrum.*, vol. 77, no. 3, p. 033904, Mar. 2006.

[65] J. C. Moore, "Gel permeation chromatography. I. A new method for molecular weight distribution of high polymers," *J. Polym. Sci. Part A Gen. Pap.*, vol. 2, no. 2, pp. 835–843, Feb. 1964.

[66] M. Persson, G. S. Lorite, H. E. Kokkonen, S.-W. Cho, P. P. Lehenkari, M. Skrifvars, and J. Tuukkanen, "Effect of bioactive extruded PLA/HA composite films on focal adhesion formation of preosteoblastic cells," *Colloids Surfaces B Biointerfaces*, vol. 121, pp. 409–416, 2014.

[67] E. Llorens, S. Calderón, L. J. del Valle, and J. Puiggalí, "Polybiguanide (PHMB) loaded in PLA scaffolds displaying high hydrophobic, biocompatibility and antibacterial properties," *Mater. Sci. Eng. C*, vol. 50, pp. 74–84, 2015.

[68] C. Ribeiro, V. Sencadas, C. M. Costa, J. L. Gómez Ribelles, and S. Lanceros-Méndez, "Tailoring the morphology and crystallinity of poly(L-lactide acid) electrospun membranes," *Sci. Technol. Adv. Mater.*, vol. 12, p. 015001, 2011.

[69] G. Kister, G. Cassanas, and M. Vert, "Effects of morphology, conformation and configuration on the IR and Raman spectra of various poly(lactic acid)s," *Polymer (Guildf).*, vol. 39, no. 2, pp. 267–273, 1998.

[70] L. T. Sin, A. R. Rahmat, and W. A. W. A. Rahman, *Polylactic Acid: PLA Biopolymer Technology and Applications*. William Andrew, 2012.

[71] G. F. de Paula, G. I. Netto, and L. H. C. Mattoso, "Physical and chemical characterization of poly(hexamethylene biguanide) hydrochloride," *Polymers (Basel).*, vol. 3, pp. 928–941, 2011.

[72] L. Chen, L. Bromberg, T. A. Hatton, and G. C. Rutledge, "Electrospun cellulose acetate fibers containing chlorhexidine as a bactericide," *Polymer (Guildf).*, vol. 49, pp. 1266–1275, 2008.

[73] S. Kumar and S. B. Rai, "Spectroscopic studies of L -arginine molecule," *J. Pure Appl. Phys.*, vol. 48, no. April, pp. 251–255, 2010.

[74] E. Llorens Domenjó, "Advanced electrospun scaffolds based on biodegradable polylactide and poly(butylene succinate) for controlled drug delivery and tissue engineering," Universitat Politècnica de Catalunya, 2014.

[75] G. Xia and C. Wolz, "Phages of Staphylococcus aureus and their impact on host evolution," *Infect. Genet. Evol.*, vol. 21, pp. 593–601, 2014.